

DMC DATA PRODUCT MANUAL



AUTHOR

GARY CROWLEY

DOCUMENT NUMBER

0115056

ISSUE

02

DATE OF ISSUE

12-Feb-2010

STATUS

FINAL

THIS DOCUMENT IS THE PROPERTY OF DMC INTERNATIONAL IMAGING LIMITED. IT IS SUBJECT TO ALTERATION WITHOUT NOTICE AND MUST NOT BE COPIED OR USED FOR ANY PURPOSE OTHER THAN THAT FOR WHICH IT HAS BEEN SUPPLIED.

DMC International Imaging Ltd.,

Tycho House,
20 Stephenson Road,
Surrey Research Park,
Guildford,
Surrey,
GU2 7YE,
UK

Tel: +44 1483 804299

Fax: +44 1483 803804

	DMC DATA PRODUCT MANUAL	DATE: 12-Feb-2010
		DOC NO: 0115056
		ISSUE: 02
		STATUS: FINAL

TABLE OF CONTENTS

1	Document Revision Status.....	6
2	Scope.....	7
3	Applicable Documents.....	7
4	Related Documents.....	7
5	Acronyms and Abbreviations.....	8
6	Units of Measurement.....	9
7	Data Products	11
8	DMC Imager Payload	11
	8.1 SLIM-6 Imager Design	12
	8.2 SLIM-6-22 Imager Design.....	15
	8.3 Sensor Model	17
	8.4 Spectral Filters	19
9	Orbit	22
10	Radiance Calculation.....	24
	10.1 L1R and L1T Products	24
	10.1.1 Reading the Scaling Coefficients for L1R and L1T Products.....	24
	10.2 LOR Products.....	25
	10.2.1 Reading the Scaling Coefficients for LOR Products.....	25
11	Metadata	26
	11.1 L1R and L1T Products	26
	11.2 LOR Products.....	27
12	Reflectance Calculation	28
13	DMC DIMAP	29
14	Image Processing	39
	14.1 Radiometric Correction.....	39
	14.2 Georeferencing.....	39
	14.3 Band Registration	39
	14.4 Bank Mosaic.....	40
	14.5 Orthorectification.....	40
15	Filename Format	43
	15.1 L1R and L1T Products	43
	15.2 LOR Products.....	43
	15.3 Framed L1R and L1T Products	44
	15.4 Framed LOR Products.....	44
16	Special Notes on DMC Data	46
	16.1 DN Range and Special DN Values.....	46
	16.2 Holes.....	46
	16.3 Band Fringes.....	47
	16.4 Bank Shift	48
17	Frequently Asked Questions.....	49
	17.1 Radiometry	49
	17.2 Geometry.....	51
	17.3 Data Quality.....	51
Appendix A:	Spectral Transmission Profiles.....	53
Appendix B:	DIMAP Sample – L1R Product	79
Appendix C:	DIMAP Sample – L1T Product	85
Appendix D:	Radiometric Calibration Report.....	90

	DMC DATA PRODUCT MANUAL	DATE: 12-Feb-2010
		DOC NO: 0115056
		ISSUE: 02
		STATUS: FINAL

Appendix E:	Orthorectification Procedure	115
Appendix F:	Keystone Image Orthorectification - Technical Summary	120
Appendix G:	Weblinks	127

FIGURES

Figure 1:	The SLIM-6 imager	12
Figure 2:	Eastman Kodak KL10203 Linear CCD.....	13
Figure 3:	Detector and channel layout of the SLIM-6 imager	14
Figure 4:	Detector and channel layout of the SLIM-6-22 imager	16
Figure 5:	DMC sensor model.....	17
Figure 6:	Image processing chain	41
Figure 7:	Software used in the processing chain.....	42
Figure 8:	Image artefacts due to holes.....	46
Figure 9:	Holes in one band	46
Figure 10:	Holes in all bands	47
Figure 11:	Fringes along the edge of a DMC image.....	47
Figure 12:	Bank shift across the top of a dual bank DMC image.....	48
Figure 13:	KLI-10203 Quantum Efficiency Curve	50
Figure 14:	Site location map showing Antarctic and Greenland test sites (green boxes).....	93
Figure 15:	Red even pixels – DU000009pm (integration time 1,500 μ s).....	94
Figure 16:	Red even pixels – DU000010pm (integration time 2,400 μ s).....	94
Figure 17:	Deep Space image (DU000010pm red even pixels).....	95
Figure 18:	Pacific Ocean at night image (DU000020pm red even pixels).....	95
Figure 19:	Comparison of Antarctic scenes DU00001cpm (left) and DU00001apm (right).....	96
Figure 20:	Ratio of the two plots in Figure 19	96
Figure 21:	Railroad Valley calibration site (DMC image)	97
Figure 22:	Comparison of dark images DU000009pm (left) and DU000010pm (right)	98
Figure 23:	Analysis of the two plots in Figure 22 - ratio (left); magnitude difference (right)	98
Figure 24:	Comparison of the dark images for the red even pixels on Imager0	99
Figure 25:	Comparison of the Antarctic images for the red even pixels on Imager0	100
Figure 26:	Ratio of Antarctic plots from Figure 25 for the red even pixels on Imager0	101
Figure 27:	Subsection of a UK-DMC image over Greenland.....	102
Figure 28:	Comparison of responses for images acquired when yaw=0° and yaw=180°	103
Figure 29:	Response of red even pixels on Imager0 for equally illuminated scene (DU000420pm) ..	104
Figure 30:	Railroad Valley test site (ASTER image provided by RSG)	105
Figure 31:	Filter response curves for the green spectral filter on Imager0 and Imager1	107
Figure 32:	Example data detailing the atmospheric conditions	108
Figure 33:	Example data detailing the radiometry.....	108
Figure 34:	Example data showing the derived absolute radiance values	109
Figure 35:	Histogram of original data (left); histogram of data after calibration (right)	111
Figure 36:	Comparison of the calibrated data (left) and the raw data (right).....	113
Figure 37:	Keystone Workstation Workspace.....	115
Figure 38:	Control Point List	116
Figure 39:	Distribution of GCPs.....	117
Figure 40:	Adjust Rigorous Model	118
Figure 41:	Standardised Residual Error of GCPs	119
Figure 42:	Generic LOS model for optical sensors.....	121

TABLES

Table 1: DMC data products	11
Table 2: SLIM-6 class imager characteristics	12
Table 3: Imagers on the DMC missions	12
Table 4: Single channel optical specification for the SLIM-6 imager	13
Table 5: Single channel optical specification for the SLIM-6-22 imager	15
Table 6: SLIM-6 sensor model parameters	17
Table 7: SLIM-6-22 sensor model parameters for Deimos-1	18
Table 8: SLIM-6-22 sensor model parameters for UK-DMC2	18
Table 9: SLIM-6 spectral channel specification	20
Table 10: SLIM-6-22 spectral channel specification	21
Table 11: Nominal orbital parameters	22
Table 12: Nominal orbital parameters for Deimos-1	22
Table 13: Nominal orbital parameters for UK-DMC2	23
Table 14: DMC satellite numbers	23
Table 15: Radiance conversion formulae	24
Table 16: TIFF tags containing rescale information for the LOR product	26
Table 17: Product metadata description	27
Table 18: $E_{0\lambda}$ for the Chance spectrum CHKUR (MODTRAN 4.0) model	28
Table 19: $E_{0\lambda}$ for the Thuillier 2002 model	28
Table 20: Filename convention parameter description	45
Table 21: DMC NE Δ L values	52
Table 22: Landsat band-averaged dark-noise levels NE Δ L	52
Table 23: Acquisition details for the images in Figure 28	104
Table 24: List of acquisitions over the RRV test site in July 2004	106
Table 25: Pixel location and DN values from image scene DU00017dpm	106
Table 26: View zenith angles for the UK-DMC image acquisitions	107
Table 27: Comparison of data variation retention during scaling	112

EQUATIONS

Equation 1: TOA radiance conversion formula for L1R and L1T products	24
Equation 2: TOA radiance conversion formula for LOR products	25
Equation 3: TOA reflectance conversion formula	28
Equation 4	109
Equation 5	110
Equation 6	110
Equation 7	111
Equation 8	111

EXAMPLES

Example 1: <Quality_Assessment> - RMS Error in Metres	33
---	----

	DMC DATA PRODUCT MANUAL	DATE: 12-Feb-2010
		DOC NO: 0115056
		ISSUE: 02
		STATUS: FINAL

Example 2: <Quality_Assessment> - RMS Error in Decimal Degrees33

Example 3: <Coordinate_Reference_System> - EPSG Geodetic Parameters.....35

Example 4: <Coordinate_Reference_System> - Custom Geodetic Parameters35

Example 5: <Image_Display> - No Data Value36

Example 6: <Dataset_Sources> - EPSG Geodetic Parameters.....38

Example 7: <Dataset_Sources> - Custom Geodetic Parameters38

	DMC DATA PRODUCT MANUAL	DATE: 12-Feb-2010
		DOC NO: 0115056
		ISSUE: 02
		STATUS: FINAL

1 DOCUMENT REVISION STATUS

Issue	Date	Name	Change Reference
01	27-Jun-2008	Gary Crowley	ALL
02	12-Feb-2010	Gary Crowley	<ul style="list-style-type: none"> • Added Exo-atmospheric solar irradiance tables. • Updated filenaming convention. • Updated DIMAP metadata information for the tag <Quality_Assessment>. • Added reference document used to determine the NEΔL. • Added information on the SLIM-6-22 imager. • Added applicable information for UK-DMC2. • Added applicable information for Deimos-1. • Added spectral transmission profiles for and Deimos-1 and UK-DMC2. • Added technical summary on the Keystone Image Orthorectification.

	DMC DATA PRODUCT MANUAL	DATE: 12-Feb-2010
		DOC NO: 0115056
		ISSUE: 02
		STATUS: FINAL

2 SCOPE

The data products supplied by DMCII are derived from images acquired by the DMC satellites. The primary payload on the DMC satellites is the SLIM-6 class of imagers manufactured by SSTL, UK.

This manual will aid users in their analysis of the data products to maximise the information they can extract from the DMC images by providing a thorough description of the data products, the imaging payload, the calibration procedure and the orthorectification process.

3 APPLICABLE DOCUMENTS

These are documents that are owned or controlled by DMCII or SSTL. Applicable documents identified in the following text are identified by **AD#n**, where "n" indicates the actual document, from the following list:

AD#	Reference	Title
01	0062733	Post-launch Calibration of the UK-DMC Satellite Sensor
02	0105469	Orthorectification Procedure
03	0052791	DMC 32m MS Filter Spectral Response Profiles
04	0104039	DMC DIMAP: A Technical Note On The Dimap Metadata Format For DMCII Products
05	0074903	Metadata Files Distributed with the DMC Images
06	0075257	Radiance Calculation Formulae for DMC Images
07	0049911	DMC Image Format
09	0086432	TIFF Tags for Radiance Calculation
09	0112168	FAQ on DMC Data Supplied to ESA for Europe 2007
10	0115064	Beijing-1 32m MS Filter Spectral Response Profiles

4 RELATED DOCUMENTS

These are external documents that are NOT owned or controlled by DMCII or SSTL. Reference documents identified in the following text are identified by **RD#n**, where "n" indicates the actual document, from the following list:

RD#	Reference	Title
01		TIFF Revision 6.0
02		Dimap Dictionary: Generic Profile Version 1.1 (Ed. May 9, 2006)
03		Dimap Dictionary: SPOT Scene Profile Version 1.1.2 (Ed. May 9, 2006)
04		KLI-10203 Datasheet Revision No. 6
05		Landsat-7 ETM+ On-Orbit Reflective-Band Radiometric Characterization <i>IEEE TRANSACTIONS ON GEOSCIENCE AND REMOTE SENSING, VOL. 42, NO. 12, DECEMBER 2004</i>
06		Keystone Image Orthorectification

	DMC DATA PRODUCT MANUAL	DATE: 12-Feb-2010
		DOC NO: 0115056
		ISSUE: 02
		STATUS: FINAL

5 ACRONYMS AND ABBREVIATIONS

The following acronyms and abbreviations are used within this document:

Acronym	Description
AOCS	Attitude and Orbit Control System
BIL	Band Interleave by Line
CCD	Charge Coupled Device
CGIAR	Consultative Group for International Agricultural Research
CGIAR-CSI	CGIAR - Consortium for Spatial Information
CHKUR	Chance-Kurucz
CIAT	International Centre for Tropical Agriculture
CRS	Coordinate Reference System
DEM	Digital Elevation Model
DIMAP	Digital Image Map
DMC	Disaster Monitoring Constellation
DMCII	DMC International Imaging Ltd.
DN	Digital Number
DTM	Digital Terrain Model
ECI	Earth Centred Inertial
ECR	Earth Centred Rotating
EO	Earth Observation
EOST	Earth Observation Scheduling Task
EPSG	European Petroleum Survey Group
ETM+	Enhanced Thematic Mapper Plus
FoV	Field of View
GCP	Ground Control Point
GCS	Geographic Coordinate System
GeoTIFF	Geo-referenced Tagged Image File Format
GLCF	Global Land Cover Facility
GLOBE	Global Land One-km Base Elevation
GSD	Ground Sample Distance
HDDR	Hard Drive Data Recorder
HTML	Hypertext Markup Language
IFD	Image File Directory
iFoV	Instantaneous Field of View
IP	Image Point
KWS	Keystone Workstation
LEO	Low Earth Orbit
LOS	Line Of Sight
LTAN	Local Time Ascending Node
LUT	Look-Up Table
MODTRAN	Moderate Resolution Atmospheric Transmission
MSI	Multi-Spectral Imager
NEΔL	Noise Equivalent Difference in Radiance
NGDC	National Geophysical Data Center
NIR	Near Infrared
NOAA	National Oceanic and Atmospheric Administration
NRT	Near Real-Time

	DMC DATA PRODUCT MANUAL	DATE: 12-Feb-2010
		DOC NO: 0115056
		ISSUE: 02
		STATUS: FINAL

Acronym	Description
OBC	On-Board Computer
OGP	International Association of Oil & Gas Producers
PAN	Panchromatic
QE	Quantum Efficiency
RGB	Red Green Blue
RMS	Root Mean Square
RMSE	Root Mean Square Error
RRV	Railroad Valley
RSG	Remote Sensing Group at The University of Arizona
SLIM-6	Surrey Linear Imager – 6 Channels
SLIM-6-22	Surrey Linear Imager – 6 Channels - 22 metre
SNR	Signal to Noise Ratio
SRTM	Shuttle Radar Topography Mission
SSDR	Solid State Data Recorder
SSTL	Surrey Satellite Technology Ltd.
TIFF	Tagged Image File Format
TLE	Two-Line Element
TIm	Telemetry
TM	Thematic Mapper
TOA	Top of Atmosphere
TP	Tie Point
UTC	Universal Time Coordinated
UTM	Universal Transverse Mercator
WGS84	World Geodetic System 1984
XML	Extensible Markup Language

6 UNITS OF MEASUREMENT

The following units of measurement are used within this document:

Unit	Description
°	Degree
µm	Micrometre = 10 ⁻⁶ m
µs	Microsecond = 10 ⁻⁶ s
arc sec	Arc second = 1/3600 °
AU	Astronomical Unit
B	Bytes
b	Bits
bps	Bits per second
GB	Gigabyte = 10 ⁹ B
kg	Kilogram
km	Kilometre = 10 ³ m
kms ⁻¹	Kilometres per second = 10 ³ ms ⁻¹
m	Metre
MB	Megabyte = 10 ⁶ B
Mbps	Megabits per second = 10 ⁶ bps
min	Minute = 60 s

Unit	Description
mm	Millimetre = 10^{-3} m
ms	Millisecond = 10^{-3} s
ms^{-1}	Metres per second
nm	Nanometre = 10^{-9} m
ns	Nanosecond = 10^{-9} s
rad	Radian
s	Second
sr	Steradian
TB	Terabyte = 10^{12} B
W	Watt
$\text{Wm}^{-2}\text{sr}^{-1}\mu\text{m}^{-1}$	Watts per square metre steradian micrometre

	DMC DATA PRODUCT MANUAL	DATE: 12-Feb-2010
		DOC NO: 0115056
		ISSUE: 02
		STATUS: FINAL

7 DATA PRODUCTS

DMCII currently offers the data products outlined in Table 1, which are derived from the multi-spectral images captured by the SLIM-6 class imagers.

Product	Description
L0R	Raw satellite data split into the 3 spectral bands (NIR, Red and Green) with a radiometric correction applied to all bands.
L1R	Band registered product derived from the L0R product.
L1T	Orthorectified product derived from the L1R product using manually collected GCPs from Landsat ETM+ data and SRTM DEM V3 ¹ data.

Table 1: DMC data products

The SRTM DEM V3 only covers the Earth's land mass between $\pm 60^\circ$ latitude. Where the acquired image exceeds $\pm 60^\circ$ latitude, orthorectification will be performed using the 1km GLOBE DEM² supplied by NGDC.

The L1T products are produced using the reference and DEM datasets specified in Table 1 and projected to UTM / WGS84 by default. However, it is possible to orthorectify DMC images to any projection using any reference and DEM datasets as supplied by the customer.

All data products are delivered in the TIFF and GeoTIFF image formats.

8 DMC IMAGER PAYLOAD

The primary DMC imaging payload is the SLIM-6 class imager built by SSTL UK, which is an evolution of multi-spectral imagers flown on previous SSTL missions. The design of the SLIM-6 class imagers provides a 3 spectral band, nadir pointing imager capable of providing high and mid-resolution images of the Earth's surface when operating in a sun-synchronous low Earth orbit.

There are currently two imagers in the SLIM-6 class of imagers, the SLIM-6 and the SLIM-6-22. The following tables give the top level characteristics of the imagers and the missions that are currently using them.

¹ Void-filled SRTM DEM V3, 2006, International Centre for Tropical Agriculture (CIAT), available from the CGIAR-CSI SRTM 90m Database: <http://srtm.csi.cgiar.org>

² The GLOBE DEM is supplied by NOAA, available from NGDC <http://www.ngdc.noaa.gov/mgg/topo/globe.html>

	DMC DATA PRODUCT MANUAL	DATE: 12-Feb-2010
		DOC NO: 0115056
		ISSUE: 02
		STATUS: FINAL

Imager	Imager Type	GSD at Nadir	Spectral Bands
SLIM-6	Optical	31.822 m	NIR Red Green
SLIM-6-22	Optical	22.001 m	NIR Red Green

Table 2: SLIM-6 class imager characteristics

DMC	Imager
AlSat-1	SLIM-6
Beijing-1	SLIM-6
Deimos-1	SLIM-6-22
NigeriaSat-1	SLIM-6
UK-DMC	SLIM-6
UK-DMC2	SLIM-6-22

Table 3: Imagers on the DMC missions

8.1 SLIM-6 Imager Design

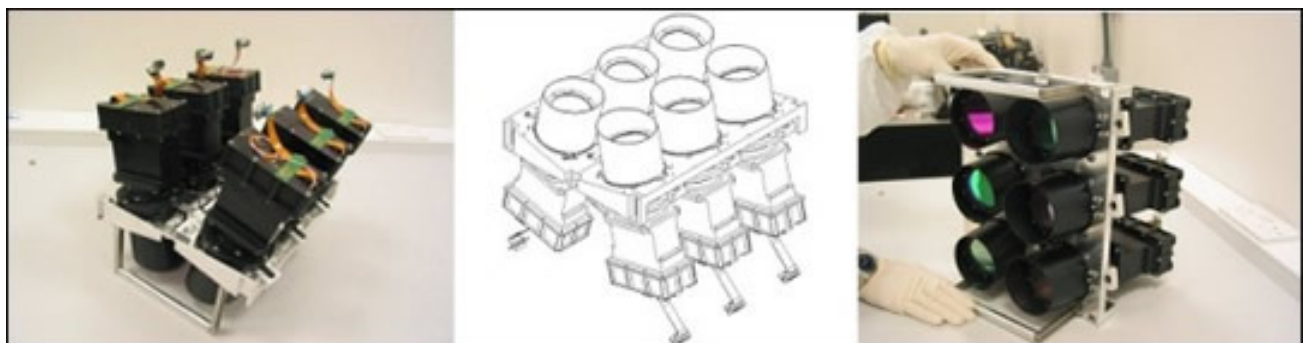


Figure 1: The SLIM-6 imager

The SLIM-6 imager is a dual bank linear CCD push broom imager utilising the orbital motion of the DMC platform to capture radiation reflected from the Earth's surface within a 600 km swath.

The spectral filter of each channel is protected by a fused silica radiation absorption window, which is positioned on the space facing side of the filter. The spectral filters are located in front of the camera lens. Each of the 6 SLIM-6 imager channels has a linear CCD array at its focal plane.

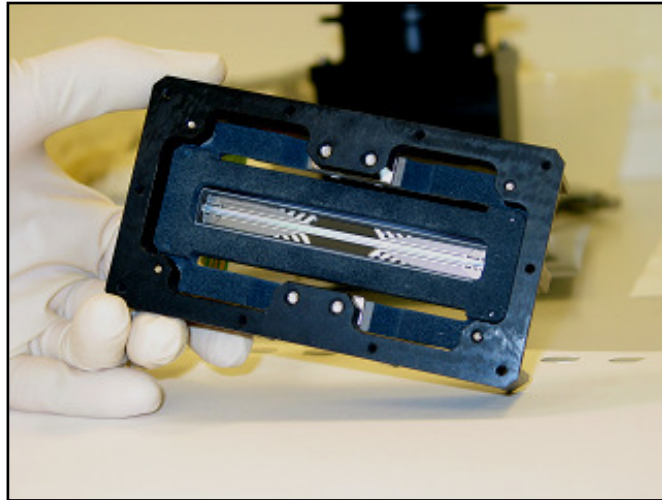


Figure 2: Eastman Kodak KL10203 Linear CCD

	Specification
Sensor	Eastman Kodak KLI-10203 Linear CCD: Number of Detectors = 10,224 ³ Detector Size = 7.0 μm x 7.0 μm Data Capture = 11-bit ⁴
Lens	Schneider Apo-Componon HM 150mm focal length, f/6.3 Focal length = 150.9 mm F-number = f/6.3
iFoV	46.388×10^{-6} rad = 0.00266° = 9.568 arc sec
FoV	$2 \times \text{TAN}^{-1} [(7.0 \times 10^{-6} \times 5100) / (150.9 \times 10^{-3})] = 26.62^\circ$
GSD	31.822 m at nadir
Swath	$31.822 \times 10200 = 324.58$ km

Table 4: Single channel optical specification for the SLIM-6 imager

³ Only 10,200 detectors are used for image capture. The other 24 detectors are used to measure the dark current.

⁴ Only the most significant 8-bits of data are captured to the storage device.

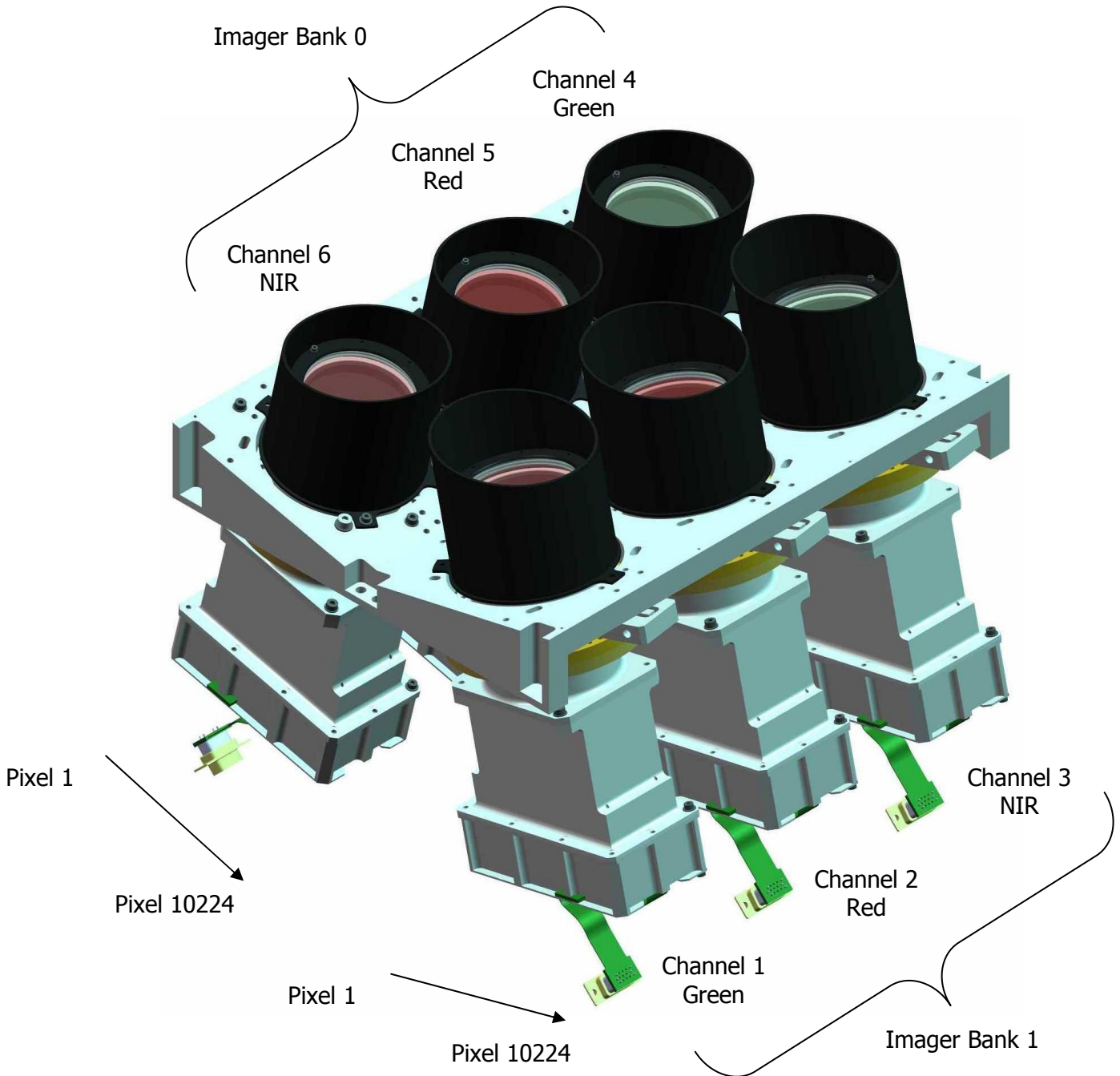


Figure 3: Detector and channel layout of the SLIM-6 imager

8.2 SLIM-6-22 Imager Design

The SLIM-6-22 imager is a dual bank linear CCD push broom imager utilising the orbital motion of the DMC platform to capture radiation reflected from the Earth's surface within a 660 km swath.

The spectral filter of each channel is protected by a fused silica radiation absorption window, which is positioned on the space facing side of the filter. The spectral filters are located in front of the camera lens. Each of the 6 SLIM-6-22 imager channels has a linear CCD array at its focal plane.

	Specification
Sensor	Eastman Kodak KLI-14403 Linear CCD: Number of Detectors = 14,436 ⁵ Detector Size = 5.0 μm x 5.0 μm Data Capture = 14-bit ⁶
Lens	Custom designed double Gaussian derivative lens Focal length = 155.9 mm F-number = f/53
iFoV	32.1×10^{-6} rad = 0.00184° = 6.62 arc sec
FoV	$2 \times \text{TAN}^{-1} [(5.0 \times 10^{-6} \times 7190) / (155.9 \times 10^{-3})] = 25.97^\circ$
GSD	22.001 m at nadir
Swath	340 km (Earth's curvature included in calculation)

Table 5: Single channel optical specification for the SLIM-6-22 imager

⁵ Only 14,404 detectors are used for image capture. The other 32 detectors are used to measure the dark current.

⁶ Only the most significant 8-bits or 10-bits of data are captured to the storage device.

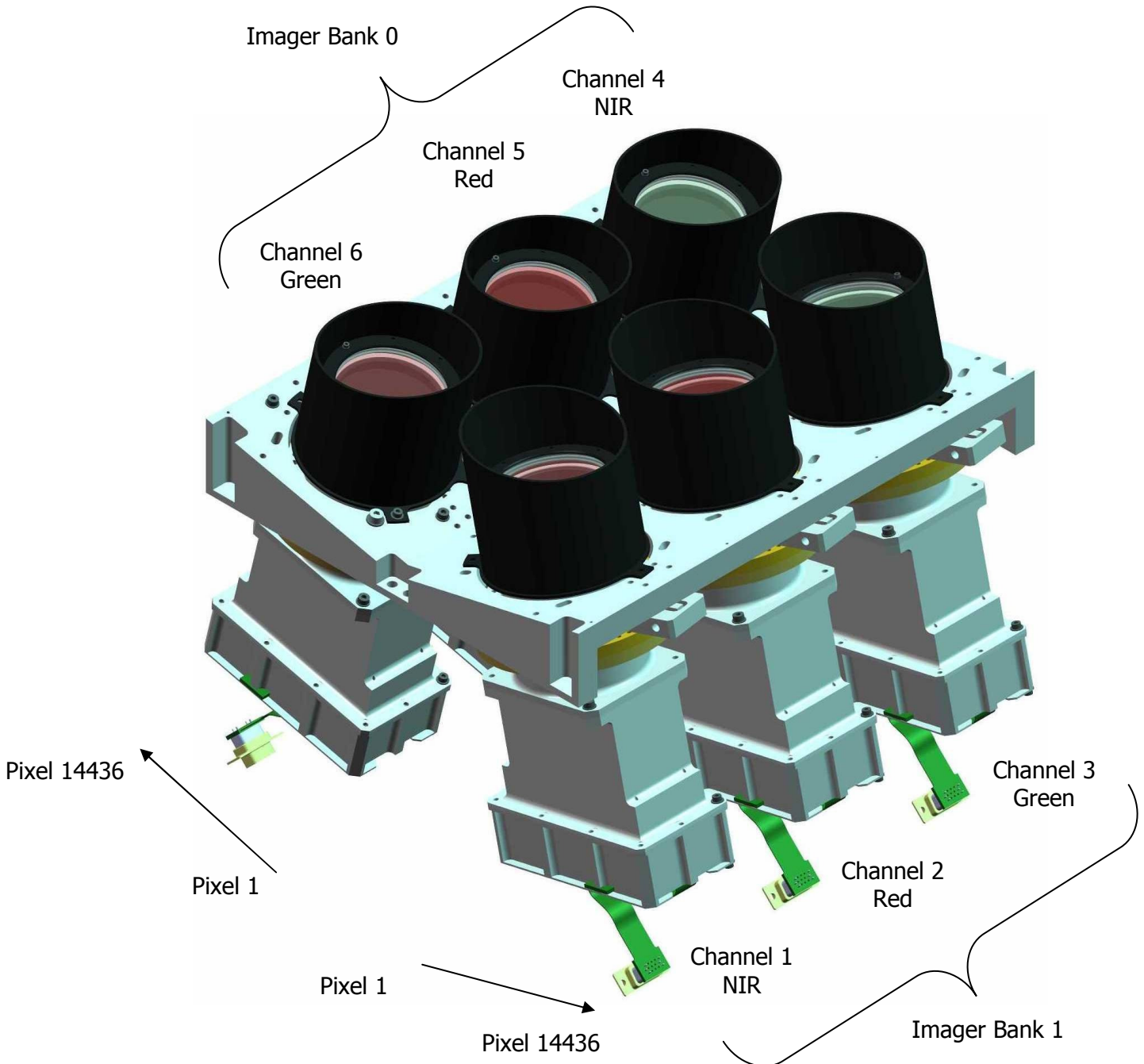


Figure 4: Detector and channel layout of the SLIM-6-22 imager

8.3 Sensor Model

The SLIM-6 class imager is composed of 2 banks, each bank consisting of 3 channels (NIR, Red, Green spectral bands). The 2 imager banks are mounted at an angle to provide a total imaging swath of over 600 km and an overlap between the simultaneously acquired images.

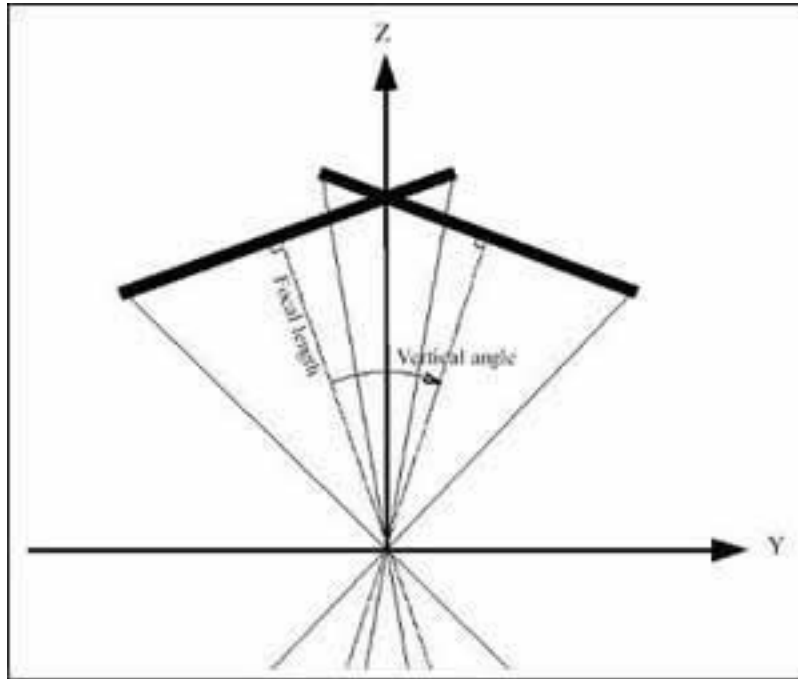


Figure 5: DMC sensor model

Parameter	Nominal Value
Vertical Angle	25.2896°
Focal Length	21,557 detector units
Number of Detectors	10,224
Overlap Between Imager Banks	567 detectors
Clock Period	800 ns
Scan Line Duration	4.8 ms

Table 6: SLIM-6 sensor model parameters

Parameter	Nominal Value
Vertical Angle	25.17°
Focal Length	31,200 detector units
Number of Detectors	14,436
Overlap Between Imager Banks	460.8 detectors
Clock Period	212.12 ns
Scan Line Duration	3.24 ms

Table 7: SLIM-6-22 sensor model parameters for Deimos-1

Parameter	Nominal Value
Vertical Angle	25.2°
Focal Length	31,200 detector units
Number of Detectors	14,436
Overlap Between Imager Banks	450.3 detectors
Clock Period	200 ns
Scan Line Duration	3.24 ms

Table 8: SLIM-6-22 sensor model parameters for UK-DMC2

	DMC DATA PRODUCT MANUAL	DATE: 12-Feb-2010
		DOC NO: 0115056
		ISSUE: 02
		STATUS: FINAL

8.4 Spectral Filters

The spectral filters used in the SLIM-6 class imagers were manufactured by Barr Associates Inc., USA using the same materials and processes as the spectral filters on the Landsat ETM+ instrument. The spectral bandwidth and channel characteristics are outlined in Table 9 and Table 10 along with the equivalent Landsat ETM+ spectral channel.

Spectral transmission profiles for the fused silica radiation absorption windows and the DMC spectral band filters can be found in Appendix A. These profiles were generated by Barr Associates Inc., USA.



DMC DATA PRODUCT MANUAL

DATE: 12-Feb-2010

DOC NO: 0115056

ISSUE: 02

STATUS: FINAL

Spectral Band Description	Spectral Band ID	Imager ID	Channel ID	Spectral Bandwidth	iFoV	GSD at Nadir	Equivalent Landsat ETM+ Spectral Channel
NIR	0	0	6	0.77 – 0.90 μm	46.388×10^{-6} rad	31.822 m	ETM+4
		1	3	0.77 – 0.90 μm	46.388×10^{-6} rad	31.822 m	ETM+4
RED	1	0	5	0.63 – 0.69 μm	46.388×10^{-6} rad	31.822 m	ETM+3
		1	2	0.63 – 0.69 μm	46.388×10^{-6} rad	31.822 m	ETM+3
GREEN	2	0	4	0.52 – 0.60 μm	46.388×10^{-6} rad	31.822 m	ETM+2
		1	1	0.52 – 0.60 μm	46.388×10^{-6} rad	31.822 m	ETM+2

Table 9: SLIM-6 spectral channel specification



DMC DATA PRODUCT MANUAL

DATE: 12-Feb-2010

DOC NO: 0115056

ISSUE: 02

STATUS: FINAL

Spectral Band Description	Spectral Band ID	Imager ID	Channel ID	Spectral Bandwidth	iFoV	GSD at Nadir	Equivalent Landsat ETM+ Spectral Channel
GREEN	0	0	6	0.52 – 0.60 μm	32.1×10^{-6} rad	22.001 m	ETM+2
		1	3	0.52 – 0.60 μm	32.1×10^{-6} rad	22.001 m	ETM+2
RED	1	0	5	0.63 – 0.69 μm	32.1×10^{-6} rad	22.001 m	ETM+3
		1	2	0.63 – 0.69 μm	32.1×10^{-6} rad	22.001 m	ETM+3
NIR	2	0	4	0.77 – 0.90 μm	32.1×10^{-6} rad	22.001 m	ETM+4
		1	1	0.77 – 0.90 μm	32.1×10^{-6} rad	22.001 m	ETM+4

Table 10: SLIM-6-22 spectral channel specification

9 ORBIT

The DMC is a constellation of EO satellites operating in a low Earth orbit. Each satellite in the constellation is phased at 90° to the next to enable a daily revisit of a point target on the Earth's surface.

The nominal orbital parameters for AlSat-1, Beijing-1, NigeriaSat-1 and UK-DMC at the start of their mission are described in Table 11.

Parameter	Nominal Value
Orbit Type	Sun Synchronous
Altitude	686 km
Inclination	98.2°
Orbital Period	98.4 min
LTAN	10:15 UTC
Orbital Velocity	7.5 kms ⁻¹
Ground Velocity	6.8 kms ⁻¹

Table 11: Nominal orbital parameters

The nominal orbital parameters for Deimos-1 at the start of their mission are described in Table 12.

Parameter	Nominal Value
Orbit Type	Sun Synchronous
Altitude	667 km
Inclination	98.1°
Orbital Period	98.1 min
LTAN	11:10 UTC
Orbital Velocity	7.5 kms ⁻¹
Ground Velocity	6.8 kms ⁻¹

Table 12: Nominal orbital parameters for Deimos-1

The nominal orbital parameters for UK-DMC2 at the start of their mission are described in Table 13.

Parameter	Nominal Value
Orbit Type	Sun Synchronous
Altitude	659 km
Inclination	98.06°
Orbital Period	97.9 min
LTAN	10:45 UTC
Orbital Velocity	7.5 kms ⁻¹
Ground Velocity	6.8 kms ⁻¹

Table 13: Nominal orbital parameters for UK-DMC2

Updated TLE can be found on the internet for each satellite. The satellite numbers for identification are given in Table 14.

Satellite	Satellite Number
AlSat-1	27559
Beijing-1	28890
Deimos-1	35681
NigeriaSat-1	27941
UK-DMC	27942
UK-DMC2	35683

Table 14: DMC satellite numbers

10 RADIANCE CALCULATION

When calculating the TOA radiance values for DMC images, there are two formulae that can be used. The correct formula to use will depend upon the product level of the image.

Table 15 is a quick reference to illustrate the correct formula that should be used to convert the DN values to TOA radiance values, depending on the product level.

Product Level	Formula
L0R	Equation 2
L1R	Equation 1
L1T	Equation 1

Table 15: Radiance conversion formulae

10.1 L1R and L1T Products

Equation 1 is the convention used in the DIMAP files. This formula should only be applied to DMC images that are processed to the L1R or L1T product levels.

$$\text{RADIANCE} = \left[\frac{\text{DN}}{\text{RESCALE GAIN}} \right] + \text{RESCALE BIAS}$$

Equation 1: TOA radiance conversion formula for L1R and L1T products

The DN parameter in Equation 1 is scaled radiance. The rescale gain and rescale bias terms are unitless scaling coefficients used to convert the scaled radiance back to true TOA radiance.

The scaling coefficients (rescale gain and rescale bias) are unique for every image and these unique coefficients are stored in the metadata files that accompany every L1R and L1T product.

The unit of radiance is Watts per square metre steradian micrometre ($\text{Wm}^{-2}\text{sr}^{-1}\mu\text{m}^{-1}$).

10.1.1 Reading the Scaling Coefficients for L1R and L1T Products

These rescale gain and rescale bias values can be extracted from the DIMAP file or read from the html file via a web browser.

	DMC DATA PRODUCT MANUAL	DATE: 12-Feb-2010
		DOC NO: 0115056
		ISSUE: 02
		STATUS: FINAL

See §11.1 for more information on the metadata files for L1R and L1T products.

10.2 LOR Products

Equation 2 is the convention used by DMCI when rescaling the scaled radiance. This formula should only be applied to DMC images that are processed to the LOR product level.

$$\text{RADIANCE} = [\text{DN} \times \text{RESCALE GAIN}] + \text{RESCALE BIAS}$$

Equation 2: TOA radiance conversion formula for LOR products

The DN parameter in Equation 2 is scaled radiance. The rescale gain and rescale bias terms are unitless scaling coefficients used to convert the scaled radiance back to true TOA radiance.

The scaling coefficients (rescale gain and rescale bias) are unique for every image and these unique coefficients are stored in the TIFF tags of the LOR products.

The unit of radiance is Watts per square metre steradian micrometre ($\text{Wm}^{-2}\text{sr}^{-1}\mu\text{m}^{-1}$).

10.2.1 Reading the Scaling Coefficients for LOR Products

This section describes how to extract the scaling coefficients from the TIFF tags of the LOR product, but it assumes a working knowledge of TIFF file structures and the TIFF Image File Directory (IFD). The tags to look for are given in Table 16.

Data relevant to radiance calculations is stored in its own private block. The block has the same format as a standard IFD, which is defined by the TIFF Revision 6.0 specification, including the use of the Value Offset field to either contain or point to the data. The block is referenced by a custom tag in the main IFD, which contains the offset from the beginning of the file of the start of the Smart-i IFD.

1. Search the TIFF IFD for a tag with the ID value of 0xFE0B. The Type of this tag is LONG, and the Count value is set to one.
2. Use the Value Offset from the tag to set the position of the next file-read operation. If successful, this will be set to the start of the Smart-i IFD.
3. Read two bytes from the file: this SHORT value contains the number of tags in the Smart-i IFD.
4. Read up to n tags, where n is the SHORT value that has just been read in.

As with the TIFF standard IFD, the end of the custom IFD is followed by four bytes, which will always be set to NULL for Smart-i.

	DMC DATA PRODUCT MANUAL	DATE: 12-Feb-2010
		DOC NO: 0115056
		ISSUE: 02
		STATUS: FINAL

Tag ID	Tag Type	Tag Name	Tag Description
0xC000	DOUBLE	NIR Rescale Bias	Rescale Bias value for the Near Infra-Red band.
0xC001	DOUBLE	NIR Rescale Gain	Rescale Gain value for the Near Infra-Red band.
0xC002	DOUBLE	Red Rescale Bias	Rescale Bias value for the Red band.
0xC003	DOUBLE	Red Rescale Gain	Rescale Gain value for the Red band.
0xC004	DOUBLE	Green Rescale Bias	Rescale Bias value for the Green band.
0xC005	DOUBLE	Green Rescale Gain	Rescale Gain value for the Green band.

Table 16: TIFF tags containing rescale information for the L0R product

11 METADATA

The DMC products are generated using two different software tools, which results in the metadata for each product being stored in a different format.

11.1 L1R and L1T Products

The L1R and L1T products are generated by Keystone with the metadata captured in several files. However, the primary source of the product's metadata is the DIMAP (.dim) file. More information on the contents of the DIMAP file can be found in §13, RD#02 and RD#03.

The L1R and L1T data products are delivered in a zip file with its associated metadata files. A description of the file types contained in the zip file is given in Table 17.

	DMC DATA PRODUCT MANUAL	DATE: 12-Feb-2010
		DOC NO: 0115056
		ISSUE: 02
		STATUS: FINAL

File Extension	Description
dim	<p>The DIMAP file containing all the information about the image, such as date and time of acquisition, rescale gain and rescale bias values, ge positioning information etc.</p> <p>The L1R product level uses the tie-point⁷ transformation model to provide an approximation of the geographic extents of the image.</p>
htm	The htm file is easily read using a web browser and contains most of the information stored in the DIMAP.
jpg	The quick look image of the product that is displayed in the htm file.
sip	The SIP file is the primary metadata file for the image. It contains all the information stored in the DIMAP and a rigorous adjustment model for the image. The SIP file can only be read by an application called Keystone Workstation, developed by Spacemetric AB, SE.
tif	The actual data product.
xsl	The style sheet used to present the information stored in the htm file.

Table 17: Product metadata description

11.2 LOR Products

The LOR products are generated by the Smart-i radiometric processor and the metadata is stored in the TIFF tags of the LOR products.

TIFF tags with IDs in the range 0-0x8FFF are members of the standard TIFF header. IDs in the range 0xC000-0xCFFF are custom tags containing data that are used for calculating the radiance of the image. IDs in the range 0xFE0C are also custom tags, and contain data that have been extracted from the raw satellite image file. The special tag ID 0xFE0B is used to determine the start of the custom tag block.

See §10.2.1 for a description on how to read these tags from the TIFF file header.

⁷ The tie-point transformation model is not read by all remote sensing packages. If your software cannot read the tie-point information of the image, then please read the htm file to extract the coordinates of the vertices and apply them to the image.

12 REFLECTANCE CALCULATION

The TOA reflectance of an image can be calculated by using Equation 3, regardless of the product level, however, this does not take into account atmospheric effects.

$$\rho_{\lambda} = \frac{\pi d^2 L_{\lambda}}{E_{0\lambda} \cos\theta_s}$$

Equation 3: TOA reflectance conversion formula

Where:

ρ_{λ} = TOA reflectance in spectral band λ

d = Earth-Sun distance [AU]

L_{λ} = TOA radiance in spectral band λ [$\text{Wm}^{-2}\text{sr}^{-1}\mu\text{m}^{-1}$]

$E_{0\lambda}$ = Exo-atmospheric solar irradiance normalised for 1AU [$\text{Wm}^{-2}\mu\text{m}^{-1}$]

θ_s = Solar zenith angle [°]

TOA radiance values can be extracted by applying the scaling coefficients as described in §10. As the date and time of image acquisition is known, then the Earth-Sun distance and solar zenith angle can be calculated. Two sets of exo-atmospheric solar irradiance values are given in Table 18 and Table 19, due to the two solar irradiance models used in their calculation.

Spectral Band	Exo-atmospheric Solar Irradiance [$\text{Wm}^{-2}\mu\text{m}^{-1}$]		
	Deimos-1 <i>SLIM-6-22</i>	UK-DMC <i>SLIM-6</i>	UK-DMC2 <i>SLIM-6-22</i>
NIR	1036	1048	1036
Red	1561	1564	1561
Green	1811	1841	1811

Table 18: $E_{0\lambda}$ for the Chance spectrum CHKUR (MODTRAN 4.0) model

Spectral Band	Exo-atmospheric Solar Irradiance [$\text{Wm}^{-2}\mu\text{m}^{-1}$]		
	Deimos-1 <i>SLIM-6-22</i>	UK-DMC <i>SLIM-6</i>	UK-DMC2 <i>SLIM-6-22</i>
NIR	1032	1042	1032
Red	1537	1546	1537
Green	1808	1811	1808

Table 19: $E_{0\lambda}$ for the Thuillier 2002 model

	DMC DATA PRODUCT MANUAL	DATE: 12-Feb-2010
		DOC NO: 0115056
		ISSUE: 02
		STATUS: FINAL

Equation 3 is just a conversion of the radiance at sensor into TOA reflectance. The actual TOA reflectance values are dependent, not just on the surface reflectance, but also on the atmospheric absorptions and scattering, which are not determined by this simple conversion.

An alternative to this simple calculation of reflectance is to use a radiative transfer code such as MODTRAN or 6S, which can assess scattering and absorption effects of the atmosphere and give true surface reflectance, rather than TOA reflectance.

13 DMC DIMAP

The metadata for L1R and L1T products are contained within the DIMAP (.dim) files. The DMC DIMAP is based upon the DIMAP generic profile version 1.1 developed by SpotImage and CNES, and is implemented through the use of XML.

Some elements of the DIMAP are not clearly defined and open for data providers to define their own parameters. For such elements used in the DMC DIMAP, a description of these elements and examples will be given in this section.

Appendix B and Appendix C contain a full DIMAP sample for the L1R and L1T products, respectively.

Documentation on DIMAP version 1.1 and the DIMAP XML implementation can be found at the following URL:

<http://www.spotimage.fr/dimap/spec/documentation/refdoc.htm>

The DIMAP elements and their implementation are described in documents RD#02 and RD#03, which can be found at the following URL:

<http://www.spotimage.fr/dimap/spec/dictionary/dictionary.htm>

	DMC DATA PRODUCT MANUAL	DATE: 12-Feb-2010
		DOC NO: 0115056
		ISSUE: 02
		STATUS: FINAL

<Quality_Assessment>

The following DIMAP elements and sub-elements have values and attributes that are unique to DMC data products. A full description of these elements and sub-elements and how they are implemented can be found in RD#02.

```

<Quality_Assessment>
  <QUALITY_TABLES>
    <Quality_Parameter>
      <QUALITY_PARAMETER_DESC>
      <QUALITY_PARAMETER_CODE>
      <QUALITY_PARAMETER_VALUE>

```

Details on the values and attributes of the elements and sub-elements that are unique to DMC data products can be found in the tables below.

Element	Element Value	Attribute	Attribute Value
<QUALITY_TABLES>	SPACEMETRIC	version	1.0
Description			
Quality assessment table labelled as "SPACEMETRIC" – version 1.0.			

Element	Element Value	Attribute	Attribute Value
<QUALITY_PARAMETER_DESC>	Number of control points	N/A	N/A
<QUALITY_PARAMETER_CODE>	SPACEMETRIC:NGCP	N/A	N/A
<QUALITY_PARAMETER_VALUE>	<i>variable</i>	N/A	N/A
Description			
Describes the number of GCPs collected to derive the model for the data product.			

	DMC DATA PRODUCT MANUAL	DATE: 12-Feb-2010
		DOC NO: 0115056
		ISSUE: 02
		STATUS: FINAL

Element	Element Value	Attribute	Attribute Value
<QUALITY_PARAMETER_DESC>	Root Mean Square residual error X component	N/A	N/A
<QUALITY_PARAMETER_CODE>	SPACEMETRIC:RMSX	N/A	N/A
<QUALITY_PARAMETER_VALUE>	<i>variable</i>	unit	<ul style="list-style-type: none"> • DEG • M

Description

Describes the RMS error in the x-direction of the data product. The units will depend upon the GCS and projection used.

"DEG" – Decimal Degrees
"M" – Metres

Typical units for DMC data products are decimal degrees for CS of type "GEOGRAPHIC" and metres for CS of type "PROJECTED", but others are available.

Element	Element Value	Attribute	Attribute Value
<QUALITY_PARAMETER_DESC>	Root Mean Square residual error Y component	N/A	N/A
<QUALITY_PARAMETER_CODE>	SPACEMETRIC:RMSY	N/A	N/A
<QUALITY_PARAMETER_VALUE>	<i>variable</i>	unit	<ul style="list-style-type: none"> • DEG • M

Description

Describes the RMS error in the y-direction of the data product. The units will depend upon the GCS and projection used.

"DEG" – Decimal Degrees
"M" – Metres

Typical units for DMC data products are decimal degrees for CS of type "GEOGRAPHIC" and metres for CS of type "PROJECTED", but others are available.

	DMC DATA PRODUCT MANUAL	DATE: 12-Feb-2010
		DOC NO: 0115056
		ISSUE: 02
		STATUS: FINAL

Element	Element Value	Attribute	Attribute Value
<QUALITY_PARAMETER_DESC>	Scene altitude (meter)	N/A	N/A
<QUALITY_PARAMETER_CODE>	SPACEMETRIC:ALTITUDE	N/A	N/A
<QUALITY_PARAMETER_VALUE>	<i>variable</i>	N/A	N/A

Description
Describes the altitude (in metres) of the satellite when the image was acquired.

Element	Element Value	Attribute	Attribute Value
<QUALITY_PARAMETER_DESC>	Sensor azimuth at scene center (deg)	N/A	N/A
<QUALITY_PARAMETER_CODE>	SPACEMETRIC:SENSOR_AZIMUTH	N/A	N/A
<QUALITY_PARAMETER_VALUE>	<i>variable</i>	N/A	N/A

Description
Describes the sensor azimuth (in decimal degrees) at scene centre.

Element	Element Value	Attribute	Attribute Value
<QUALITY_PARAMETER_DESC>	Sensor elevation at scene center (deg)	N/A	N/A
<QUALITY_PARAMETER_CODE>	SPACEMETRIC:SENSOR_ELEVATION	N/A	N/A
<QUALITY_PARAMETER_VALUE>	<i>variable</i>	N/A	N/A

Description
Describes the sensor elevation (in decimal degrees) at scene centre.

Example 1: <Quality_Assessment> - RMS Error in Metres

```

<Quality_Assessment>
  <QUALITY_TABLES version="1.0">SPACEMETRIC</QUALITY_TABLES>
  <Quality_Parameter>
    <QUALITY_PARAMETER_DESC>Number of control
points</QUALITY_PARAMETER_DESC>
    <QUALITY_PARAMETER_CODE>SPACEMETRIC:NGCP</QUALITY_PARAMETER_CODE>
    <QUALITY_PARAMETER_VALUE>28</QUALITY_PARAMETER_VALUE>
  </Quality_Parameter>
  <Quality_Parameter>
    <QUALITY_PARAMETER_DESC>Root Mean Square residual error X
component</QUALITY_PARAMETER_DESC>
    <QUALITY_PARAMETER_CODE>SPACEMETRIC:RMSX</QUALITY_PARAMETER_CODE>
    <QUALITY_PARAMETER_VALUE unit="M">13.2</QUALITY_PARAMETER_VALUE>
  </Quality_Parameter>
  <Quality_Parameter>
    <QUALITY_PARAMETER_DESC>Root Mean Square residual error Y
component</QUALITY_PARAMETER_DESC>
    <QUALITY_PARAMETER_CODE>SPACEMETRIC:RMSY</QUALITY_PARAMETER_CODE>
    <QUALITY_PARAMETER_VALUE unit="M">10.5</QUALITY_PARAMETER_VALUE>
  </Quality_Parameter>
</Quality_Assessment>

```

Example 2: <Quality_Assessment> - RMS Error in Decimal Degrees

```

<Quality_Assessment>
  <QUALITY_TABLES version="1.0">SPACEMETRIC</QUALITY_TABLES>
  <Quality_Parameter>
    <QUALITY_PARAMETER_DESC>Number of control
points</QUALITY_PARAMETER_DESC>
    <QUALITY_PARAMETER_CODE>SPACEMETRIC:NGCP</QUALITY_PARAMETER_CODE>
    <QUALITY_PARAMETER_VALUE>0</QUALITY_PARAMETER_VALUE>
  </Quality_Parameter>
  <Quality_Parameter>
    <QUALITY_PARAMETER_DESC>Root Mean Square residual error X
component</QUALITY_PARAMETER_DESC>
    <QUALITY_PARAMETER_CODE>SPACEMETRIC:RMSX</QUALITY_PARAMETER_CODE>
    <QUALITY_PARAMETER_VALUE
unit="DEG">0.28647889756541156</QUALITY_PARAMETER_VALUE>
  </Quality_Parameter>
  <Quality_Parameter>
    <QUALITY_PARAMETER_DESC>Root Mean Square residual error Y
component</QUALITY_PARAMETER_DESC>
    <QUALITY_PARAMETER_CODE>SPACEMETRIC:RMSY</QUALITY_PARAMETER_CODE>
    <QUALITY_PARAMETER_VALUE
unit="DEG">0.20970255301788127</QUALITY_PARAMETER_VALUE>
  </Quality_Parameter>
</Quality_Assessment>

```

<Coordinate_Reference_System>

The following DIMAP elements and sub-elements have values and attributes that are unique to DMC data products. A full description of these elements and sub-elements and how they are implemented can be found in RD#02.

```

<Coordinate_Reference_System>
  <GEO_TABLES>
    <Horizontal_CS>
      <HORIZONTAL_CS_CODE>
      <HORIZONTAL_CS_TYPE>
      <HORIZONTAL_CS_NAME>

```

Details on the values and attributes of the elements and sub-elements that are unique to DMC data products can be found in the tables below.

Element	Element Value	Attribute	Attribute Value
<GEO_TABLES>	<ul style="list-style-type: none"> EPSG CUSTOM 	version	<i>variable</i>
Description			
System used to identify the geodetic parameters.			
"EPSG" - parameters are defined in the EPSG database version 6.13.			
"CUSTOM" - user specified parameters.			

Element	Element Value	Attribute	Attribute Value
<HORIZONTAL_CS_CODE>	<i>variable</i>	N/A	N/A
Description			
Unique identification code that defines the horizontal CS used by the data product. This code relates to the geodetic table defined by the element <GEO_TABLES>. The code is variable, but it is prefixed by the geodetic table used followed by ":", i.e. "EPSG:4258" or "CUSTOM:50008".			
To avoid overlapping of the horizontal CS codes from the EPSG database, all CUSTOM horizontal CS codes (i.e. not defined in the EPSG database) will start at 50001.			

	DMC DATA PRODUCT MANUAL	DATE: 12-Feb-2010
		DOC NO: 0115056
		ISSUE: 02
		STATUS: FINAL

Element	Element Value	Attribute	Attribute Value
<HORIZONTAL_CS_TYPE>	<ul style="list-style-type: none"> GEOGRAPHIC PROJECTED 	N/A	N/A
Description			
<p>Describes the type of horizontal CS used.</p> <p>"GEOGRAPHIC" – Horizontal CS is not projected. "PROJECTED" – Horizontal CS is a cartographic projection.</p>			

Element	Element Value	Attribute	Attribute Value
<HORIZONTAL_CS_NAME>	<i>variable</i>	N/A	N/A
Description			
Name of the horizontal CS used by the data product.			

Example 3: <Coordinate_Reference_System> - EPSG Geodetic Parameters

```

<Coordinate_Reference_System>
  <GEO_TABLES>EPSG</GEO_TABLES>
  <Horizontal_CS>
    <HORIZONTAL_CS_CODE>EPSG:4258</HORIZONTAL_CS_CODE>
    <HORIZONTAL_CS_TYPE>GEOGRAPHIC</HORIZONTAL_CS_TYPE>
    <HORIZONTAL_CS_NAME>ETRS89</HORIZONTAL_CS_NAME>
    ...
  </Horizontal_CS>
</Coordinate_Reference_System>

```

Example 4: <Coordinate_Reference_System> - Custom Geodetic Parameters

```

<Coordinate_Reference_System>
  <GEO_TABLES>CUSTOM</GEO_TABLES>
  <Horizontal_CS>
    <HORIZONTAL_CS_CODE>CUSTOM:50008</HORIZONTAL_CS_CODE>
    <HORIZONTAL_CS_TYPE>PROJECTED</HORIZONTAL_CS_TYPE>
    <HORIZONTAL_CS_NAME>ED50 / Turkish Lambert 2007</HORIZONTAL_CS_NAME>
    ...
  </Horizontal_CS>
</Coordinate_Reference_System>

```

<Image_Display>

The following DIMAP elements and sub-elements have values and attributes that are unique to DMC data products. A full description of these elements and sub-elements and how they are implemented can be found in RD#02.

```

<Image_Display>
  <Special_Value>
    <SPECIAL_VALUE_INDEX>
    <SPECIAL_VALUE_TEXT>

```

Details on the values and attributes of the elements and sub-elements that are unique to DMC data products can be found in the tables below.

Element	Element Value	Attribute	Attribute Value
<SPECIAL_VALUE_INDEX>	0	N/A	N/A
<SPECIAL_VALUE_TEXT>	nodata	N/A	N/A
Description			
Data points in the product that have a DN value of 0 are described as being data points of no significance and should be ignored in any analysis performed.			

Example 5: <Image_Display> - No Data Value

```

<Image_Display>
  ...
  <Special_Value>
    <SPECIAL_VALUE_INDEX>0</SPECIAL_VALUE_INDEX>
    <SPECIAL_VALUE_TEXT>nodata</SPECIAL_VALUE_TEXT>
  </Special_Value>
  ...
</Image_Display>

```

	DMC DATA PRODUCT MANUAL	DATE: 12-Feb-2010
		DOC NO: 0115056
		ISSUE: 02
		STATUS: FINAL

<Dataset_Sources>

Due to the nature of the DIMAP format, there is the potential for data to be duplicated under different elements. In the case of the <Dataset_Sources> element there is a sub-element called <Coordinate_Reference_System>, which contains the same information as the <Coordinate_Reference_System> element that preceded it. Information about this element has been documented for completeness.

The following DIMAP elements and sub-elements have values and attributes that are unique to DMC data products. A full description of these elements and sub-elements and how they are implemented can be found in RD#02.

```

<Dataset_Sources>
  <Coordinate_Reference_System>
    <GEO_TABLES>
      <Horizontal_CS>
        <HORIZONTAL_CS_CODE>
        <HORIZONTAL_CS_TYPE>
        <HORIZONTAL_CS_NAME>

```

Details on the values and attributes of the elements and sub-elements that are unique to DMC data products can be found in the tables below.

Element	Element Value	Attribute	Attribute Value
<GEO_TABLES>	<ul style="list-style-type: none"> • EPSG • CUSTOM 	version	<i>variable</i>
Description			
System used to identify the geodetic parameters.			
"EPSG" - parameters are defined in the EPSG database version 6.13.			
"CUSTOM" - user specified parameters.			

Element	Element Value	Attribute	Attribute Value
<HORIZONTAL_CS_CODE>	<i>variable</i>	N/A	N/A
Description			
Unique identification code that defines the horizontal CS used by the data product. This code relates to the geodetic table defined by the element <GEO_TABLES>. The code is variable, but it is prefixed by the geodetic table used followed by ":", i.e. "EPSG:4258" or "CUSTOM:50008".			
To avoid overlapping of the horizontal CS codes from the EPSG database, all CUSTOM horizontal CS codes (i.e. not defined in the EPSG database) will start at 50001.			

	DMC DATA PRODUCT MANUAL	DATE: 12-Feb-2010
		DOC NO: 0115056
		ISSUE: 02
		STATUS: FINAL

Element	Element Value	Attribute	Attribute Value
<HORIZONTAL_CS_TYPE>	<ul style="list-style-type: none"> GEOGRAPHIC PROJECTED 	N/A	N/A
Description			
<p>Describes the type of horizontal CS used.</p> <p>"GEOGRAPHIC" – Horizontal CS is not projected. "PROJECTED" – Horizontal CS is a cartographic projection.</p>			

Element	Element Value	Attribute	Attribute Value
<HORIZONTAL_CS_NAME>	<i>variable</i>	N/A	N/A
Description			
Name of the horizontal CS used by the data product.			

Example 6: <Dataset_Sources> - EPSG Geodetic Parameters

```

<Dataset_Sources>
  ...
  <Coordinate_Reference_System>
    <GEO_TABLES>EPSG</GEO_TABLES>
    <Horizontal_CS>
      <HORIZONTAL_CS_CODE>EPSG:4258</HORIZONTAL_CS_CODE>
      <HORIZONTAL_CS_TYPE>GEOGRAPHIC</HORIZONTAL_CS_TYPE>
      <HORIZONTAL_CS_NAME>ETRS89</HORIZONTAL_CS_NAME>
      ...
    </Horizontal_CS>
  </Coordinate_Reference_System>
  ...
</Dataset_Sources>

```

Example 7: <Dataset_Sources> - Custom Geodetic Parameters

```

<Dataset_Sources>
  ...
  <Coordinate_Reference_System>
    <GEO_TABLES>CUSTOM</GEO_TABLES>
    <Horizontal_CS>
      <HORIZONTAL_CS_CODE>CUSTOM:50008</HORIZONTAL_CS_CODE>
      <HORIZONTAL_CS_TYPE>PROJECTED</HORIZONTAL_CS_TYPE>
      <HORIZONTAL_CS_NAME>ED50 / Turkish Lambert
      2007</HORIZONTAL_CS_NAME>
      ...
    </Horizontal_CS>
  </Coordinate_Reference_System>
  ...
</Dataset_Sources>

```

	DMC DATA PRODUCT MANUAL	DATE: 12-Feb-2010
		DOC NO: 0115056
		ISSUE: 02
		STATUS: FINAL

14 IMAGE PROCESSING

The raw images acquired by the DMC satellites undergo various processing stages to reach their final deliverable product. The generation of each product level is performed by various software applications at different stages of the process. The image processing chain implemented is displayed in Figure 6 and the software responsible at each stage of the process is shown in Figure 7.

14.1 Radiometric Correction

The radiometric correction is performed by applying a LUT to the image. This allows each pixel to be corrected individually, based upon the detector that captured it. The LUT is generated based on calibration images collected over the test site in Rail Road Valley, Nevada, USA.

This correction converts the raw image from an 8-bit DN image to a 32-bit radiance image. In order to keep the image file size low, the radiance image is then scaled back to an 8-bit DN image. However, the image is scaled to the range of DN=1 to DN=254. Pixels with DN=0 are special value pixels representing pixels of no data and can be ignored during analysis.

The scaling coefficients are preserved in the metadata for the product and converting the DN image back to a radiance image is a simple task described in §10.

The radiometric correction process is performed by the Smart-i radiometric processor and the output from this process is the LOR product.

A full report on the radiometric calibration of the DMC satellites can be found in Appendix D.

14.2 Georeferencing

The georeferencing process uses tie-point transformation to generate a model to apply to the final L1R product. The model is generated based upon the attitude and ephemeris data stored in the metadata of the LOR product.

The GCS used for the final L1R product is the WGS84 (EPSG:4326).

The georeferencing process is performed during the import of the LOR product files, before the band registration process.

14.3 Band Registration

The band registration process is performed on the single band LOR products output from the radiometric correction process. The three spectral bands from one imager bank are co-registered to provide a 3-band RGB image.

	DMC DATA PRODUCT MANUAL	DATE: 12-Feb-2010
		DOC NO: 0115056
		ISSUE: 02
		STATUS: FINAL

Geometric correction is also performed during this stage of the processing to remove the following sources of geometric distortion from the image:

- Sensor Geometry
- Lens Distortion
- Curvature of the Earth
- Rotation of the Earth
- Spacecraft Attitude
- Spacecraft Motion

If the image was acquired as a single bank image event, then the process for the L1R product ends here. If the image was acquired as a dual bank image event, then the two single bank L1R products are passed on to the bank mosaic processing stage.

The band registration process is performed by Keystone and the output from this process is the L1R product for a single bank image event.

14.4 Bank Mosaic

The bank mosaic process is performed on the single bank L1R products output from the band registration process. The two single bank images are mosaiced together at the point of overlap between the two images.

The bank mosaic process is performed by Keystone and the output from this process is the L1R product for a dual bank image event.

14.5 Orthorectification

The orthorectification process is a two stage process; GCP collection and image rectification.

The first stage involves manual GCP collection against a standard reference data set and DEM using an application called Keystone Workstation. Each GCP updates the georeferencing of the L1R product and includes the height information from the DEM, thus correcting image distortions due to the Earth's topography. The output from the GCP collection is a rigorous image model to pass on to the next stage of the process.

The second and final stage of the process is image rectification. This process is performed by Keystone, which rectifies the L1R product using the updated image model produced in the first stage.

The final output from the orthorectification process is the L1T product rectified to the defined projection.

The orthorectification process is a flexible process whereby GCP collection can be performed using any reference data set and DEM provided, and the final L1T product can be rectified to any projection requested.

A full description of the orthorectification procedure can be found in Appendix E.

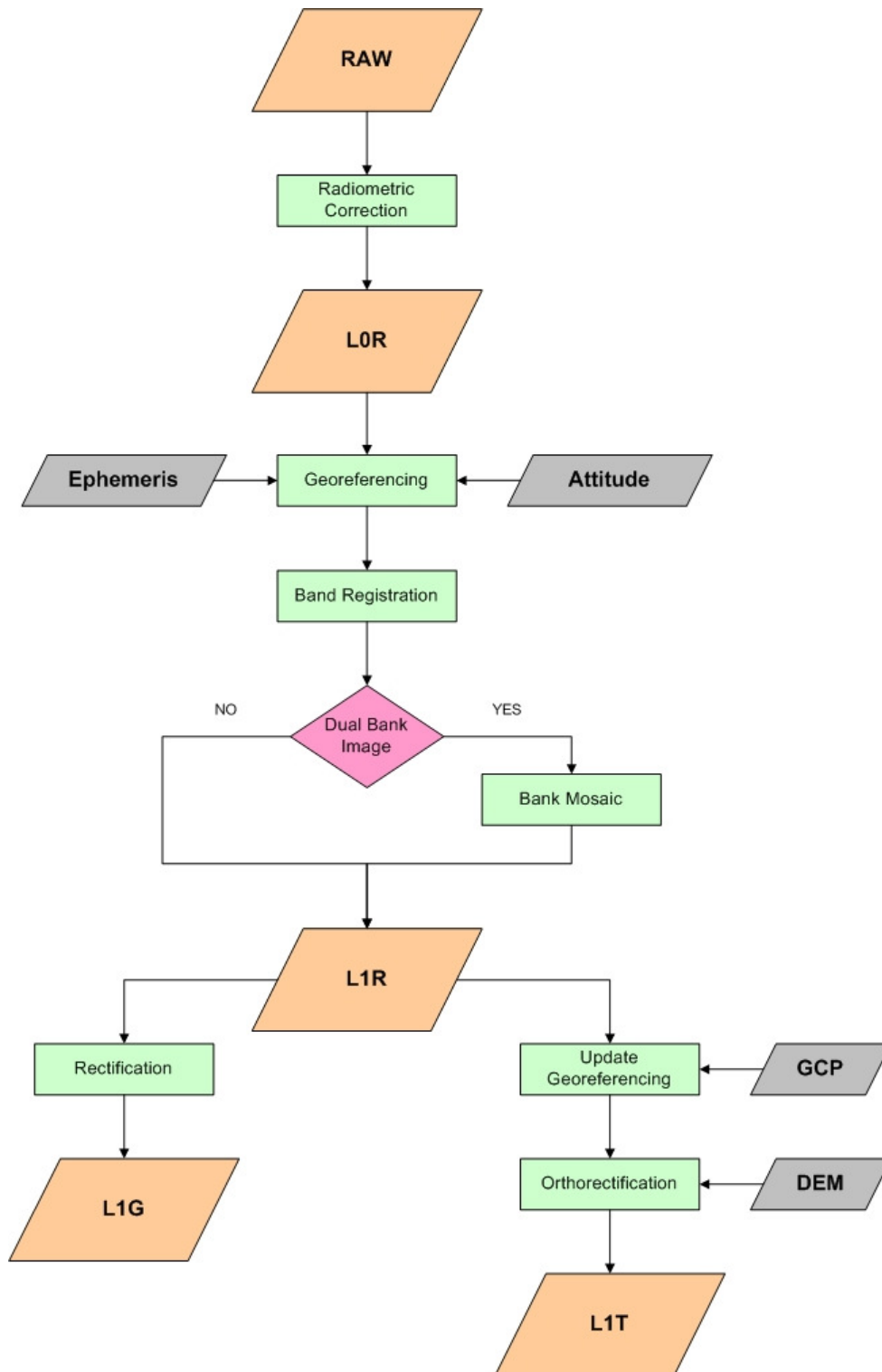


Figure 6: Image processing chain

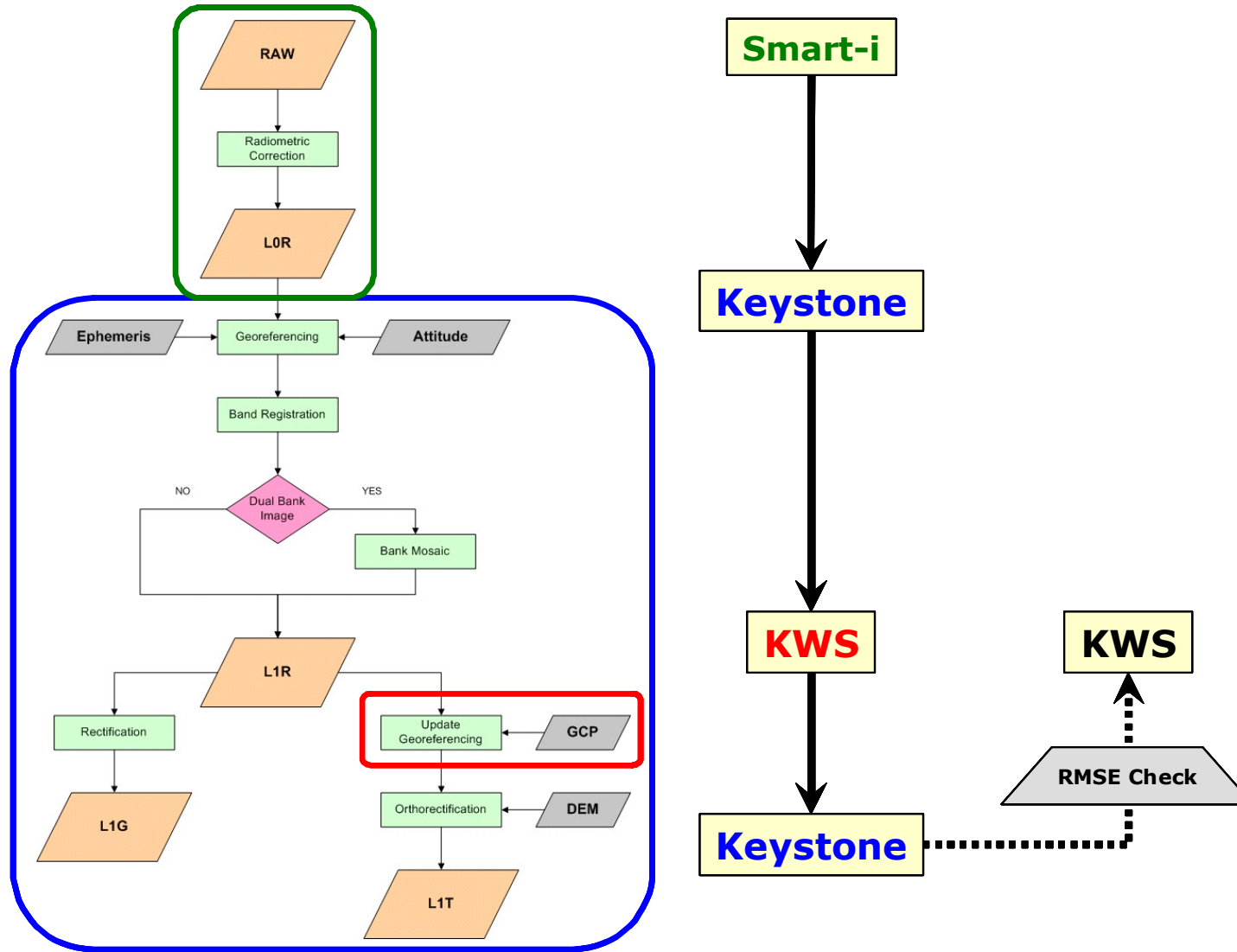


Figure 7: Software used in the processing chain

	DMC DATA PRODUCT MANUAL	DATE: 12-Feb-2010
		DOC NO: 0115056
		ISSUE: 02
		STATUS: FINAL

15 FILENAME FORMAT

The products derived from DMC images of a nominal size, will assume the filename convention specified in §15.1 and §15.2. However, due to the imaging capabilities of Beijing-1, Deimos-1 and UK-DMC2, the filename convention for long strip images will assume the format described in §15.3 and §15.4.

A full description of the parameters used in each filename convention can found in Table 20.

15.1 L1R and L1T Products

The filename convention for L1R and L1T products will assume the general format:

sseeeeeeb_p.ext

Example:

DA000123p_L1R.tif
 DN0004d8s_L1T.tif
 DU00010cT_L1R.tif
 DU00010cT_L1T.tif

15.2 L0R Products

The filename convention for L0R products will assume the general format:

sseeeeeebc_p.ext

Example:

DU00010cp0_L0R.tif
 DU00010cp1_L0R.tif
 DU00010cp2_L0R.tif
 DU00010cs0_L0R.tif
 DU00010cs1_L0R.tif
 DU00010cs2_L0R.tif

	DMC DATA PRODUCT MANUAL	DATE: 12-Feb-2010
		DOC NO: 0115056
		ISSUE: 02
		STATUS: FINAL

15.3 Framed L1R and L1T Products

For long image strips acquired by Beijing-1, Deimos-1 and UK-DMC2, the filename convention for L1R and L1T products will assume the general format:

sseeeee SL_EL_b_p.ext

Example:

```
DC000610_000000_010499_p_L1R.tif
DC000610_000000_010499_s_L1R.tif
DC000610_010000_020499_p_L1T.tif
DC000610_010000_020499_s_L1T.tif
```

15.4 Framed L0R Products

For long image strips acquired by Beijing-1, Deimos-1 and UK-DMC2, the filename convention for L0R products will assume the general format:

sseeeee SL_EL_bc_p.ext

Example:

```
DC000610_000000_010499_p0_L0R.tif
DC000610_000000_010499_p1_L0R.tif
DC000610_000000_010499_p2_L0R.tif
DC000610_000000_010499_s0_L0R.tif
DC000610_000000_010499_s1_L0R.tif
DC000610_000000_010499_s2_L0R.tif
DC000610_010000_020499_p0_L0R.tif
DC000610_010000_020499_p1_L0R.tif
DC000610_010000_020499_p2_L0R.tif
DC000610_010000_020499_s0_L0R.tif
DC000610_010000_020499_s1_L0R.tif
DC000610_010000_020499_s2_L0R.tif
```

	DMC DATA PRODUCT MANUAL	DATE: 12-Feb-2010
		DOC NO: 0115056
		ISSUE: 02
		STATUS: FINAL

Parameter	Description	Value
ss	Satellite Name	DA AlSat-1 DC Beijing-1 DE Deimos-1 DN NigeriaSat-1 DU UK-DMC U2 UK-DMC2
eeeeee	Event ID Number	Unique 6 digit hexadecimal value
SL	Scene Start Line Number	6 digit scene start line number
EL	Scene End Line Number	6 digit scene end line number
b	Imager Bank	p Primary imager bank s Secondary imager bank T Two imager banks mosaiced
c	Imager Spectral Channel	0 NIR spectral channel 1 Red spectral channel 2 Green spectral channel
p	Product Level	L0R As described in Table 1 L1R As described in Table 1 L1T As described in Table 1
ext	File Extension	tif TIFF / GeoTIFF image file format

Table 20: Filename convention parameter description

16 SPECIAL NOTES ON DMC DATA

16.1 DN Range and Special DN Values

During the radiometric correction of an image, there is a scaling process that scales all pixels containing valid image data to the range DN=1-254, whereas pixels containing no data are set to DN=0.

16.2 Holes

Holes are lost data packets that are caused by interference during data downlink. Figure 8 shows the artefacts seen in a DMC image where holes are present.

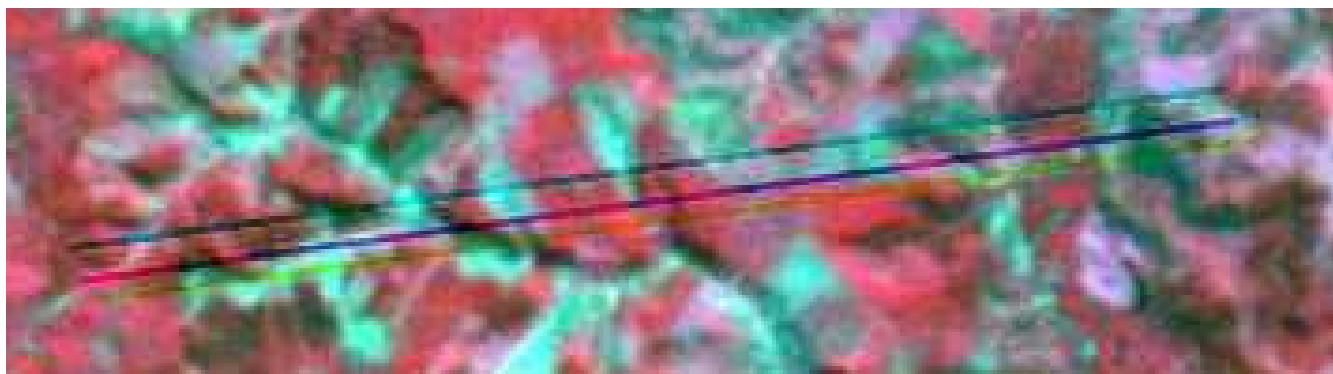


Figure 8: Image artefacts due to holes

To prevent holes in an image, the DMC groundstations implement a system that detects the lost data packets and subsequently sends a request to the satellite to transmit the lost data packet again. Because of this system, it is very rare for a DMC image to contain holes.

The holes exhibit themselves in an image as pixels of no data, i.e. DN=0, and can be present in any or all bands at any point within the image.

For example, from the illustration in Figure 9, holes may occur at one or many points in the image and only occur in the NIR band, in which case only the NIR band will show these pixels as being DN=0; the red and green bands will still contain valid data at these points.

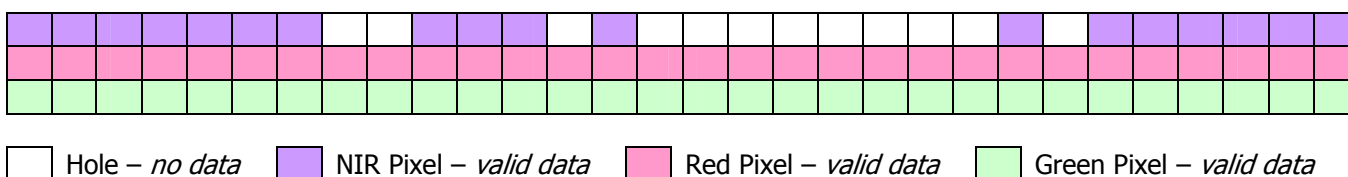
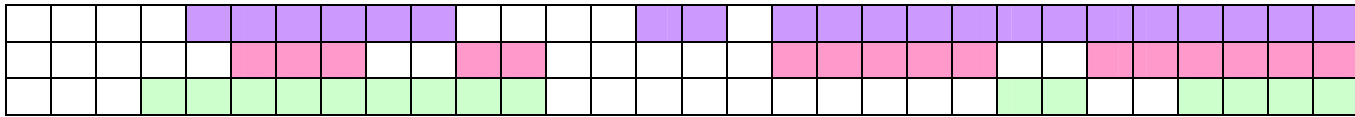


Figure 9: Holes in one band

Another example could be where holes are present at one or many points in the image and occur in all three bands, so all three bands will show these pixels as being DN=0, as illustrated in Figure 10.



Hole – *no data*
 NIR Pixel – *valid data*
 Red Pixel – *valid data*
 Green Pixel – *valid data*

Figure 10: Holes in all bands

16.3 Band Fringes

Fringes occur in all DMC products and are the result of the realignment of the spectral channels in the imager bank during the band registration process. These fringes are visible at the edges of the image and appear as colour bands, as shown in Figure 11.

Due to the physical nature of the SLIM-6 class imager (see §8), each spectral channel effectively points to slightly different locations on the ground. During the band registration process, the spectral bands are realigned to produce the 3-band multispectral image. Fringes occur in the areas where the rows and columns of the spectral bands do not overlap or partially overlap.

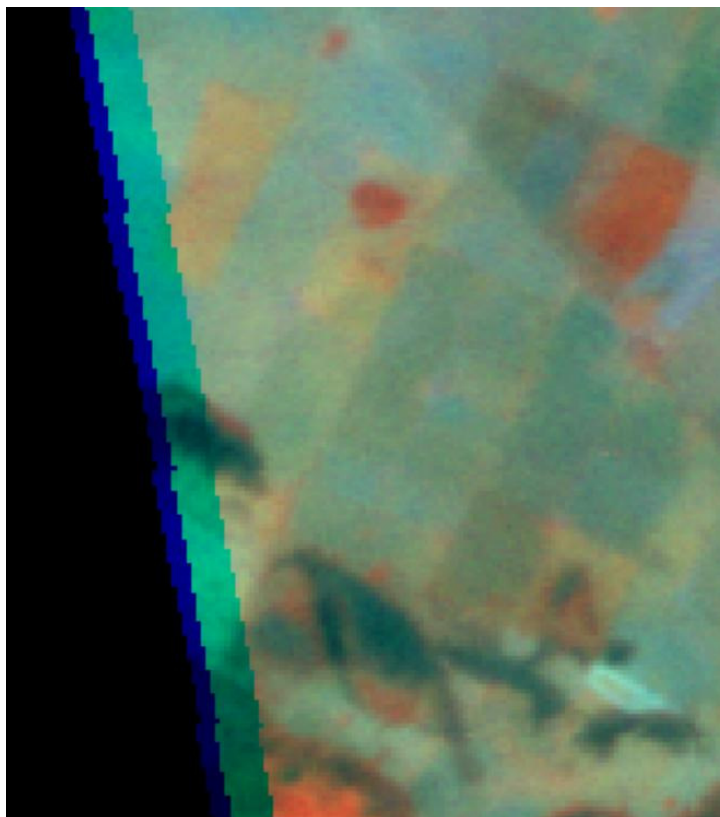


Figure 11: Fringes along the edge of a DMC image

16.4 Bank Shift

The bank shift occurs in all dual bank images and is exhibited as a vertical step in the image, which is visible along the top and bottom edges of the image, as shown in Figure 12.

Apart from the differences noted between the spectral channels, there is also a difference in the alignment between the two banks of the SLIM-6 class imagers described in §8. During the bank mosaic process, the single bank images are shifted and the overlapping pixels from each image are removed to produce a seamless mosaic.

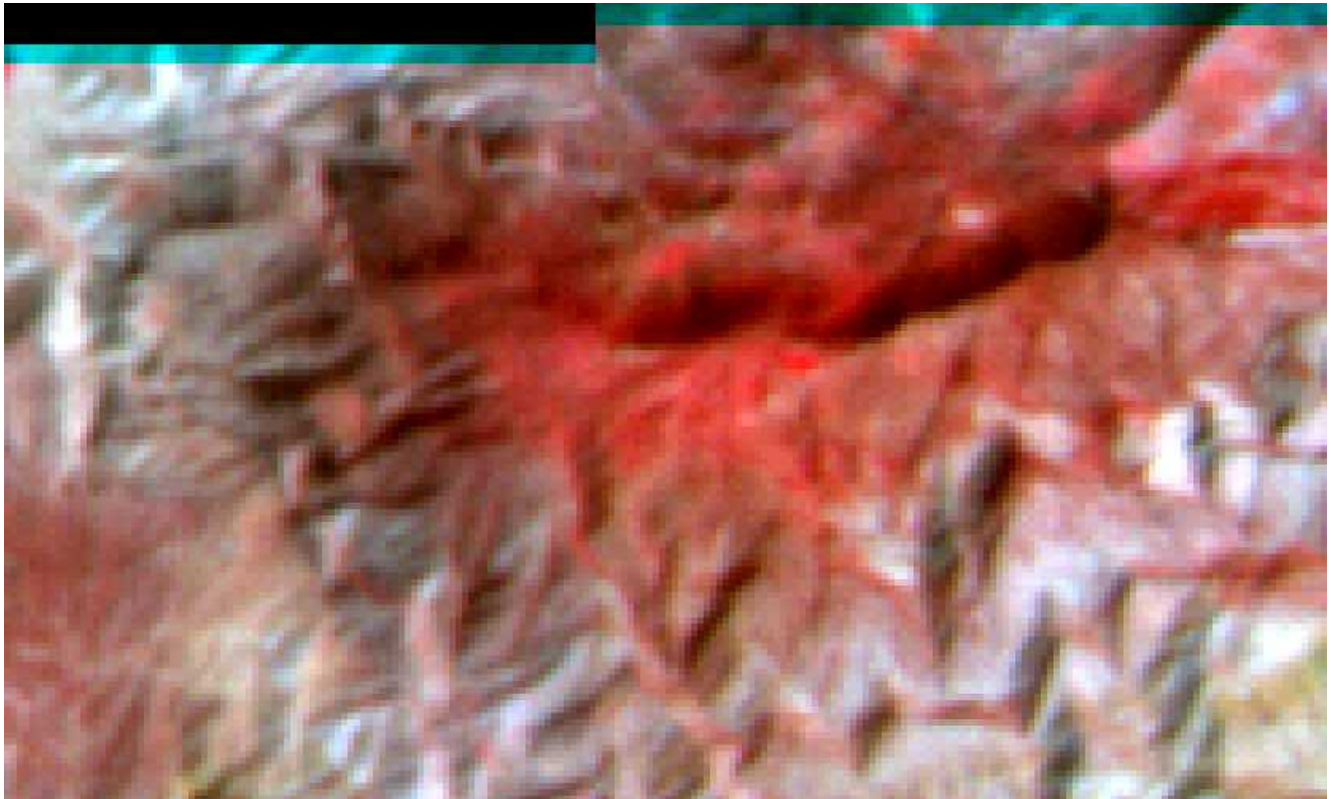


Figure 12: Bank shift across the top of a dual bank DMC image

	DMC DATA PRODUCT MANUAL	DATE: 12-Feb-2010
		DOC NO: 0115056
		ISSUE: 02
		STATUS: FINAL

17 FREQUENTLY ASKED QUESTIONS

17.1 Radiometry

What is the radiometric resolution of the data product?

Although 11 bits of data are captured in the initial data collection, only the most significant 8 bits are stored on-board and sent to the ground.

What are the units of the data product?

The data is scaled radiance with units $Wm^{-2}sr^{-1}\mu m^{-1}$. There is a scaling gain and scaling bias to apply to convert the data back into radiance, also with units $Wm^{-2}sr^{-1}\mu m^{-1}$.

The image data is scaled to fit inside a byte value, while maximising the amount of information

How accurate are the radiance values given in the data product?

The instrument is calibrated in a vicarious calibration campaign over the Railroad Valley site in Nevada, USA. The field measurements and radiance calculation is performed by the world renowned Remote Sensing Group at The University of Arizona (RSG) under Kurt Thome. The estimated accuracy given by RSG is 3-5% for the radiance calculation.

Given that only a limited number of pixels are used in the calculation, we have increased this estimate to 5-7% to cover the increased standard deviation in the estimate based on the noise in the data for the limited number of pixels used.

The absolute calibration is transferred from the few pixels calibrated to the whole array using a site at DOME-C in Antarctica.

How are cross-track illumination differences and BRDF dealt with over the calibration sites?

For the absolute site, only a few pixels are chosen to derive calibration coefficients. Pixels chosen are close to nadir to minimise BRDF effects.

For the transfer calibration in Antarctica the spacecraft is yawed prior to scene acquisition so that the imaging plane is orthogonal to the principal plane to the sun, giving equal illumination across the swath and minimising BRDF effects.

The band to band radiometry varies from scene to scene!

For any single satellite the band to band radiometry has proven to be very stable (RMS error of less than 0.34% over a three year period). However between satellites, variations of a few percent are possible due to differences in the absolute calibration of any specific satellite.

The more likely problem is that the user is looking at scaled radiances (the scaling is band and image content dependent). Convert the images to radiance using the scaling gain and bias before carrying out the comparison.

Is the data atmospherically corrected?

No. However, using a radiative transfer code and atmospheric measurements it is possible to convert the radiance (after applying the scaling gain and bias correction) to reflectance.

Is it possible to get the Quantum Efficiency (QE) of the CCD detectors?

The manufacturer’s nominal QE curve for the Eastman Kodak KL10203 Linear CCD array is given in Figure 13.

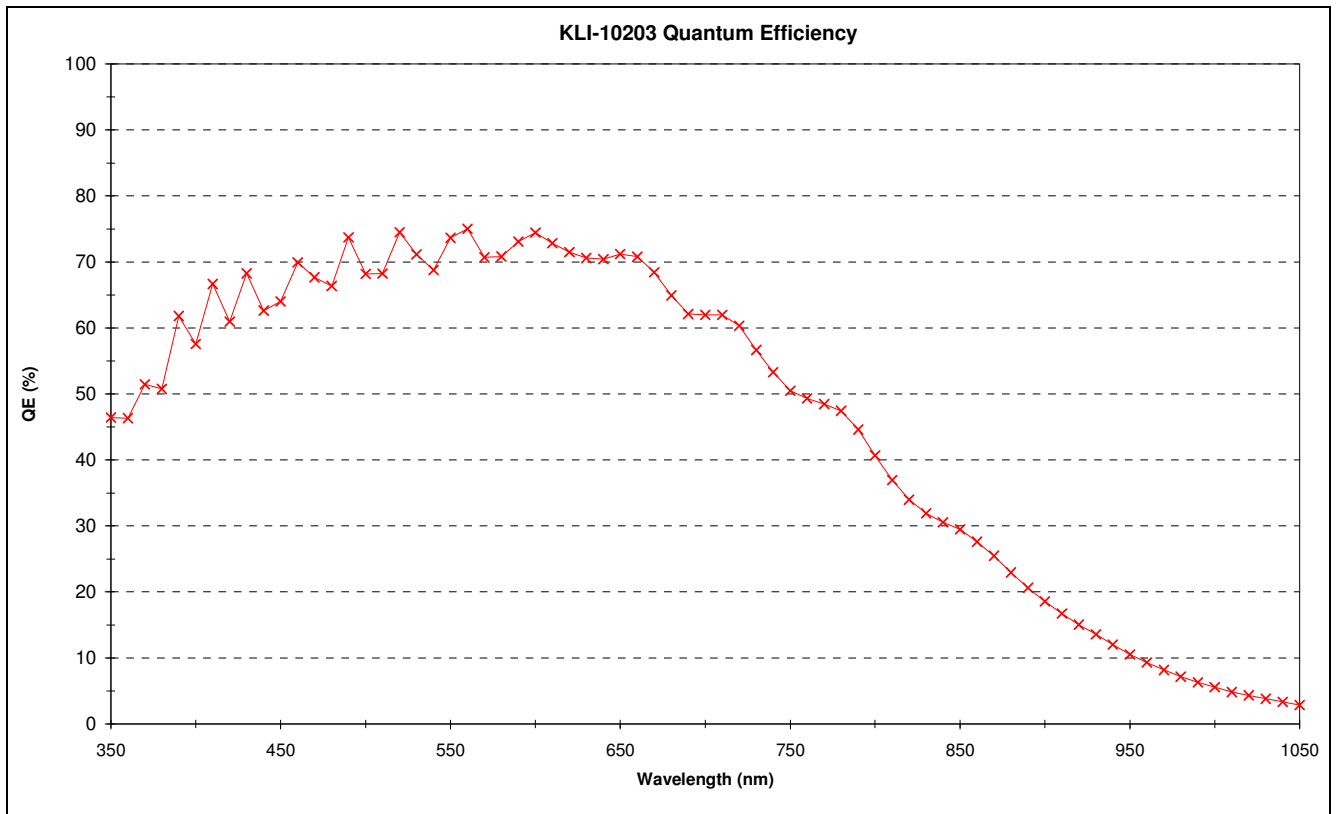


Figure 13: KLI-10203 Quantum Efficiency Curve

	DMC DATA PRODUCT MANUAL	DATE: 12-Feb-2010
		DOC NO: 0115056
		ISSUE: 02
		STATUS: FINAL

17.2 Geometry

How accurate is the band registration?

The band registration has sub-pixel accuracy, usually around 0.3 of a pixel.

How accurate is the orthorectified product?

During orthorectification, an RMS error of 0.25 of a pixel can be achieved. However, typically the RMS error is of the order of 0.5 to 0.75 of a pixel.

What map projection is used for the orthorectified image?

The image projection and EPSG code are defined in the metadata for that product. See §11 for more details. The LOR product levels are not projected.

There seem to be errors in parts of the image after the orthorectification process!

The GCPs in the orthorectification process should produce reasonable RMS errors across the scene, unless there was a significant high frequency oscillation of the spacecraft. This is very unlikely, as if this was the case, systematic biases in the errors across the scene would be noted during the orthorectification process.

17.3 Data Quality

There are some vertical striping in the imagery, is there a fault with the calibration?

Some vertical striping can be seen when the image has a small dynamic range, especially over homogeneous targets where the target DN range is very low. The small noise element caused by a separation in the odd and even detector response can produce small but noticeable effects.

What is the SNR of the DMC imagers?

For a nominal vegetated scene at mid-latitude summer the SNRs for all three bands approach 100:1, with the green spectral band having the highest SNR.

What is the NEAL of the DMC imagers?

The NEAL values for DMC have been measured for all three spectral bands and compared to the equivalent Landsat bands. The NEAL values for DMC are given in Table 21 and the values for Landsat are given in Table 22.

Band	DMC
0	0.85
1	0.87
2	0.77

Table 21: DMC NEAL values

Band	Landsat-5 TM	Landsat-7ETM+ High Gain
1	0.7	0.90
2	0.6	0.69
3	0.7	0.75
4	0.4	0.37
5	0.1	0.10
7	0.06	0.056
8 (pan)	N/A	1.4

Table 22: Landsat band-averaged dark-noise levels NEAL

The calculation used to determine the NEAL is given in RD#05.

	DMC DATA PRODUCT MANUAL	DATE: 12-Feb-2010
		DOC NO: 0115056
		ISSUE: 02
		STATUS: FINAL

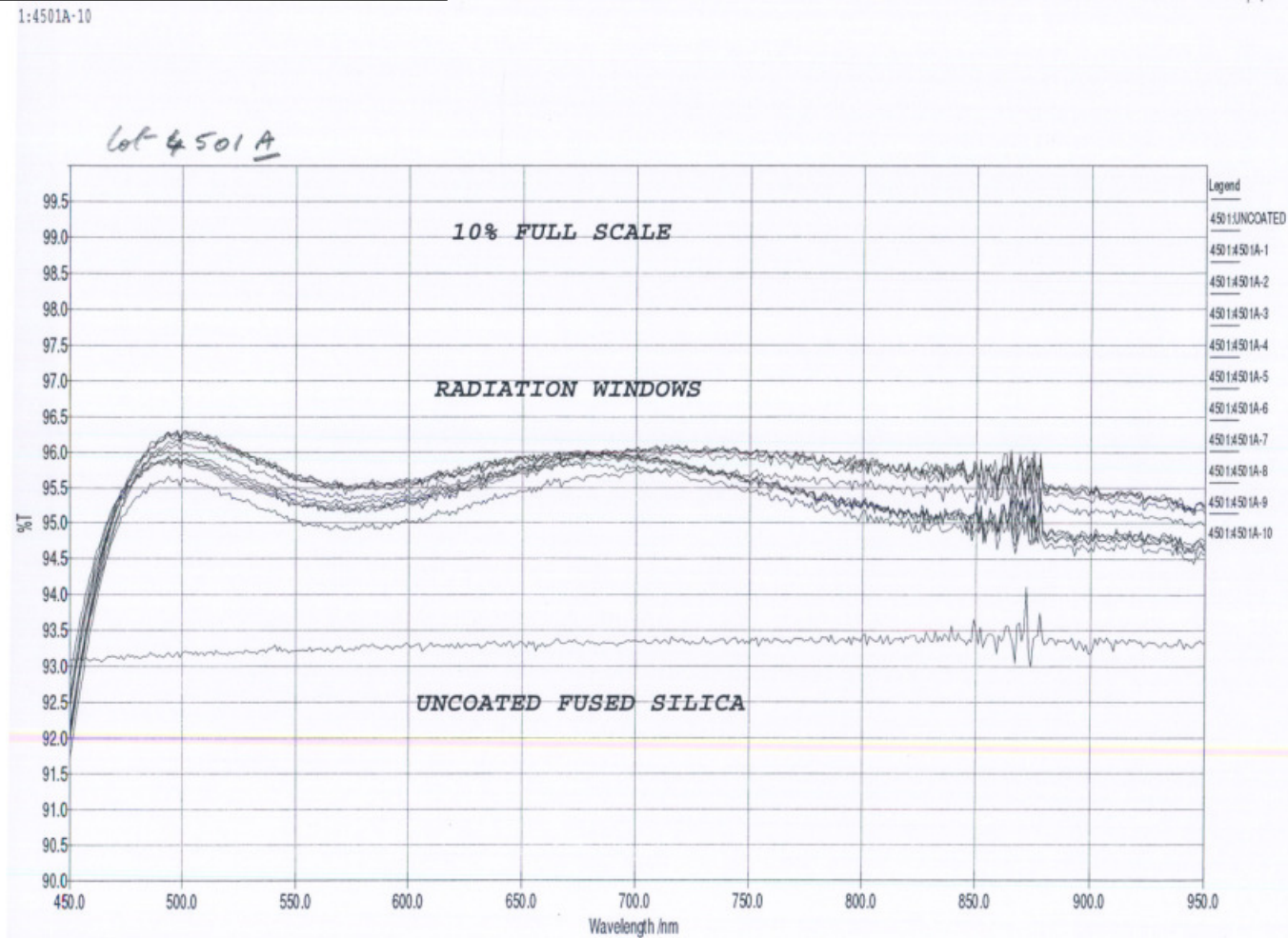
APPENDIX A: SPECTRAL TRANSMISSION PROFILES

The following plots show the spectral transmission profiles for the fused silica radiation absorption windows and the spectral band filters on the DMC spacecraft.

The level of information captured in these plots, although limited, should be enough to perform a spectral analysis.

These plots were provided by Barr Associates Inc., USA in a hard copy format only, so electronic versions detailing each point on these plots are not available. These plots were scanned for the purposes of this document.

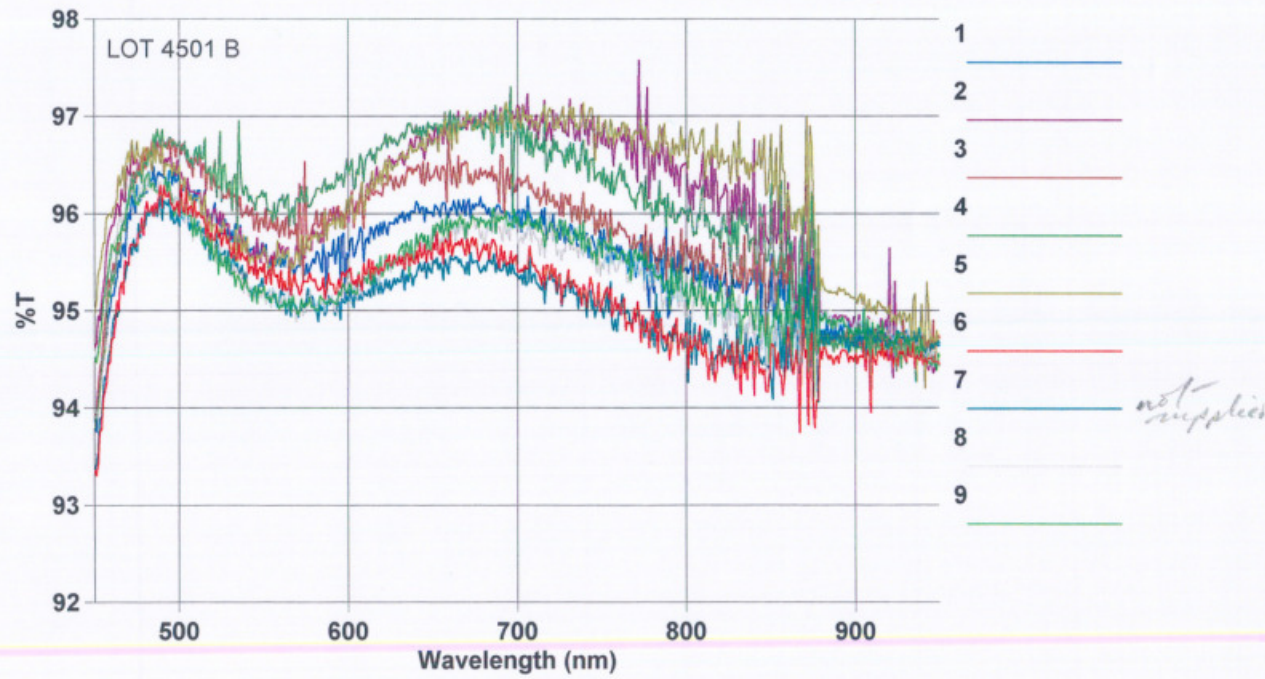
Fused Silica Radiation Absorption Windows



Fused Silica Radiation Absorption Windows

11/9/01 12:02:49 PM

Page 1 of 1

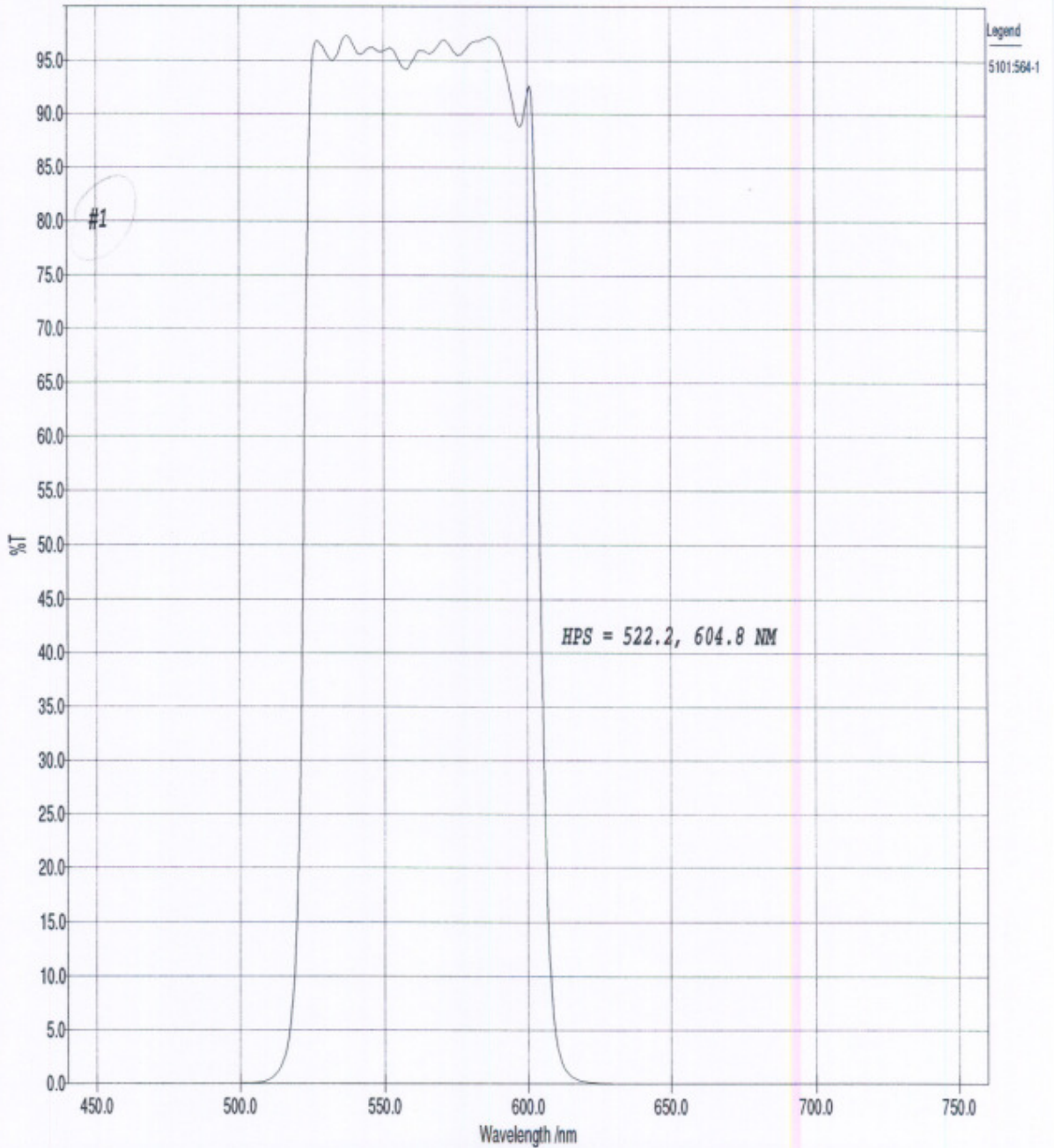


CARY 500 Spectrophotometer

AlSat-1 Green Spectral Transmission Profile

5101:564-1

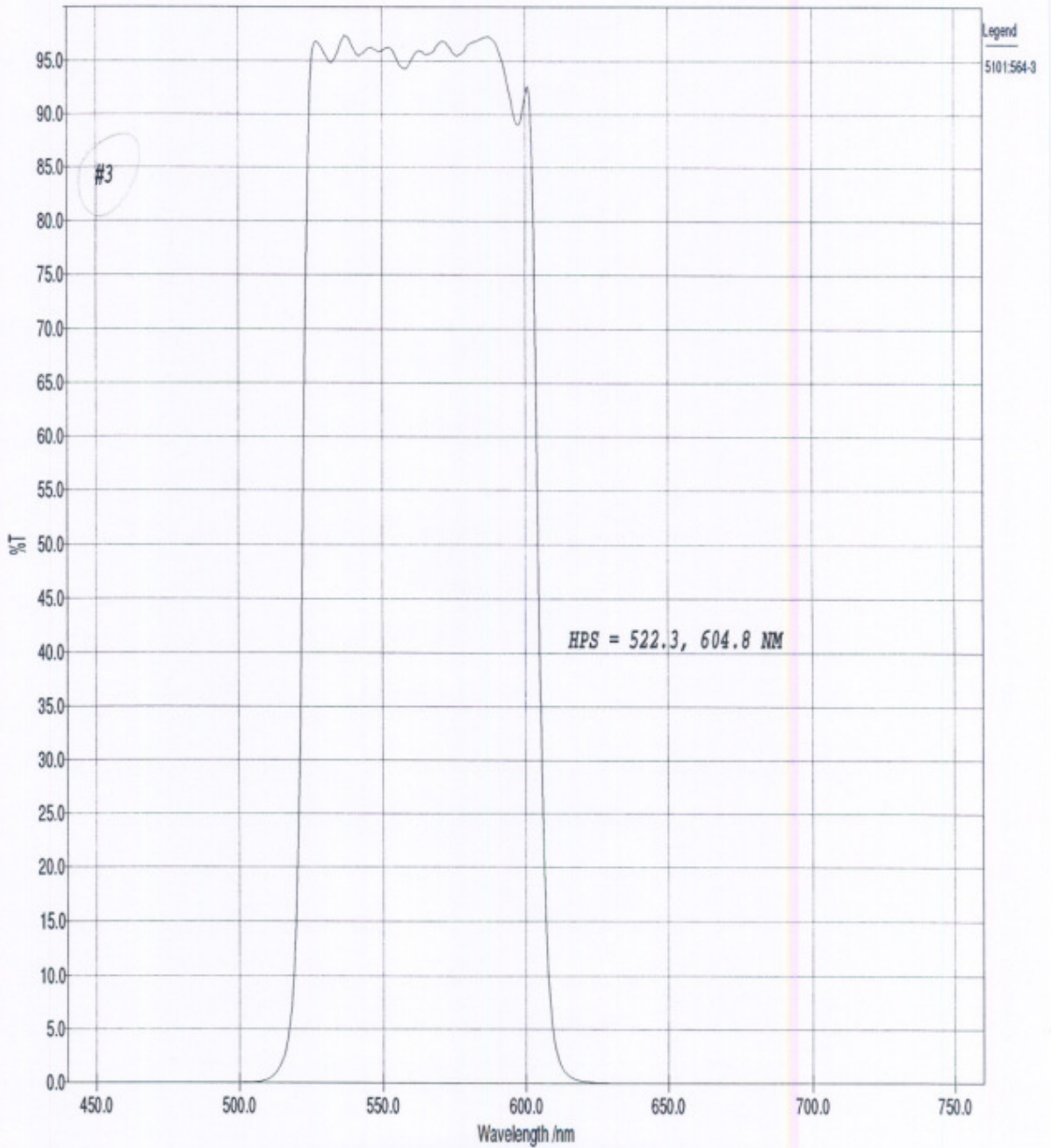
93



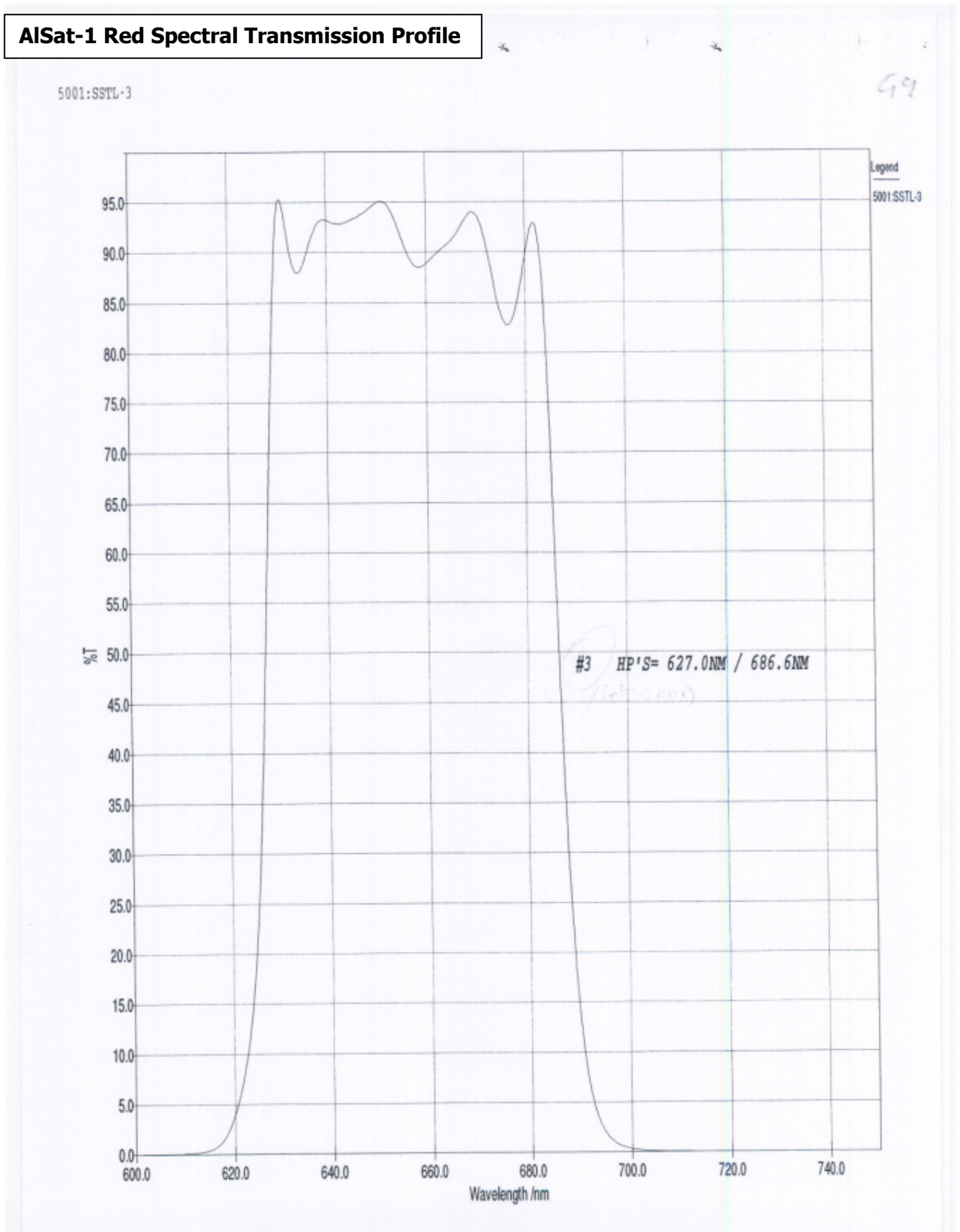
AlSat-1 Green Spectral Transmission Profile

5101:564-3

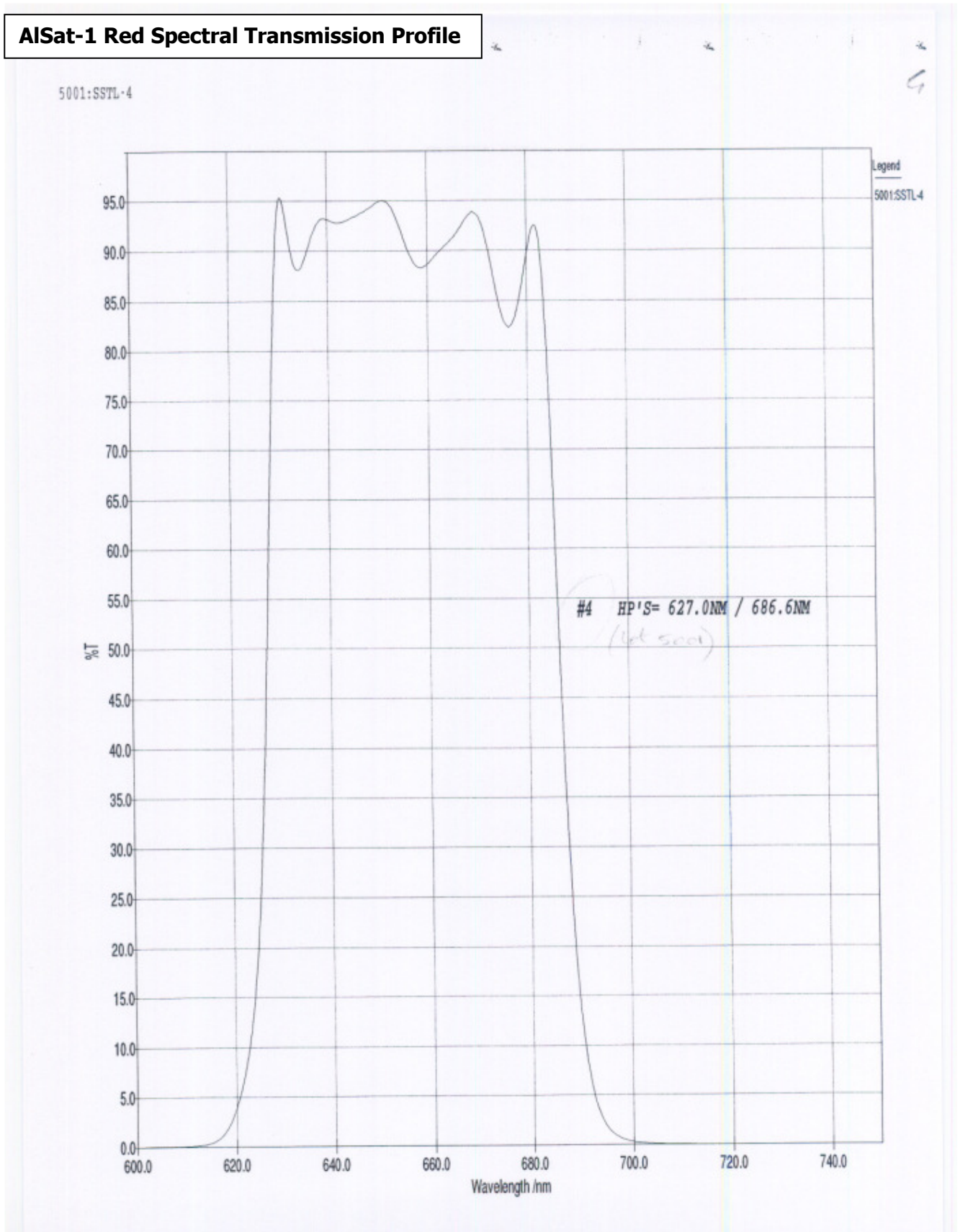
94



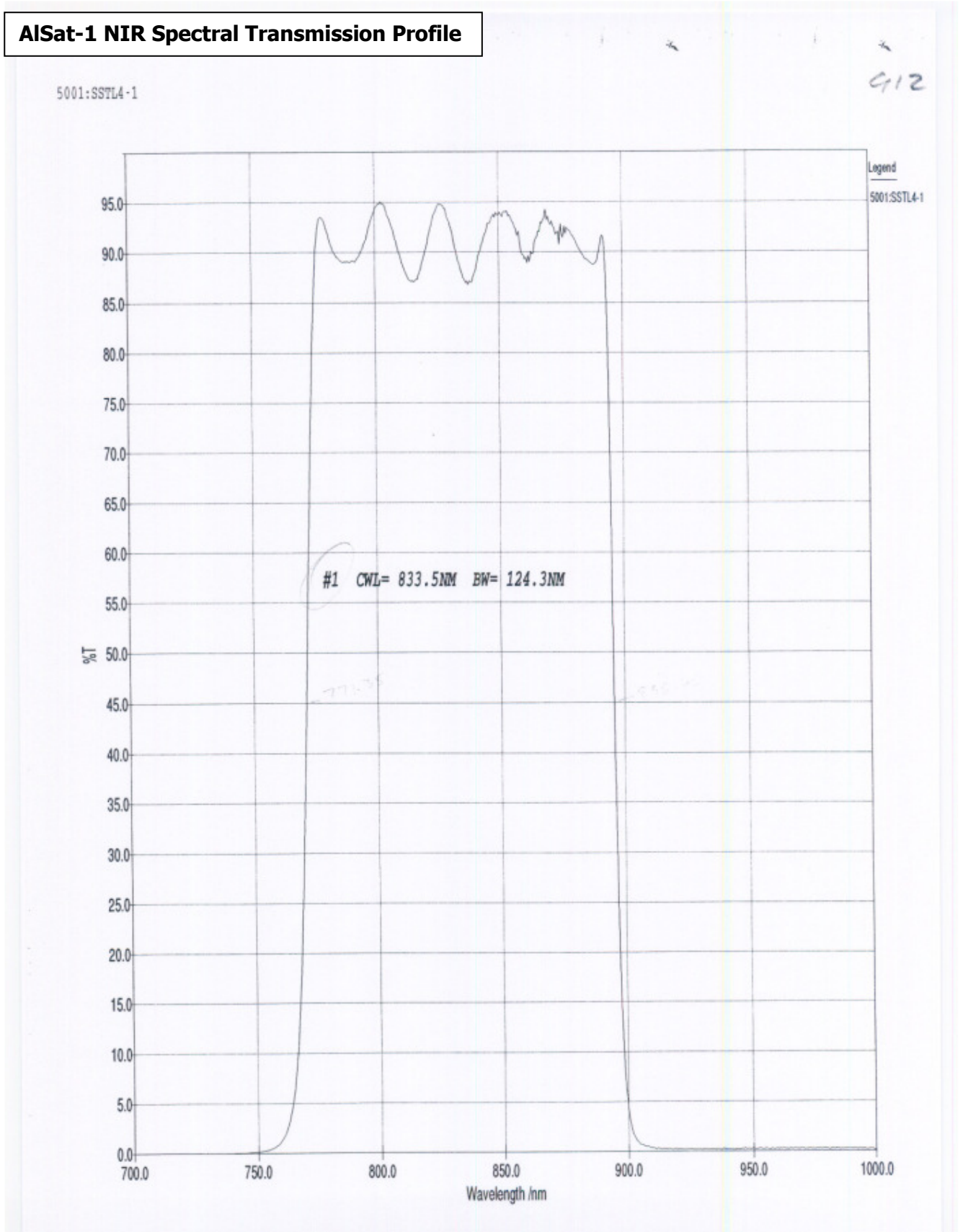
AlSat-1 Red Spectral Transmission Profile



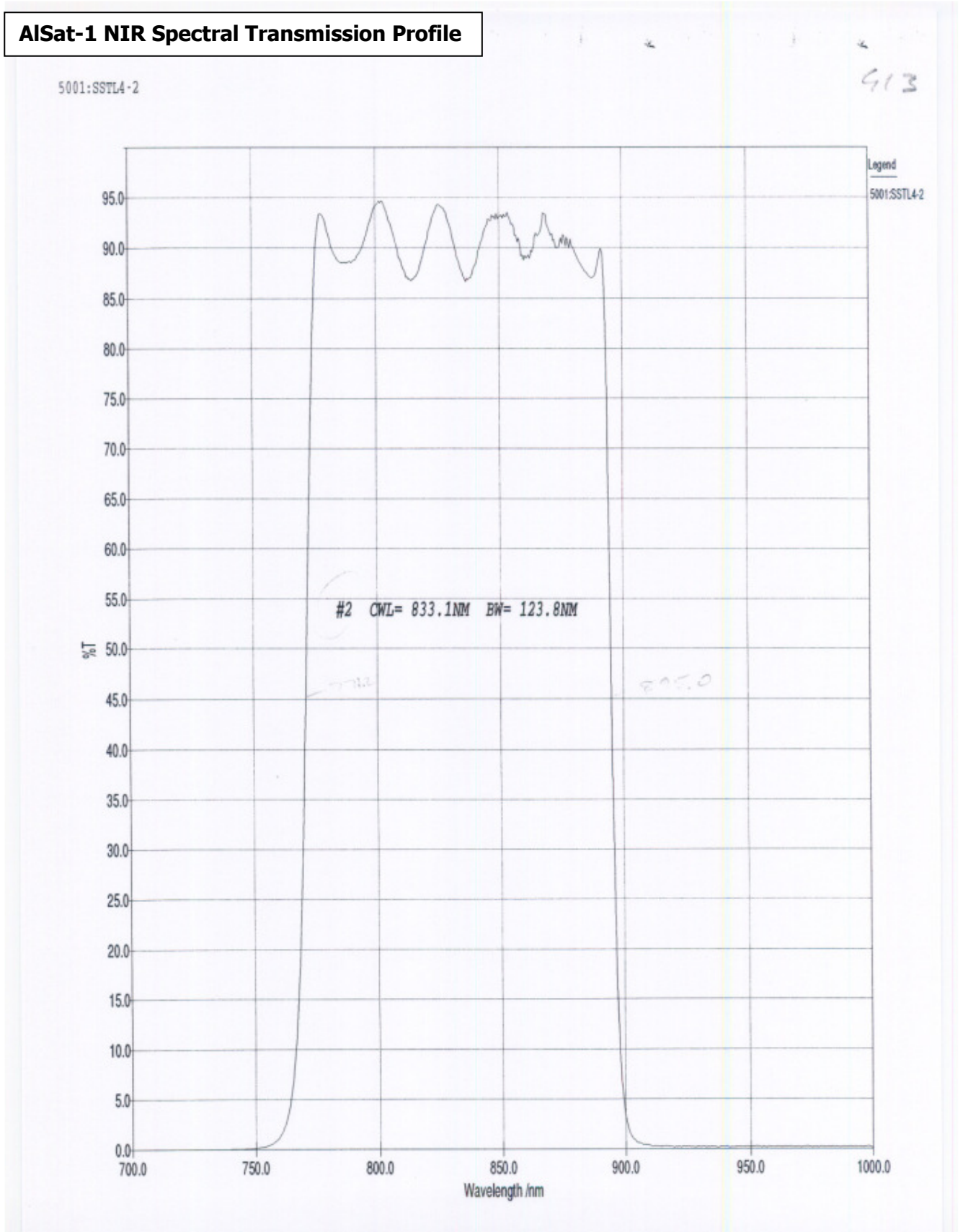
AlSat-1 Red Spectral Transmission Profile



AlSat-1 NIR Spectral Transmission Profile



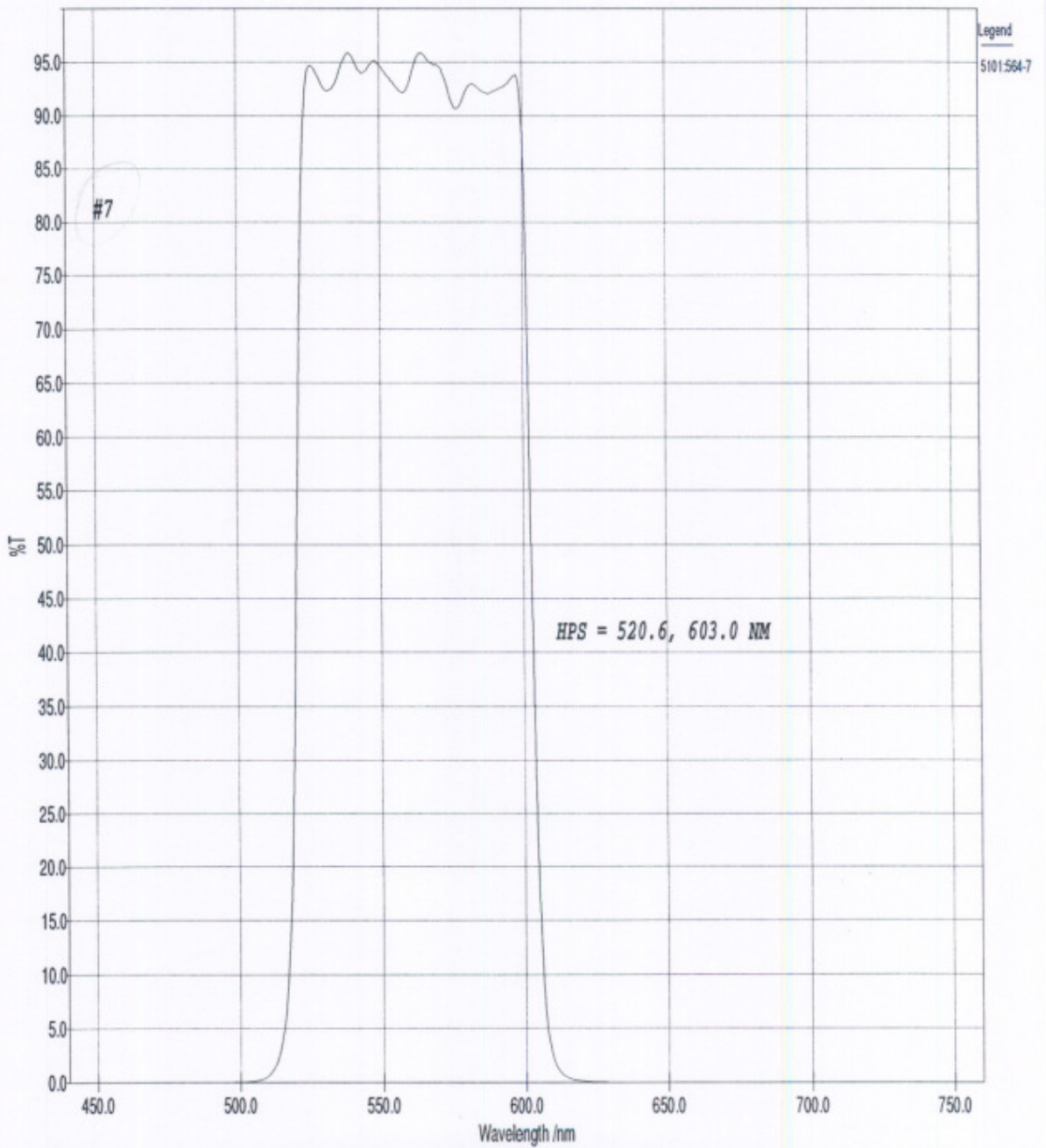
AlSat-1 NIR Spectral Transmission Profile



NigeriaSat-1 Green Spectral Transmission Profile

5101:564-7

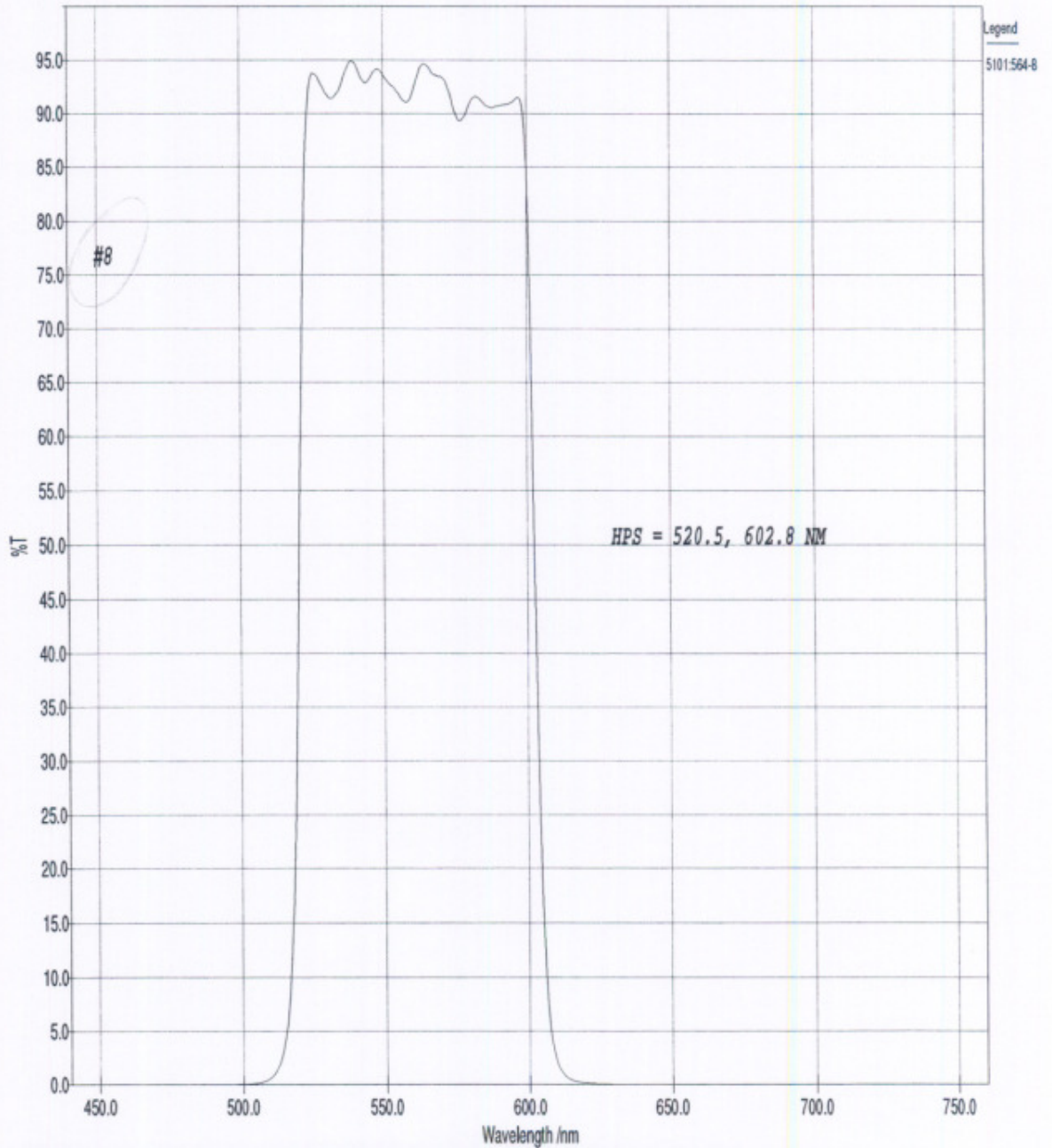
97



NigeriaSat-1 Green Spectral Transmission Profile

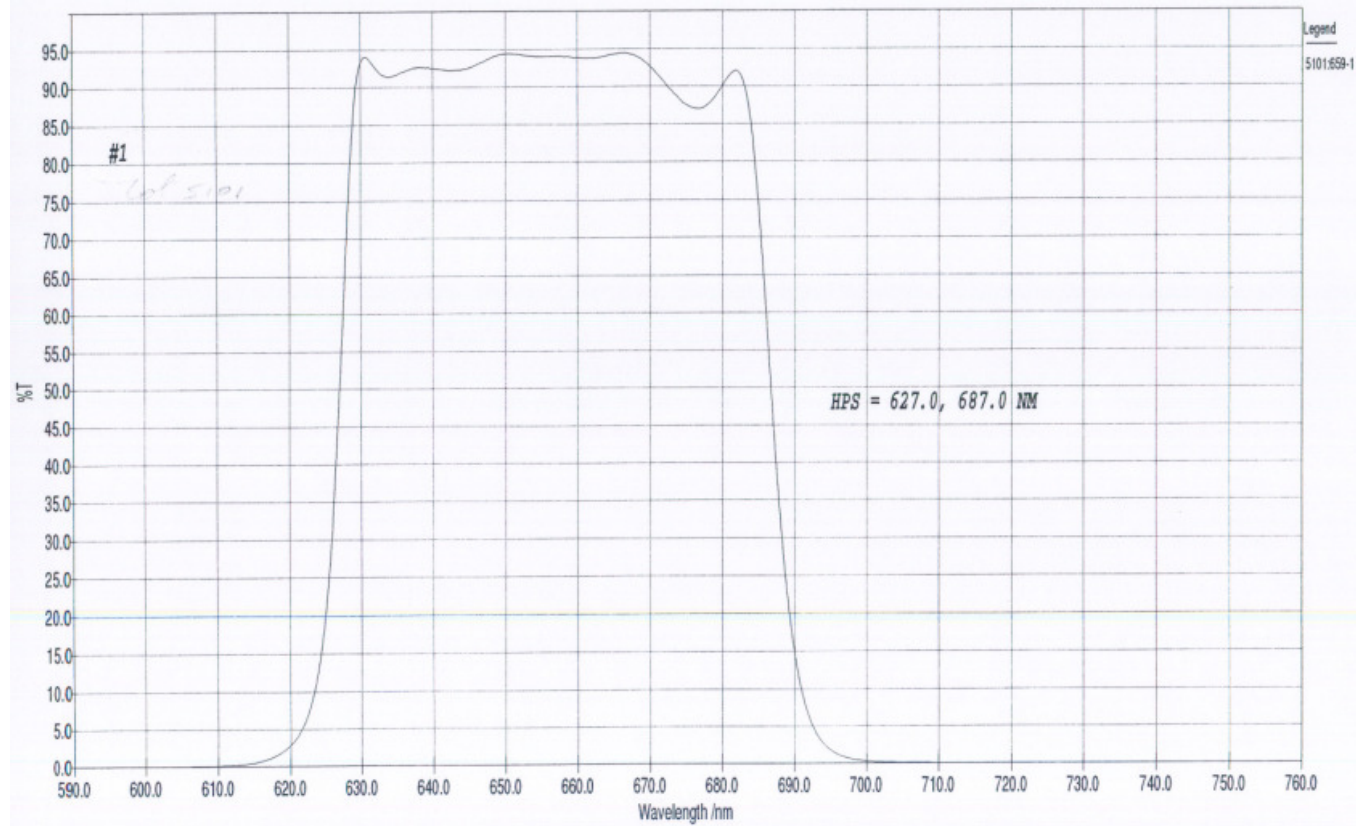
5101:564-8

48

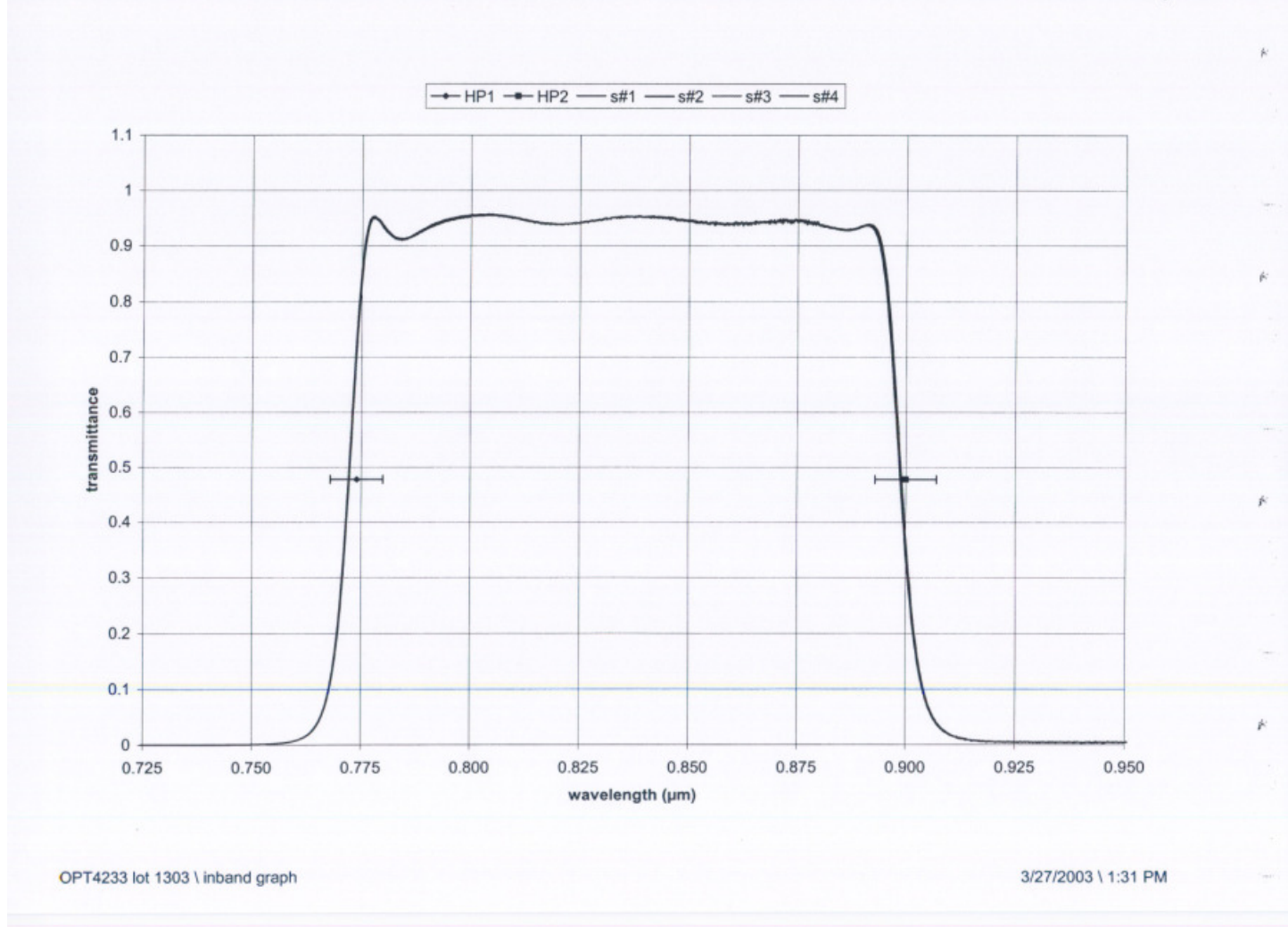


NigeriaSat-1 Red Spectral Transmission Profile (Generic)

11:659-1



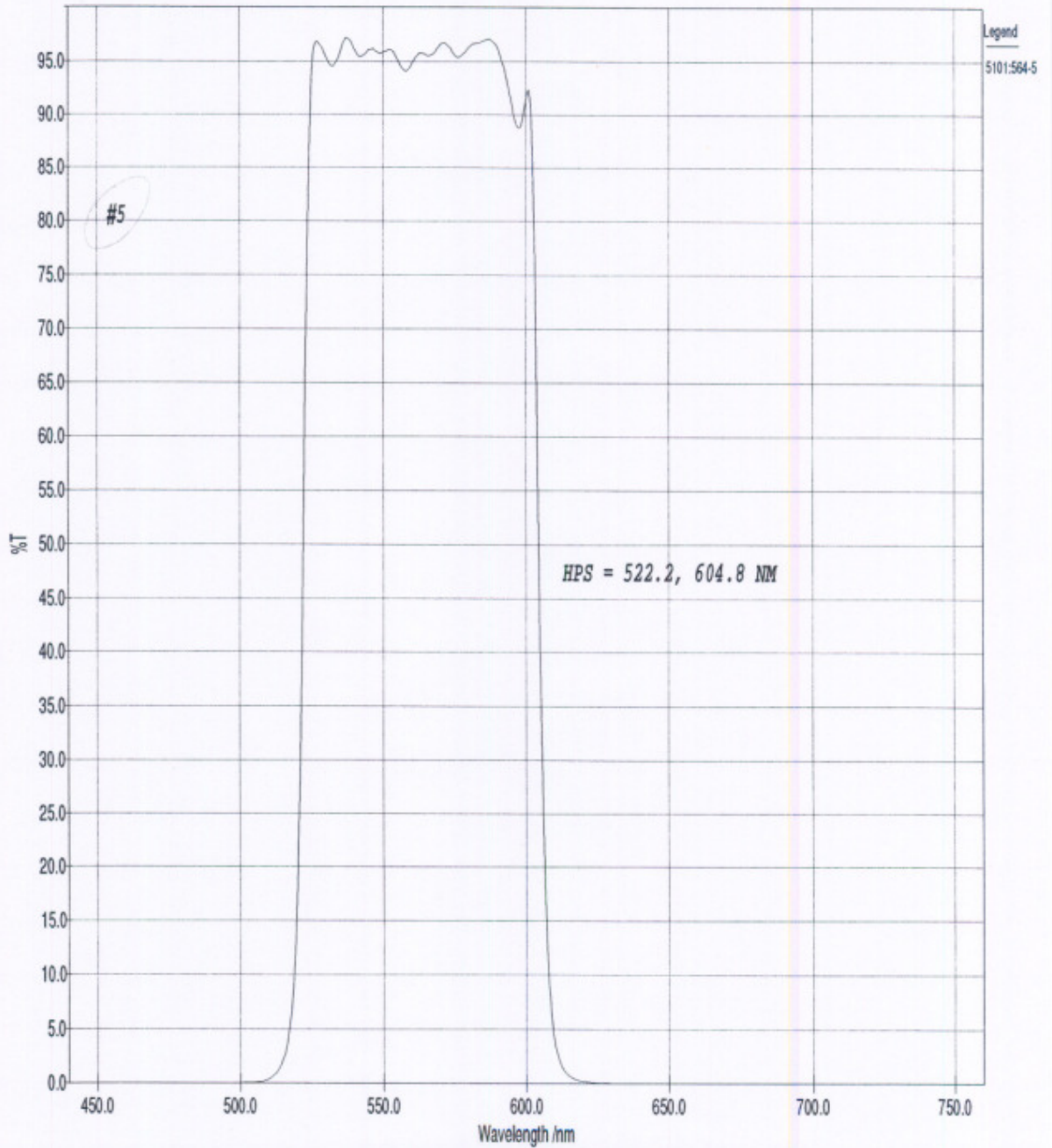
NigeriaSat-1 NIR Spectral Transmission Profile (Generic)



UK-DMC Green Spectral Transmission Profile

5101:564-5

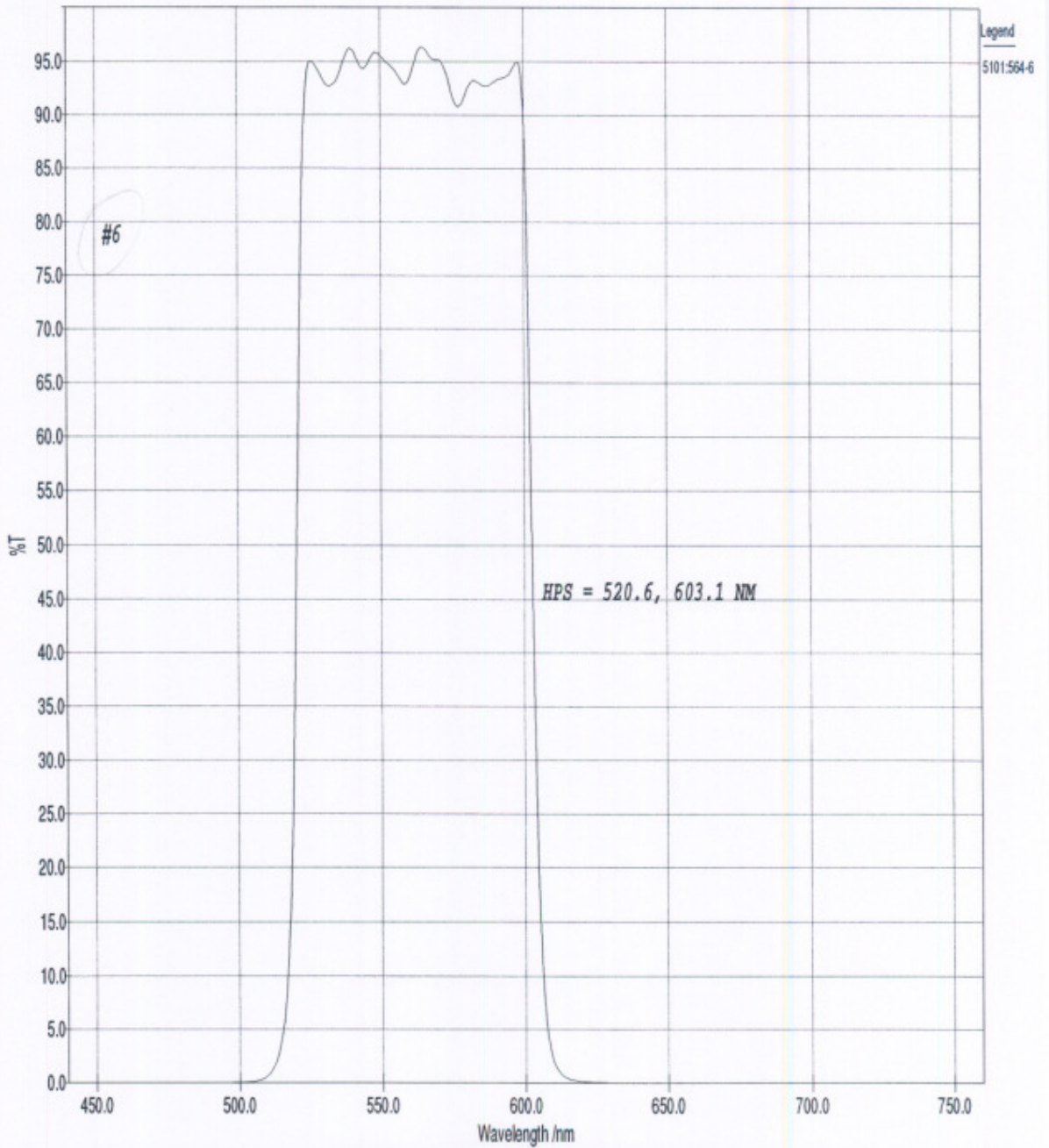
45



UK-DMC Green Spectral Transmission Profile

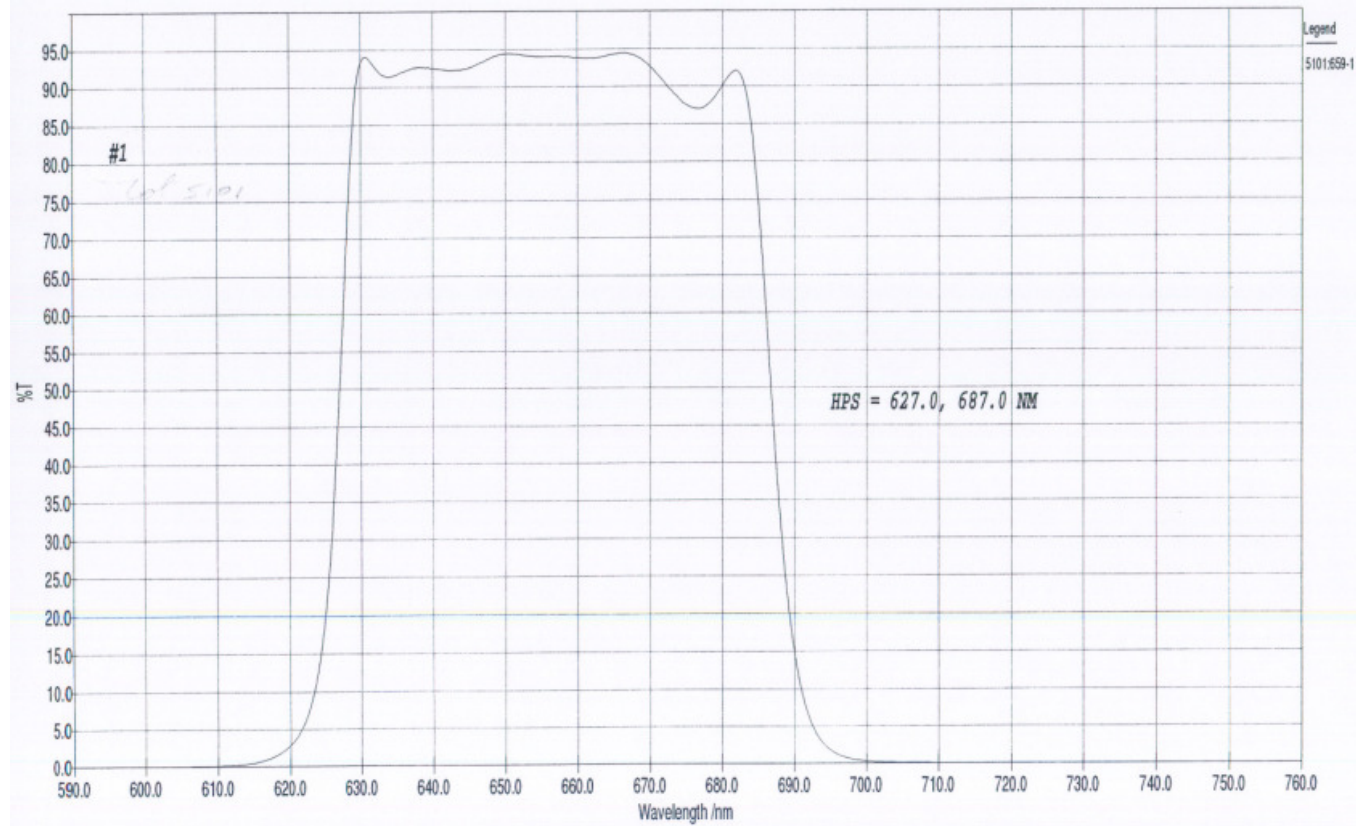
5101:564-6

46

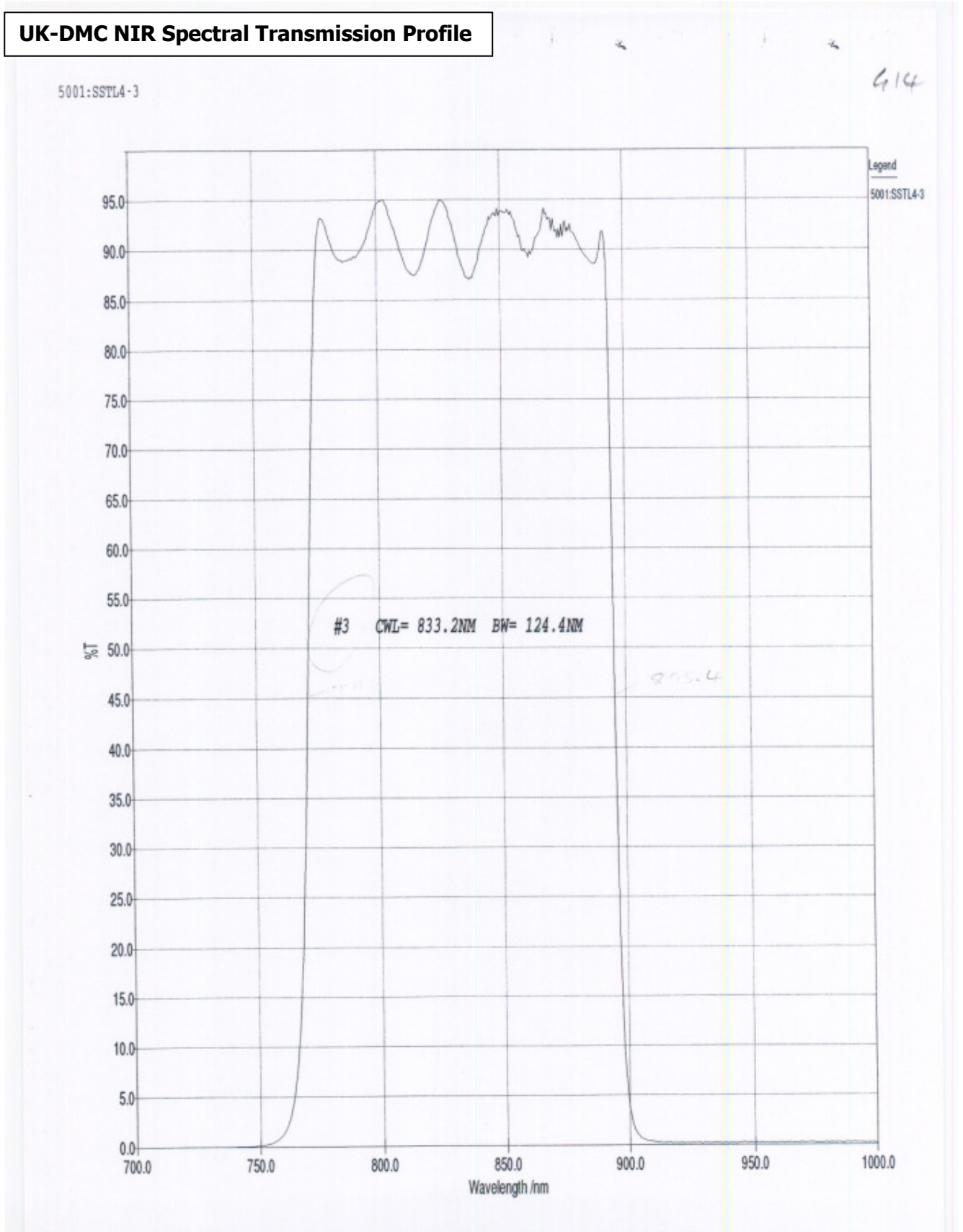


UK-DMC Red Spectral Transmission Profile (Generic)

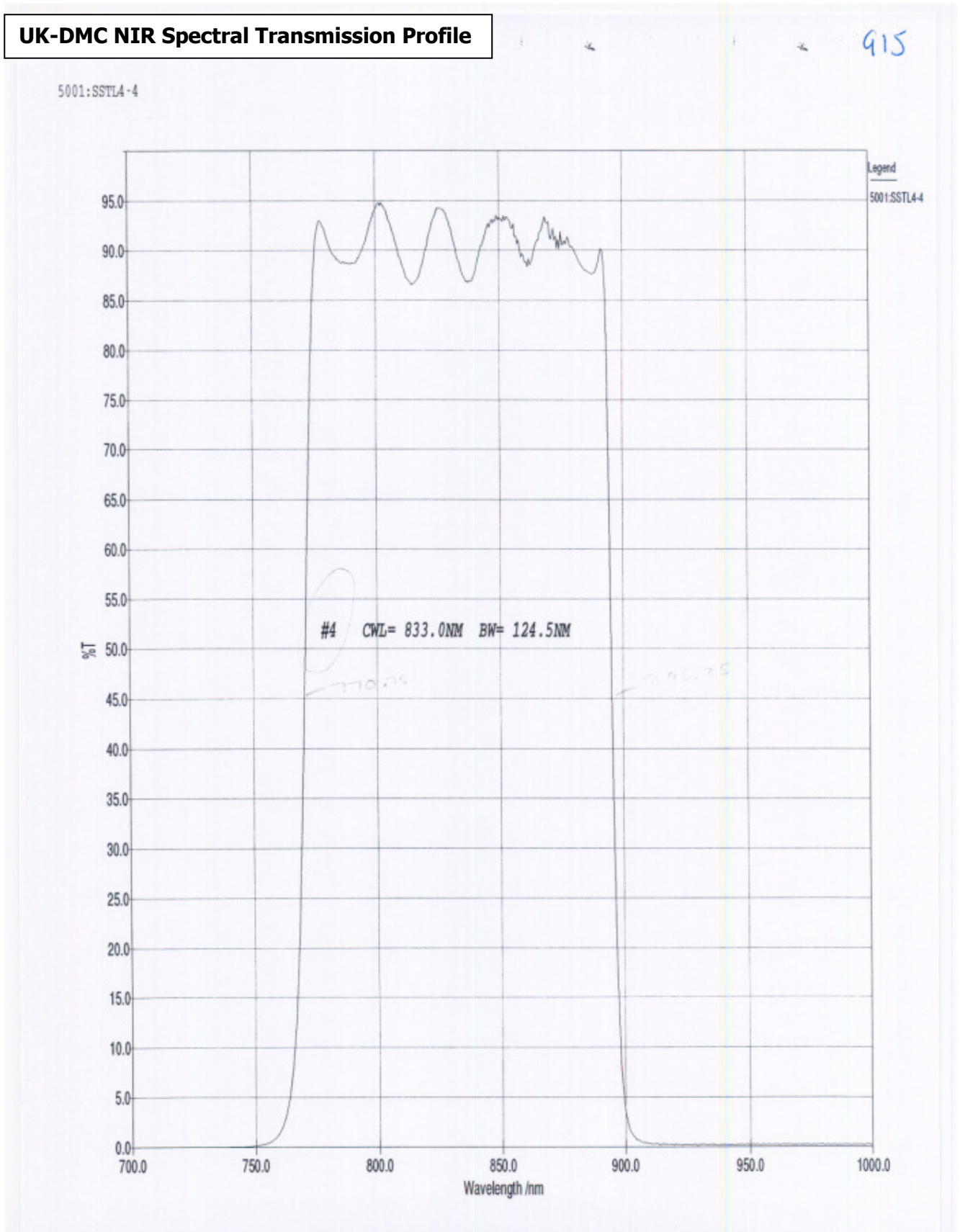
11:659-1



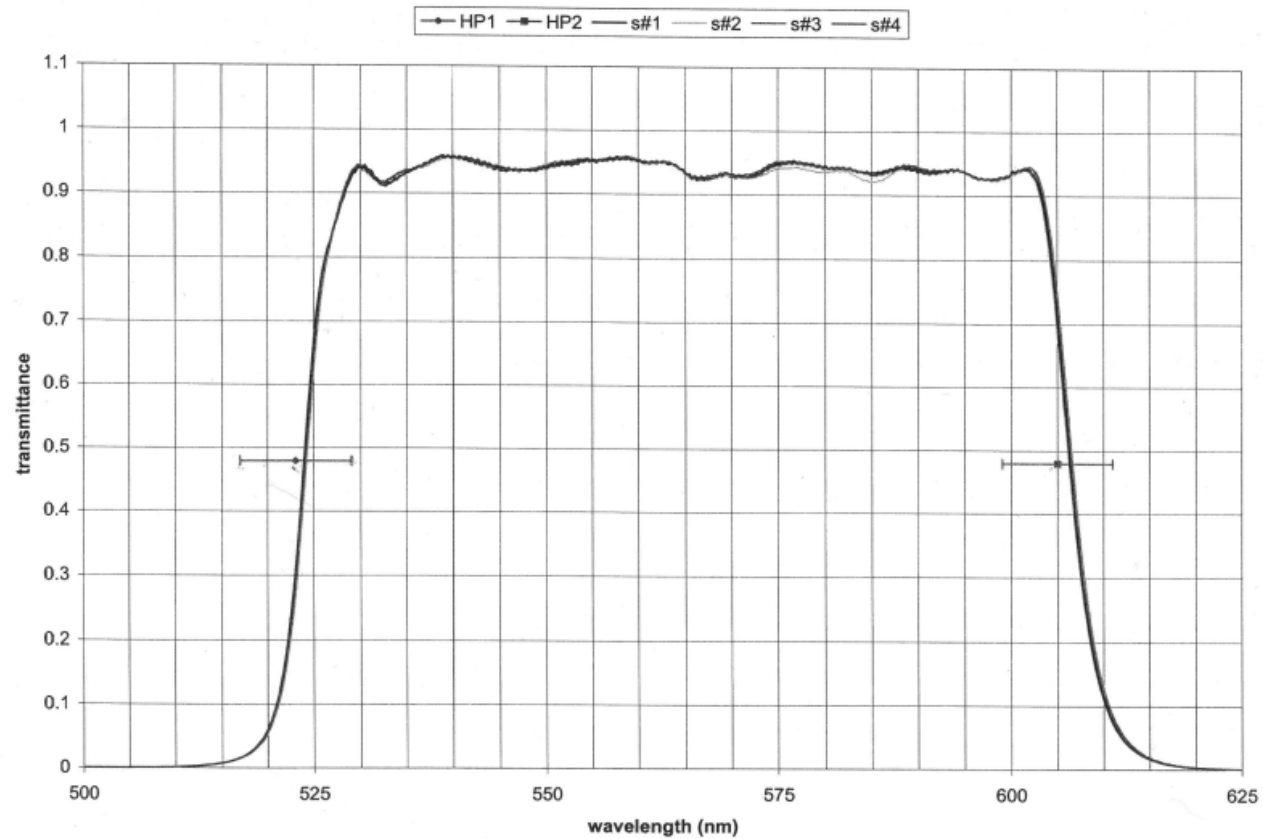
UK-DMC NIR Spectral Transmission Profile



UK-DMC NIR Spectral Transmission Profile



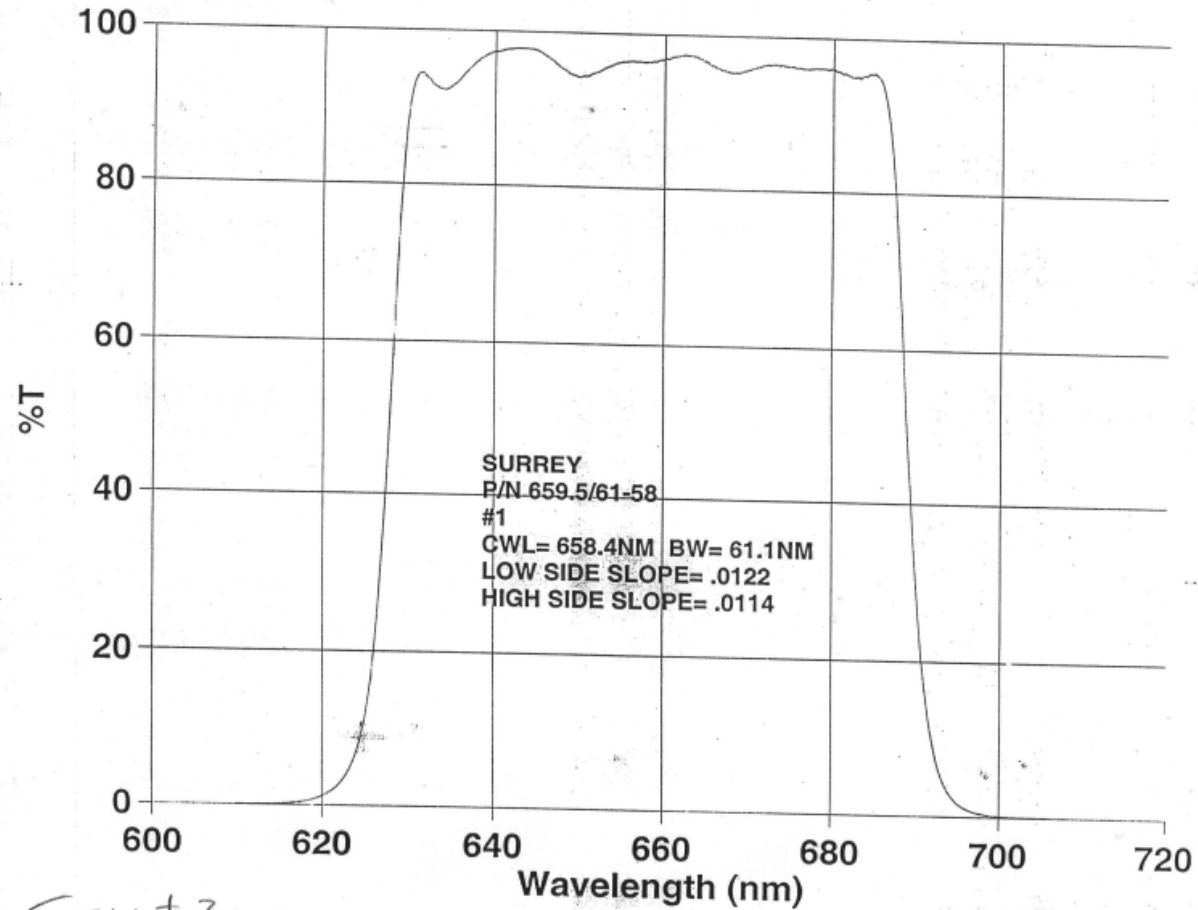
Beijing-1 Green Spectral Transmission Profile (Generic)



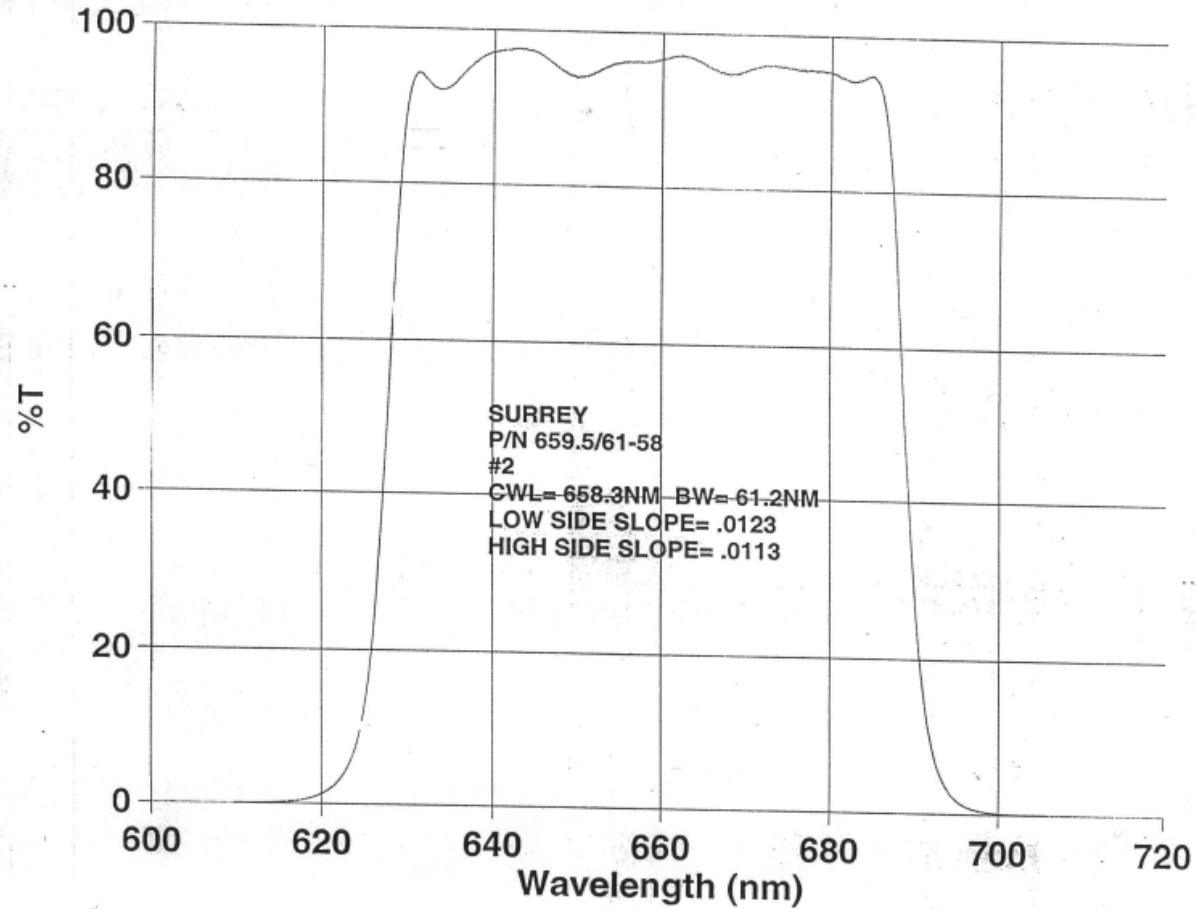
OPT4231 lot 1403 \ inband chart
ETM + 2 = GREEN

4/1/2003 \ 2:34 PM

Beijing-1 Red Spectral Transmission Profile

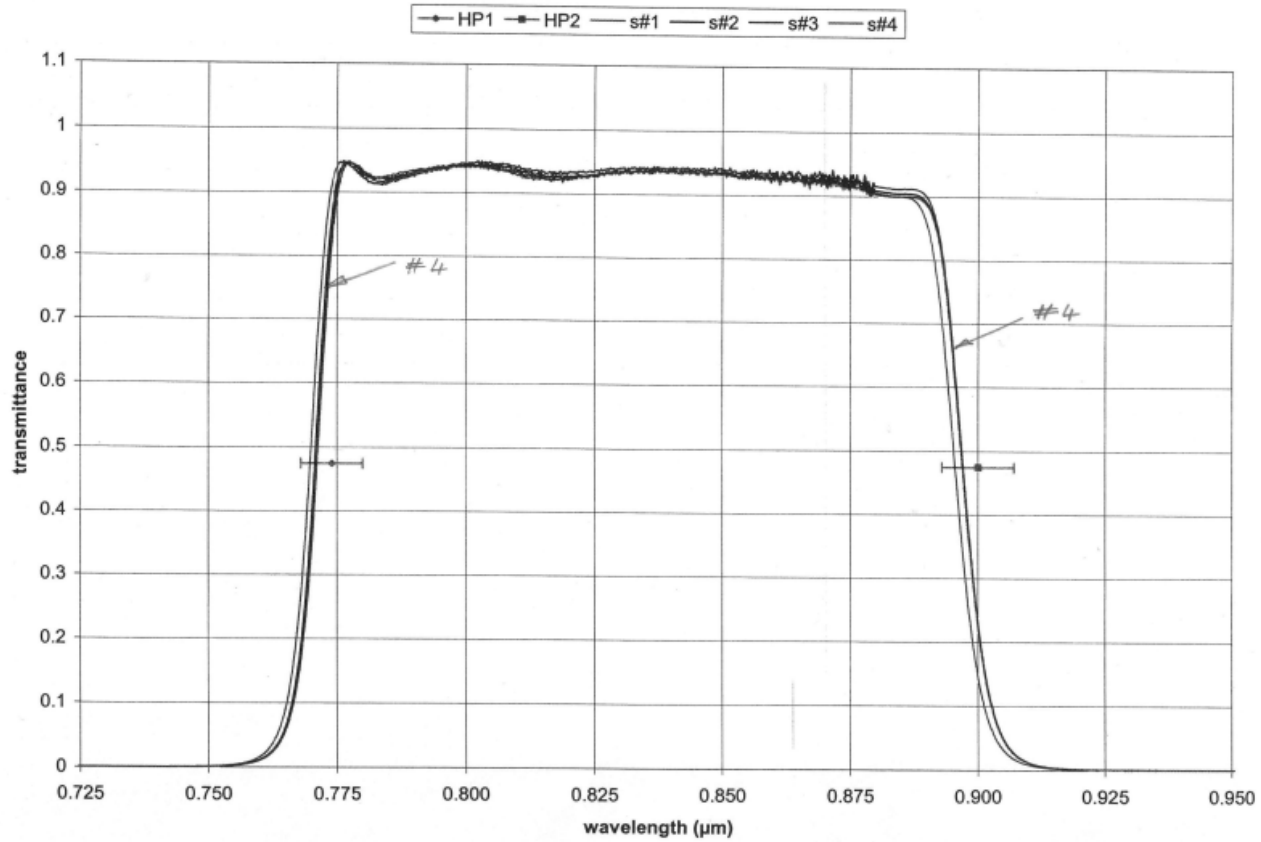


Beijing-1 Red Spectral Transmission Profile



ETM + 3 = RED

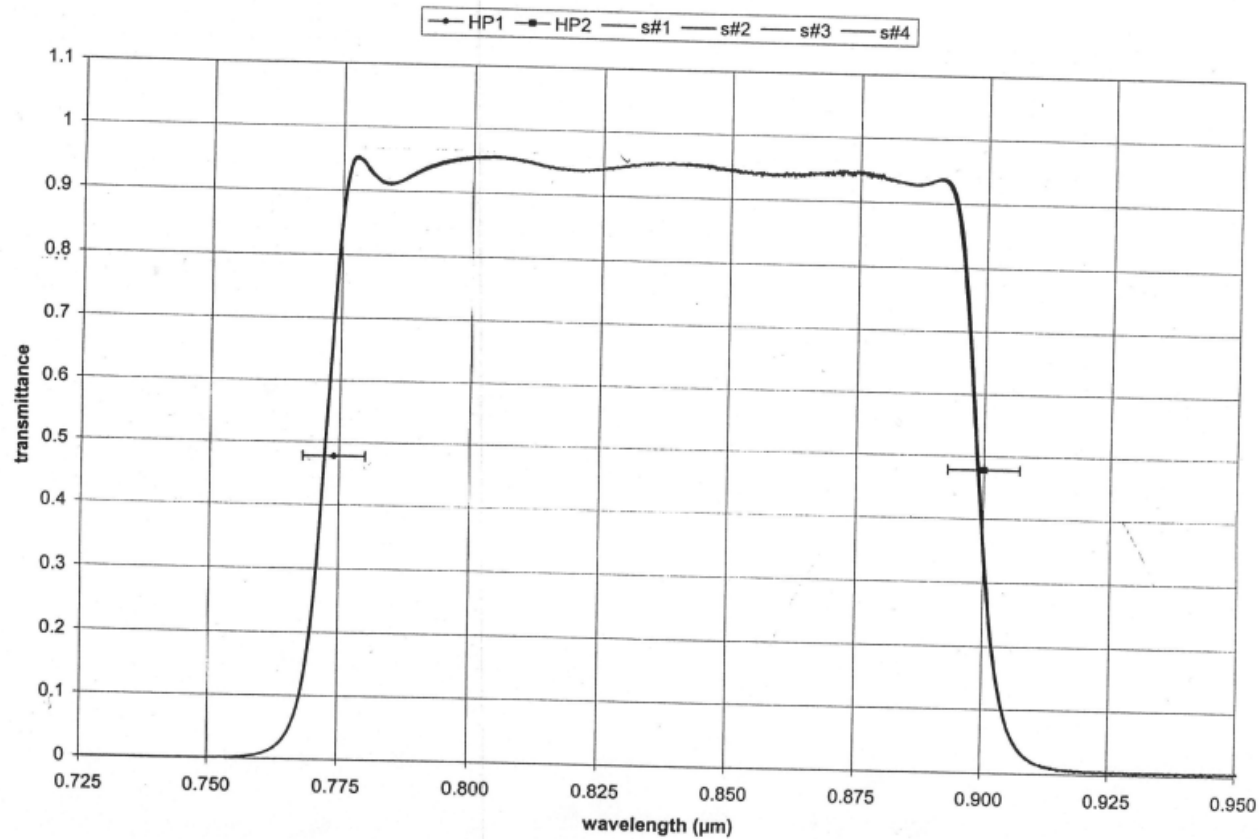
Beijing-1 NIR Spectral Transmission Profile



OPT4233 lot 1403 \ inband graph

4/11/2003 \ 1:29 PM

Beijing-1 NIR Spectral Transmission Profile



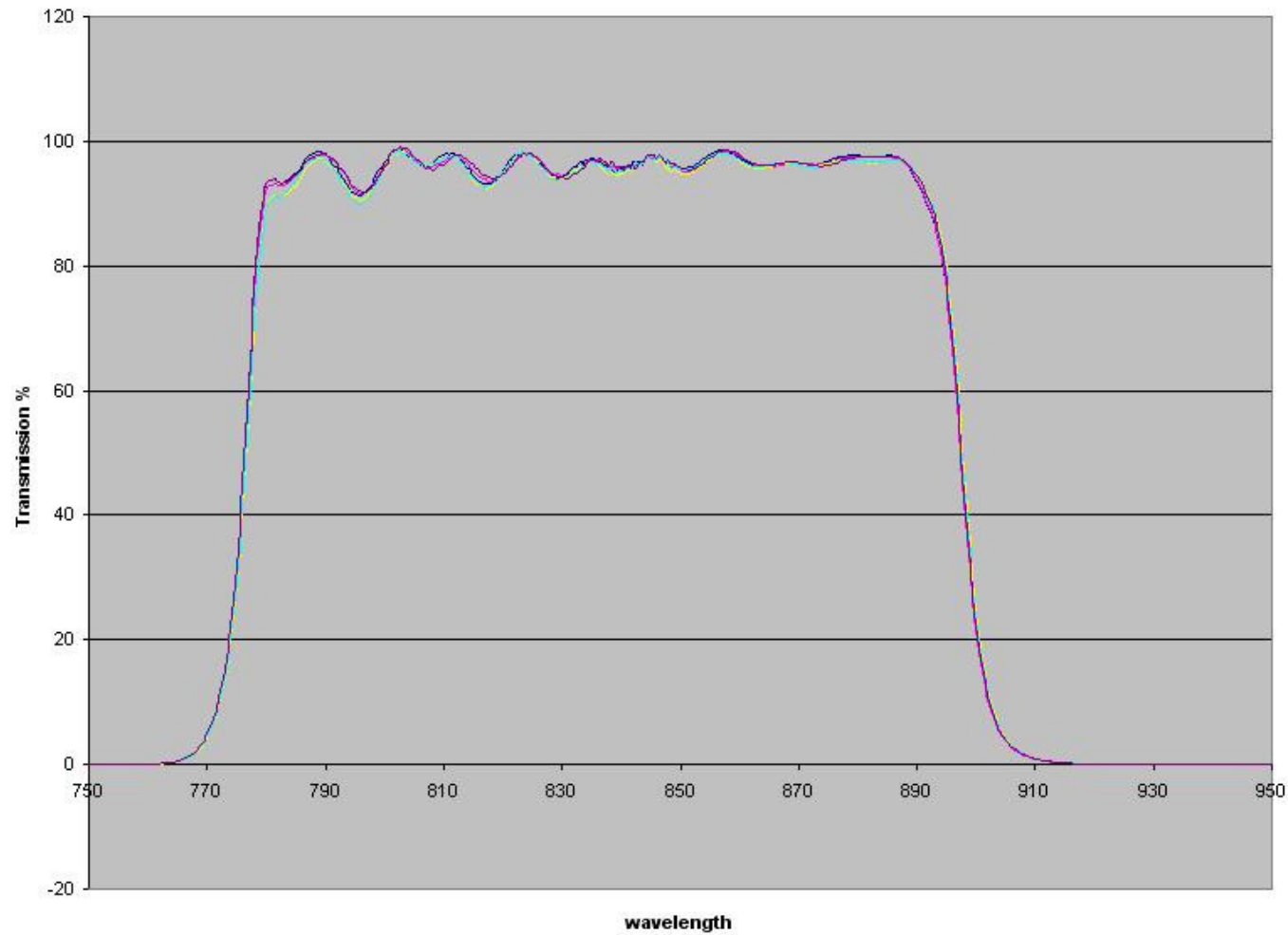
OPT4233 lot 1303 \ inband graph

ETM+4 = NIR

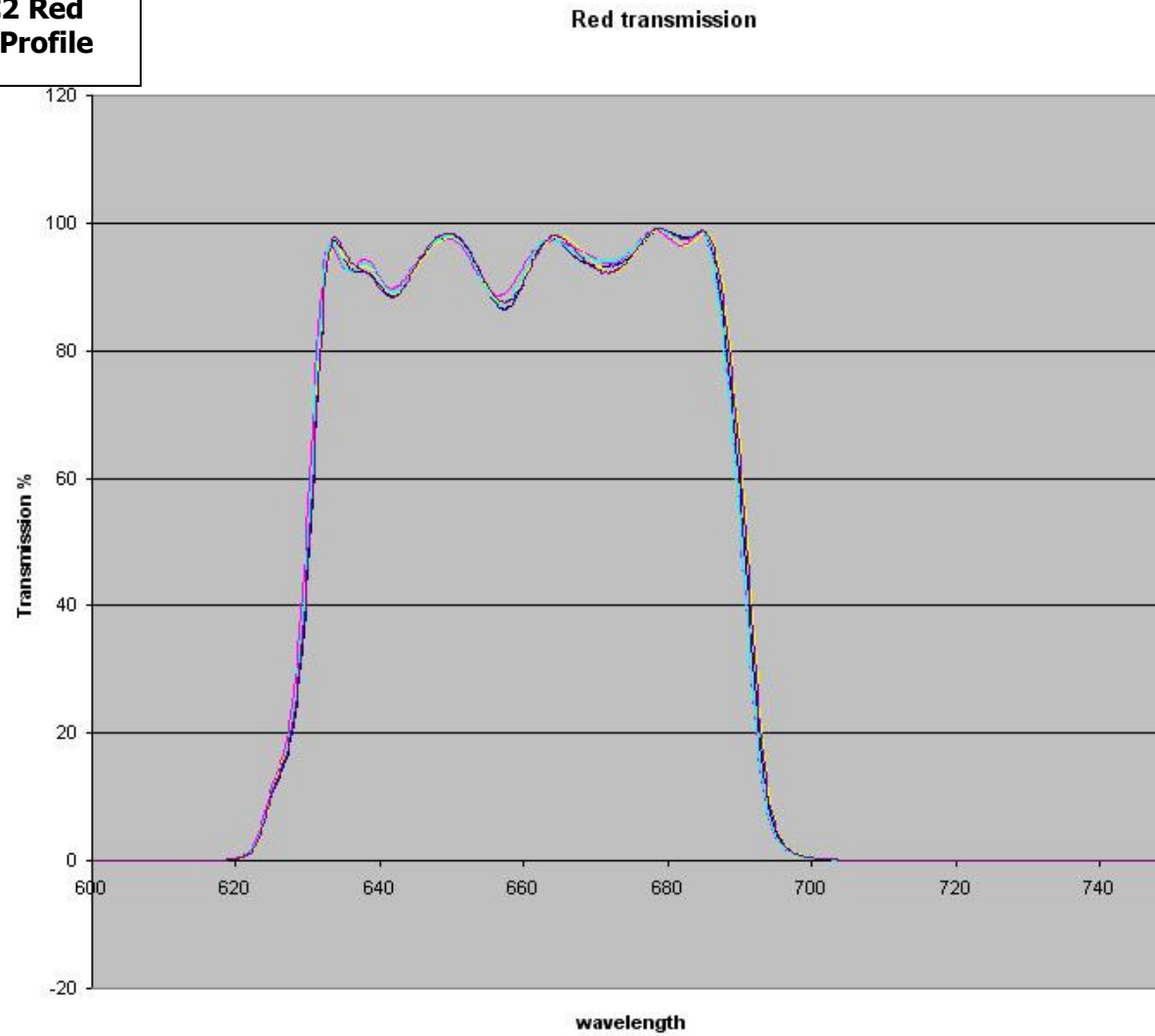
3/27/2003 \ 1:31 PM

**Deimos-1 and UK-DMC2 NIR
Spectral Transmission Profile**

NIR transmission

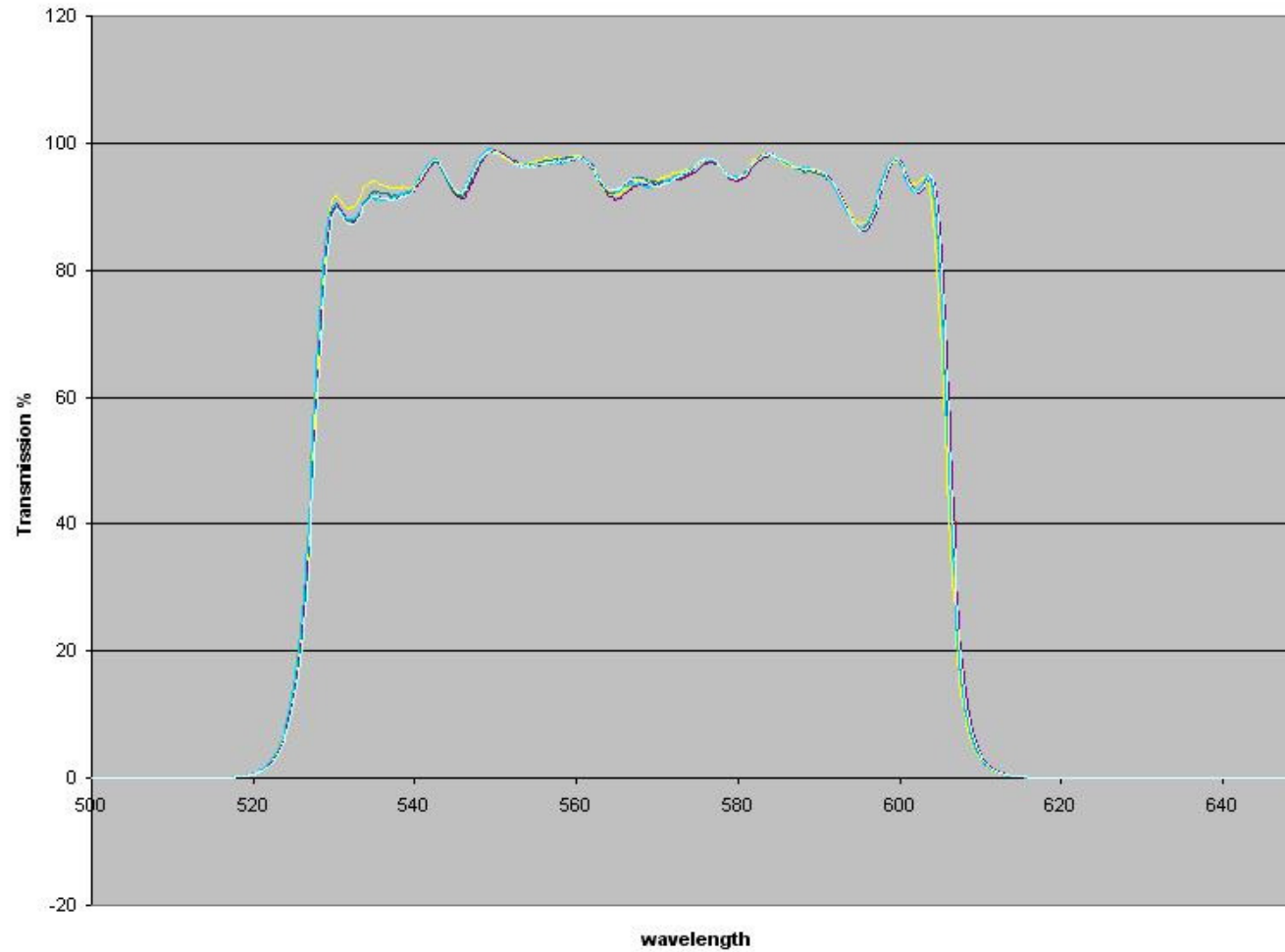


Deimos-1 and UK-DMC2 Red Spectral Transmission Profile



Deimos-1 and UK-DMC2 Green Spectral Transmission Profile

Green filter transmission



APPENDIX B: DIMAP SAMPLE – L1R PRODUCT

```

<?xml version="1.0" encoding="ISO-8859-1"?>
<?xml-stylesheet type="text/xsl" href="DU000b63T_L1R.xsl"?>
<Dimap_Document xmlns:dim="http://www.spotimage.fr/Dimap"
xmlns:xsi="http://www.w3.org/2001/XMLSchema-instance">
  <Metadata_Id>
    <METADATA_FORMAT version="1.1">DIMAP</METADATA_FORMAT>
  </Metadata_Id>
  <Dataset_Id>
    <DATASET_NAME>DU000b63T_L1R</DATASET_NAME>
    <COPYRIGHT>DMC International Imaging Ltd.</COPYRIGHT>
    <DATASET_QL_PATH href="DU000b63T_L1R_ql.jpg"/>
  </Dataset_Id>
  <Production>
    <DATASET_PRODUCER_NAME>DMC International Imaging
Ltd.</DATASET_PRODUCER_NAME>
    <DATASET_PRODUCER_URL href="http://www.dmcii.com"/>
    <DATASET_PRODUCTION_DATE>2007-09-20</DATASET_PRODUCTION_DATE>
    <PRODUCT_TYPE/>
    <JOB_ID/>
  </Production>
  <Quality_Assessment>
    <QUALITY_TABLES version="1.0">SPACEMETRIC</QUALITY_TABLES>
    <Quality_Parameter>
      <QUALITY_PARAMETER_DESC>Number of control
points</QUALITY_PARAMETER_DESC>
      <QUALITY_PARAMETER_CODE>SPACEMETRIC:NGCP</QUALITY_PARAMETER_CODE>
      <QUALITY_PARAMETER_VALUE>0</QUALITY_PARAMETER_VALUE>
    </Quality_Parameter>
    <Quality_Parameter>
      <QUALITY_PARAMETER_DESC>Root Mean Square residual error X
component</QUALITY_PARAMETER_DESC>
      <QUALITY_PARAMETER_CODE>SPACEMETRIC:RMSX</QUALITY_PARAMETER_CODE>
      <QUALITY_PARAMETER_VALUE
unit="DEG">0.27616565725305675</QUALITY_PARAMETER_VALUE>
    </Quality_Parameter>
    <Quality_Parameter>
      <QUALITY_PARAMETER_DESC>Root Mean Square residual error Y
component</QUALITY_PARAMETER_DESC>
      <QUALITY_PARAMETER_CODE>SPACEMETRIC:RMSY</QUALITY_PARAMETER_CODE>
      <QUALITY_PARAMETER_VALUE
unit="DEG">0.2125673419935354</QUALITY_PARAMETER_VALUE>
    </Quality_Parameter>
  </Quality_Assessment>
  <Dataset_Use>
    <DATASET_CONTENT>Texas, USA</DATASET_CONTENT>
  </Dataset_Use>
  <Data_Processing>
    <GEOMETRIC_PROCESSING>1R</GEOMETRIC_PROCESSING>
    <RADIOMETRIC_PROCESSING>Cubic convolution</RADIOMETRIC_PROCESSING>
  </Data_Processing>
  <Coordinate_Reference_System>
    <GEO_TABLES>EPSG</GEO_TABLES>
    <Horizontal_CS>
      <HORIZONTAL_CS_CODE>EPSG:4326</HORIZONTAL_CS_CODE>
    </Horizontal_CS>
  </Coordinate_Reference_System>

```



DMC DATA PRODUCT MANUAL

DATE: 12-Feb-2010

DOC NO: 0115056

ISSUE: 02

STATUS: FINAL

```
<HORIZONTAL_CS_TYPE>GEOGRAPHIC</HORIZONTAL_CS_TYPE>
<HORIZONTAL_CS_NAME>WGS 84</HORIZONTAL_CS_NAME>
<Geographic_CS>
  <GEOGRAPHIC_CS_NAME>WGS 84</GEOGRAPHIC_CS_NAME>
  <GEOGRAPHIC_CS_CODE>EPSG:4326</GEOGRAPHIC_CS_CODE>
  <Horizontal_Datum>
    <HORIZONTAL_DATUM_NAME>World Geodetic System
1984</HORIZONTAL_DATUM_NAME>
    <HORIZONTAL_DATUM_CODE>EPSG:6326</HORIZONTAL_DATUM_CODE>
  <Ellipsoid>
    <ELLIPSOID_NAME>WGS 84</ELLIPSOID_NAME>
    <ELLIPSOID_CODE>EPSG:7030</ELLIPSOID_CODE>
    <Ellipsoid_Parameters>
      <ELLIPSOID_MAJOR_AXIS
unit="M">6378137.0</ELLIPSOID_MAJOR_AXIS>
      <ELLIPSOID_MINOR_AXIS
unit="M">6356752.31424518</ELLIPSOID_MINOR_AXIS>
    </Ellipsoid_Parameters>
  </Ellipsoid>
  <Prime_Meridian>
    <PRIME_MERIDIAN_NAME>Greenwich</PRIME_MERIDIAN_NAME>
    <PRIME_MERIDIAN_CODE>EPSG:8901</PRIME_MERIDIAN_CODE>
    <PRIME_MERIDIAN_OFFSET
unit="DEG">0.0</PRIME_MERIDIAN_OFFSET>
  </Prime_Meridian>
</Horizontal_Datum>
</Geographic_CS>
</Horizontal_CS>
</Coordinate_Reference_System>
<Geoposition>
  <Geoposition_Points>
    <Tie_Point>
      <TIE_POINT_DATA_X>0.0</TIE_POINT_DATA_X>
      <TIE_POINT_DATA_Y>0.0</TIE_POINT_DATA_Y>
      <TIE_POINT_CRS_X unit="DEG">-100.36121700237744</TIE_POINT_CRS_X>
      <TIE_POINT_CRS_Y unit="DEG">31.35796462327202</TIE_POINT_CRS_Y>
    </Tie_Point>
    <Tie_Point>
      <TIE_POINT_DATA_X>3977.0</TIE_POINT_DATA_X>
      <TIE_POINT_DATA_Y>0.0</TIE_POINT_DATA_Y>
      <TIE_POINT_CRS_X unit="DEG">-99.07716948100622</TIE_POINT_CRS_X>
      <TIE_POINT_CRS_Y unit="DEG">31.543096941217634</TIE_POINT_CRS_Y>
    </Tie_Point>
    <Tie_Point>
      <TIE_POINT_DATA_X>7954.0</TIE_POINT_DATA_X>
      <TIE_POINT_DATA_Y>0.0</TIE_POINT_DATA_Y>
      <TIE_POINT_CRS_X unit="DEG">-97.6886624143706</TIE_POINT_CRS_X>
      <TIE_POINT_CRS_Y unit="DEG">31.72922176530387</TIE_POINT_CRS_Y>
    </Tie_Point>
    <Tie_Point>
      <TIE_POINT_DATA_X>11930.999999999998</TIE_POINT_DATA_X>
      <TIE_POINT_DATA_Y>0.0</TIE_POINT_DATA_Y>
      <TIE_POINT_CRS_X unit="DEG">-96.12077738816531</TIE_POINT_CRS_X>
      <TIE_POINT_CRS_Y unit="DEG">31.920565627568482</TIE_POINT_CRS_Y>
    </Tie_Point>
    <Tie_Point>
      <TIE_POINT_DATA_X>0.0</TIE_POINT_DATA_X>
      <TIE_POINT_DATA_Y>2577.0</TIE_POINT_DATA_Y>
```




DMC DATA PRODUCT MANUAL

DATE: 12-Feb-2010

DOC NO: 0115056

ISSUE: 02

STATUS: FINAL

```
<TIE_POINT_CRX_X unit="DEG">-100.16271084681733</TIE_POINT_CRX_X>
<TIE_POINT_CRX_Y unit="DEG">30.612565439414062</TIE_POINT_CRX_Y>
</Tie_Point>
<Tie_Point>
  <TIE_POINT_DATA_X>3977.0</TIE_POINT_DATA_X>
  <TIE_POINT_DATA_Y>2577.0</TIE_POINT_DATA_Y>
  <TIE_POINT_CRX_X unit="DEG">-98.88843259962778</TIE_POINT_CRX_X>
  <TIE_POINT_CRX_Y unit="DEG">30.796339165565442</TIE_POINT_CRX_Y>
</Tie_Point>
<Tie_Point>
  <TIE_POINT_DATA_X>7954.0</TIE_POINT_DATA_X>
  <TIE_POINT_DATA_Y>2577.0</TIE_POINT_DATA_Y>
  <TIE_POINT_CRX_X unit="DEG">-97.51068361773663</TIE_POINT_CRX_X>
  <TIE_POINT_CRX_Y unit="DEG">30.98141363769206</TIE_POINT_CRX_Y>
</Tie_Point>
<Tie_Point>
  <TIE_POINT_DATA_X>11930.999999999998</TIE_POINT_DATA_X>
  <TIE_POINT_DATA_Y>2577.0</TIE_POINT_DATA_Y>
  <TIE_POINT_CRX_X unit="DEG">-95.95515413990444</TIE_POINT_CRX_X>
  <TIE_POINT_CRX_Y unit="DEG">31.172095831106123</TIE_POINT_CRX_Y>
</Tie_Point>
<Tie_Point>
  <TIE_POINT_DATA_X>0.0</TIE_POINT_DATA_X>
  <TIE_POINT_DATA_Y>5154.0</TIE_POINT_DATA_Y>
  <TIE_POINT_CRX_X unit="DEG">-99.96652476925705</TIE_POINT_CRX_X>
  <TIE_POINT_CRX_Y unit="DEG">29.866912521196525</TIE_POINT_CRX_Y>
</Tie_Point>
<Tie_Point>
  <TIE_POINT_DATA_X>3977.0</TIE_POINT_DATA_X>
  <TIE_POINT_DATA_Y>5154.0</TIE_POINT_DATA_Y>
  <TIE_POINT_CRX_X unit="DEG">-98.70165632252848</TIE_POINT_CRX_X>
  <TIE_POINT_CRX_Y unit="DEG">30.04937964001442</TIE_POINT_CRX_Y>
</Tie_Point>
<Tie_Point>
  <TIE_POINT_DATA_X>7954.0</TIE_POINT_DATA_X>
  <TIE_POINT_DATA_Y>5154.0</TIE_POINT_DATA_Y>
  <TIE_POINT_CRX_X unit="DEG">-97.33427300658795</TIE_POINT_CRX_X>
  <TIE_POINT_CRX_Y unit="DEG">30.233452960067293</TIE_POINT_CRX_Y>
</Tie_Point>
<Tie_Point>
  <TIE_POINT_DATA_X>11930.999999999998</TIE_POINT_DATA_X>
  <TIE_POINT_DATA_Y>5154.0</TIE_POINT_DATA_Y>
  <TIE_POINT_CRX_X unit="DEG">-95.79065045117527</TIE_POINT_CRX_X>
  <TIE_POINT_CRX_Y unit="DEG">30.423520707812283</TIE_POINT_CRX_Y>
</Tie_Point>
<Tie_Point>
  <TIE_POINT_DATA_X>0.0</TIE_POINT_DATA_X>
  <TIE_POINT_DATA_Y>7731.0</TIE_POINT_DATA_Y>
  <TIE_POINT_CRX_X unit="DEG">-99.77255901774444</TIE_POINT_CRX_X>
  <TIE_POINT_CRX_Y unit="DEG">29.121014990107515</TIE_POINT_CRX_Y>
</Tie_Point>
<Tie_Point>
  <TIE_POINT_DATA_X>3977.0</TIE_POINT_DATA_X>
  <TIE_POINT_DATA_Y>7731.0</TIE_POINT_DATA_Y>
  <TIE_POINT_CRX_X unit="DEG">-98.51675287257412</TIE_POINT_CRX_X>
  <TIE_POINT_CRX_Y unit="DEG">29.30222566977647</TIE_POINT_CRX_Y>
</Tie_Point>
<Tie_Point>
```

```

<TIE_POINT_DATA_X>7954.0</TIE_POINT_DATA_X>
<TIE_POINT_DATA_Y>7731.0</TIE_POINT_DATA_Y>
<TIE_POINT_CRS_X unit="DEG">-97.15935466401667</TIE_POINT_CRS_X>
<TIE_POINT_CRS_Y unit="DEG">29.485345633894866</TIE_POINT_CRS_Y>
</Tie_Point>
<Tie_Point>
  <TIE_POINT_DATA_X>11930.999999999998</TIE_POINT_DATA_X>
  <TIE_POINT_DATA_Y>7731.0</TIE_POINT_DATA_Y>
  <TIE_POINT_CRS_X unit="DEG">-95.627207536508</TIE_POINT_CRS_X>
  <TIE_POINT_CRS_Y unit="DEG">29.67484446319718</TIE_POINT_CRS_Y>
</Tie_Point>
</Geoposition_Points>
</Geoposition>
<Raster_CS>
  <RASTER_CS_TYPE>POINT</RASTER_CS_TYPE>
</Raster_CS>
<Dataset_Frame>
  <Vertex>
    <FRAME_X unit="DEG">-100.36121700237744</FRAME_X>
    <FRAME_Y unit="DEG">31.35796462327202</FRAME_Y>
  </Vertex>
  <Vertex>
    <FRAME_X unit="DEG">-99.77248418945639</FRAME_X>
    <FRAME_Y unit="DEG">29.120725520370257</FRAME_Y>
  </Vertex>
  <Vertex>
    <FRAME_X unit="DEG">-95.62714433926318</FRAME_X>
    <FRAME_Y unit="DEG">29.67455393921758</FRAME_Y>
  </Vertex>
  <Vertex>
    <FRAME_X unit="DEG">-96.12077738816531</FRAME_X>
    <FRAME_Y unit="DEG">31.920565627568482</FRAME_Y>
  </Vertex>
</Dataset_Frame>
<Raster_Encoding>
  <NBITS>8</NBITS>
  <DATA_TYPE>BYTE</DATA_TYPE>
  <BYTEORDER>M</BYTEORDER>
</Raster_Encoding>
<Data_Access>
  <DATA_FILE_FORMAT>GEOTIFF</DATA_FILE_FORMAT>
  <Data_File>
    <DATA_FILE_PATH href="DU000b63T_L1R.tif"/>
  </Data_File>
</Data_Access>
<Raster_Dimensions>
  <NCOLS>11932</NCOLS>
  <NROWS>7733</NROWS>
  <NBANDS>3</NBANDS>
</Raster_Dimensions>
<Image_Interpretation>
  <Spectral_Band_Info>
    <BAND_INDEX>1</BAND_INDEX>
    <BAND_DESCRIPTION>NIR</BAND_DESCRIPTION>
    <PHYSICAL_GAIN>1.0749817168185152</PHYSICAL_GAIN>
    <PHYSICAL_BIAS>13.31323795165322</PHYSICAL_BIAS>
    <PHYSICAL_UNIT>W/m2/sr/m-6</PHYSICAL_UNIT>
  </Spectral_Band_Info>

```

```

<Spectral_Band_Info>
  <BAND_INDEX>2</BAND_INDEX>
  <BAND_DESCRIPTION>Red</BAND_DESCRIPTION>
  <PHYSICAL_GAIN>0.8908284414984867</PHYSICAL_GAIN>
  <PHYSICAL_BIAS>5.724840466729124</PHYSICAL_BIAS>
  <PHYSICAL_UNIT>W/m2/sr/m-6</PHYSICAL_UNIT>
</Spectral_Band_Info>
<Spectral_Band_Info>
  <BAND_INDEX>3</BAND_INDEX>
  <BAND_DESCRIPTION>Green</BAND_DESCRIPTION>
  <PHYSICAL_GAIN>1.1722234734653645</PHYSICAL_GAIN>
  <PHYSICAL_BIAS>10.417201834872332</PHYSICAL_BIAS>
  <PHYSICAL_UNIT>W/m2/sr/m-6</PHYSICAL_UNIT>
</Spectral_Band_Info>
</Image_Interpretation>
<Image_Display>
  <Band_Display_Order>
    <RED_CHANNEL>1</RED_CHANNEL>
    <GREEN_CHANNEL>2</GREEN_CHANNEL>
    <BLUE_CHANNEL>3</BLUE_CHANNEL>
  </Band_Display_Order>
  <Special_Value>
    <SPECIAL_VALUE_INDEX>0</SPECIAL_VALUE_INDEX>
    <SPECIAL_VALUE_TEXT>nodata</SPECIAL_VALUE_TEXT>
  </Special_Value>
  <Band_Statistics>
    <BAND_INDEX>1</BAND_INDEX>
    <STX_LIN_MIN>-32.36799891064808</STX_LIN_MIN>
    <STX_LIN_MAX>254.185048069092</STX_LIN_MAX>
    <STX_STDV>57.31060939594801</STX_STDV>
    <STX_MEAN>110.90852457922196</STX_MEAN>
    <STX_MIN>10.0</STX_MIN>
    <STX_MAX>243.0</STX_MAX>
  </Band_Statistics>
  <Band_Statistics>
    <BAND_INDEX>2</BAND_INDEX>
    <STX_LIN_MIN>-75.53120332858349</STX_LIN_MIN>
    <STX_LIN_MAX>255.0</STX_LIN_MAX>
    <STX_STDV>72.20814583034952</STX_STDV>
    <STX_MEAN>104.98916124729031</STX_MEAN>
    <STX_MIN>12.0</STX_MIN>
    <STX_MAX>228.0</STX_MAX>
  </Band_Statistics>
  <Band_Statistics>
    <BAND_INDEX>3</BAND_INDEX>
    <STX_LIN_MIN>-58.367896778413666</STX_LIN_MIN>
    <STX_LIN_MAX>255.0</STX_LIN_MAX>
    <STX_STDV>75.99178728851398</STX_STDV>
    <STX_MEAN>131.61157144287128</STX_MEAN>
    <STX_MIN>2.0</STX_MIN>
    <STX_MAX>245.0</STX_MAX>
  </Band_Statistics>
</Image_Display>
<Dataset_Sources>
  <Source_Information>
    <SOURCE_ID>DU000b63T</SOURCE_ID>
    <Coordinate_Reference_System>
      <GEO_TABLES>EPSG</GEO_TABLES>
    
```

```
<Horizontal_CS>
  <HORIZONTAL_CS_CODE>EPSG:4326</HORIZONTAL_CS_CODE>
  <HORIZONTAL_CS_TYPE>GEOGRAPHIC</HORIZONTAL_CS_TYPE>
  <HORIZONTAL_CS_NAME>WGS 84</HORIZONTAL_CS_NAME>
</Horizontal_CS>
</Coordinate_Reference_System>
<Source_Frame>
  <Vertex>
    <FRAME_LON unit="DEG">-96.12077740664937</FRAME_LON>
    <FRAME_LAT unit="DEG">31.920565629599768</FRAME_LAT>
  </Vertex>
  <Vertex>
    <FRAME_LON unit="DEG">-95.62765014290926</FRAME_LON>
    <FRAME_LAT unit="DEG">29.67687825042264</FRAME_LAT>
  </Vertex>
  <Vertex>
    <FRAME_LON unit="DEG">-99.16229849325259</FRAME_LON>
    <FRAME_LAT unit="DEG">29.212329892339728</FRAME_LAT>
  </Vertex>
  <Vertex>
    <FRAME_LON unit="DEG">-99.7367748166211</FRAME_LON>
    <FRAME_LAT unit="DEG">31.449295800260668</FRAME_LAT>
  </Vertex>
</Source_Frame>
<Scene_Source>
  <MISSION>UK-DMC</MISSION>
  <INSTRUMENT>SLIM-6</INSTRUMENT>
  <IMAGING_DATE>2007-07-30</IMAGING_DATE>
  <IMAGING_TIME>16:14:39</IMAGING_TIME>
  <VIEWING_ANGLE unit="DEG">1.70751061117751</VIEWING_ANGLE>
  <SUN_AZIMUTH unit="DEG">101.74181569705586</SUN_AZIMUTH>
  <SUN_ELEVATION unit="DEG">55.227078071950686</SUN_ELEVATION>
</Scene_Source>
</Source_Information>
</Dataset_Sources>
</Dimap_Document>
```

APPENDIX C: DIMAP SAMPLE – L1T PRODUCT

```

<?xml version="1.0" encoding="ISO-8859-1"?>
<?xml-stylesheet type="text/xsl" href="DU000b63T_L1T.xsl"?>
<Dimap_Document xmlns:dim="http://www.spotimage.fr/Dimap"
xmlns:xsi="http://www.w3.org/2001/XMLSchema-instance">
  <Metadata_Id>
    <METADATA_FORMAT version="1.1">DIMAP</METADATA_FORMAT>
  </Metadata_Id>
  <Dataset_Id>
    <DATASET_NAME>DU000b63T_L1T</DATASET_NAME>
    <COPYRIGHT>DMC International Imaging Ltd.</COPYRIGHT>
    <DATASET_QL_PATH href="DU000b63T_L1T_ql.jpg"/>
  </Dataset_Id>
  <Production>
    <DATASET_PRODUCER_NAME>DMC International Imaging
Ltd.</DATASET_PRODUCER_NAME>
    <DATASET_PRODUCER_URL href="http://www.dmcii.com"/>
    <DATASET_PRODUCTION_DATE>2007-09-20</DATASET_PRODUCTION_DATE>
    <PRODUCT_TYPE/>
    <JOB_ID/>
  </Production>
  <Quality_Assessment>
    <QUALITY_TABLES version="1.0">SPACEMETRIC</QUALITY_TABLES>
    <Quality_Parameter>
      <QUALITY_PARAMETER_DESC>Number of control
points</QUALITY_PARAMETER_DESC>
      <QUALITY_PARAMETER_CODE>SPACEMETRIC:NGCP</QUALITY_PARAMETER_CODE>
      <QUALITY_PARAMETER_VALUE>33</QUALITY_PARAMETER_VALUE>
    </Quality_Parameter>
    <Quality_Parameter>
      <QUALITY_PARAMETER_DESC>Root Mean Square residual error X
component</QUALITY_PARAMETER_DESC>
      <QUALITY_PARAMETER_CODE>SPACEMETRIC:RMSX</QUALITY_PARAMETER_CODE>
      <QUALITY_PARAMETER_VALUE
unit="M">11.200000000000001</QUALITY_PARAMETER_VALUE>
    </Quality_Parameter>
    <Quality_Parameter>
      <QUALITY_PARAMETER_DESC>Root Mean Square residual error Y
component</QUALITY_PARAMETER_DESC>
      <QUALITY_PARAMETER_CODE>SPACEMETRIC:RMSY</QUALITY_PARAMETER_CODE>
      <QUALITY_PARAMETER_VALUE unit="M">13.9</QUALITY_PARAMETER_VALUE>
    </Quality_Parameter>
  </Quality_Assessment>
  <Dataset_Use>
    <DATASET_CONTENT>Texas, USA</DATASET_CONTENT>
  </Dataset_Use>
  <Data_Processing>
    <GEOMETRIC_PROCESSING>1T</GEOMETRIC_PROCESSING>
    <RADIOMETRIC_PROCESSING>Cubic convolution</RADIOMETRIC_PROCESSING>
  </Data_Processing>
  <Coordinate_Reference_System>
    <GEO_TABLES>EPSG</GEO_TABLES>
    <Horizontal_CS>
      <HORIZONTAL_CS_CODE>EPSG:32614</HORIZONTAL_CS_CODE>
      <HORIZONTAL_CS_TYPE>PROJECTED</HORIZONTAL_CS_TYPE>
    </Horizontal_CS>
  </Coordinate_Reference_System>

```



DMC DATA PRODUCT MANUAL

DATE: 12-Feb-2010

DOC NO: 0115056

ISSUE: 02

STATUS: FINAL

```
<HORIZONTAL_CS_NAME>WGS 84 / UTM zone 14N</HORIZONTAL_CS_NAME>
<Projection>
  <PROJECTION_NAME>UTM zone 14N</PROJECTION_NAME>
  <PROJECTION_CODE>EPSG:16014</PROJECTION_CODE>
  <Projection_CT_Method>
    <PROJECTION_CT_NAME>Transverse Mercator</PROJECTION_CT_NAME>
    <PROJECTION_CT_CODE>EPSG:9807</PROJECTION_CT_CODE>
    <Projection_Parameters>
      <Projection_Parameter>

<PROJECTION_PARAMETER_NAME>Latitude_of_natural_origin</PROJECTION_PARAMETER_NAME>
  <PROJECTION_PARAMETER_VALUE
unit="DEG">0.0</PROJECTION_PARAMETER_VALUE>
  </Projection_Parameter>
  <Projection_Parameter>

<PROJECTION_PARAMETER_NAME>Longitude_of_natural_origin</PROJECTION_PARAMETER_NAME>
  <PROJECTION_PARAMETER_VALUE unit="DEG">-
98.9999999999999</PROJECTION_PARAMETER_VALUE>
  </Projection_Parameter>
  <Projection_Parameter>

<PROJECTION_PARAMETER_NAME>Scale_factor_at_natural_origin</PROJECTION_PARAMETER_NAME>
NAME>
<PROJECTION_PARAMETER_VALUE>0.9996</PROJECTION_PARAMETER_VALUE>
  </Projection_Parameter>
  <Projection_Parameter>

<PROJECTION_PARAMETER_NAME>False_easting</PROJECTION_PARAMETER_NAME>
  <PROJECTION_PARAMETER_VALUE
unit="M">500000.0</PROJECTION_PARAMETER_VALUE>
  </Projection_Parameter>
  <Projection_Parameter>

<PROJECTION_PARAMETER_NAME>False_northing</PROJECTION_PARAMETER_NAME>
  <PROJECTION_PARAMETER_VALUE
unit="M">0.0</PROJECTION_PARAMETER_VALUE>
  </Projection_Parameter>
  </Projection_Parameters>
</Projection_CT_Method>
</Projection>
<Geographic_CS>
  <GEOGRAPHIC_CS_NAME>WGS 84</GEOGRAPHIC_CS_NAME>
  <GEOGRAPHIC_CS_CODE>EPSG:4326</GEOGRAPHIC_CS_CODE>
  <Horizontal_Datum>
    <HORIZONTAL_DATUM_NAME>World Geodetic System
1984</HORIZONTAL_DATUM_NAME>
    <HORIZONTAL_DATUM_CODE>EPSG:6326</HORIZONTAL_DATUM_CODE>
  <Ellipsoid>
    <ELLIPSOID_NAME>WGS 84</ELLIPSOID_NAME>
    <ELLIPSOID_CODE>EPSG:7030</ELLIPSOID_CODE>
    <Ellipsoid_Parameters>
      <ELLIPSOID_MAJOR_AXIS
unit="M">6378137.0</ELLIPSOID_MAJOR_AXIS>
      <ELLIPSOID_MINOR_AXIS
unit="M">6356752.31424518</ELLIPSOID_MINOR_AXIS>
    </Ellipsoid_Parameters>
```

```

        </Ellipsoid>
        <Prime_Meridian>
            <PRIME_MERIDIAN_NAME>Greenwich</PRIME_MERIDIAN_NAME>
            <PRIME_MERIDIAN_CODE>EPSG:8901</PRIME_MERIDIAN_CODE>
            <PRIME_MERIDIAN_OFFSET
unit="DEG">0.0</PRIME_MERIDIAN_OFFSET>
        </Prime_Meridian>
    </Horizontal_Datum>
</Geographic_CS>
</Horizontal_CS>
</Coordinate_Reference_System>
<Geoposition>
    <Geoposition_Insert>
        <ULXMAP unit="M">355520.0</ULXMAP>
        <ULYMAP unit="M">3548480.0</ULYMAP>
        <XDIM unit="M">32.0</XDIM>
        <YDIM unit="M">32.0</YDIM>
    </Geoposition_Insert>
</Geoposition>
<Raster_CS>
    <RASTER_CS_TYPE>POINT</RASTER_CS_TYPE>
</Raster_CS>
<Dataset_Frame>
    <Vertex>
        <FRAME_X unit="M">751712.0</FRAME_X>
        <FRAME_Y unit="M">3548320.0</FRAME_Y>
    </Vertex>
    <Vertex>
        <FRAME_X unit="M">355680.0</FRAME_X>
        <FRAME_Y unit="M">3476320.0</FRAME_Y>
    </Vertex>
    <Vertex>
        <FRAME_X unit="M">409376.0</FRAME_X>
        <FRAME_Y unit="M">3228608.0</FRAME_Y>
    </Vertex>
    <Vertex>
        <FRAME_X unit="M">805280.0</FRAME_X>
        <FRAME_Y unit="M">3301088.0</FRAME_Y>
    </Vertex>
</Dataset_Frame>
<Raster_Encoding>
    <NBITS>8</NBITS>
    <DATA_TYPE>BYTE</DATA_TYPE>
    <BYTEORDER>M</BYTEORDER>
</Raster_Encoding>
<Data_Access>
    <DATA_FILE_FORMAT>GEOTIFF</DATA_FILE_FORMAT>
    <Data_File>
        <DATA_FILE_PATH href="DU000b63T_L1T.tif"/>
    </Data_File>
</Data_Access>
<Raster_Dimensions>
    <NCOLS>14061</NCOLS>
    <NROWS>10001</NROWS>
    <NBANDS>3</NBANDS>
</Raster_Dimensions>
<Image_Interpretation>
    <Spectral_Band_Info>

```

```

<BAND_INDEX>1</BAND_INDEX>
<BAND_DESCRIPTION>NIR</BAND_DESCRIPTION>
<PHYSICAL_GAIN>1.0749817168185152</PHYSICAL_GAIN>
<PHYSICAL_BIAS>13.31323795165322</PHYSICAL_BIAS>
<PHYSICAL_UNIT>W/m2/sr/m-6</PHYSICAL_UNIT>
</Spectral_Band_Info>
<Spectral_Band_Info>
  <BAND_INDEX>2</BAND_INDEX>
  <BAND_DESCRIPTION>Red</BAND_DESCRIPTION>
  <PHYSICAL_GAIN>0.8908284414984867</PHYSICAL_GAIN>
  <PHYSICAL_BIAS>5.724840466729124</PHYSICAL_BIAS>
  <PHYSICAL_UNIT>W/m2/sr/m-6</PHYSICAL_UNIT>
</Spectral_Band_Info>
<Spectral_Band_Info>
  <BAND_INDEX>3</BAND_INDEX>
  <BAND_DESCRIPTION>Green</BAND_DESCRIPTION>
  <PHYSICAL_GAIN>1.1722234734653645</PHYSICAL_GAIN>
  <PHYSICAL_BIAS>10.417201834872332</PHYSICAL_BIAS>
  <PHYSICAL_UNIT>W/m2/sr/m-6</PHYSICAL_UNIT>
</Spectral_Band_Info>
</Image_Interpretation>
<Image_Display>
  <Band_Display_Order>
    <RED_CHANNEL>1</RED_CHANNEL>
    <GREEN_CHANNEL>2</GREEN_CHANNEL>
    <BLUE_CHANNEL>3</BLUE_CHANNEL>
  </Band_Display_Order>
  <Special_Value>
    <SPECIAL_VALUE_INDEX>0</SPECIAL_VALUE_INDEX>
    <SPECIAL_VALUE_TEXT>nodata</SPECIAL_VALUE_TEXT>
  </Special_Value>
  <Band_Statistics>
    <BAND_INDEX>1</BAND_INDEX>
    <STX_LIN_MIN>-32.57339014206026</STX_LIN_MIN>
    <STX_LIN_MAX>248.33776104124735</STX_LIN_MAX>
    <STX_STDV>56.18223023666152</STX_STDV>
    <STX_MEAN>107.88218544959354</STX_MEAN>
    <STX_MIN>11.0</STX_MIN>
    <STX_MAX>241.0</STX_MAX>
  </Band_Statistics>
  <Band_Statistics>
    <BAND_INDEX>2</BAND_INDEX>
    <STX_LIN_MIN>-79.2137024983392</STX_LIN_MIN>
    <STX_LIN_MAX>255.0</STX_LIN_MAX>
    <STX_STDV>72.33002904174667</STX_STDV>
    <STX_MEAN>101.61137010602748</STX_MEAN>
    <STX_MIN>12.0</STX_MIN>
    <STX_MAX>237.0</STX_MAX>
  </Band_Statistics>
  <Band_Statistics>
    <BAND_INDEX>3</BAND_INDEX>
    <STX_LIN_MIN>-61.81851901297571</STX_LIN_MIN>
    <STX_LIN_MAX>255.0</STX_LIN_MAX>
    <STX_STDV>75.76671043023572</STX_STDV>
    <STX_MEAN>127.59825706261358</STX_MEAN>
    <STX_MIN>19.0</STX_MIN>
    <STX_MAX>247.0</STX_MAX>
  </Band_Statistics>

```



```
</Image_Display>
<Dataset_Sources>
  <Source_Information>
    <SOURCE_ID>DU000b63T</SOURCE_ID>
    <Coordinate_Reference_System>
      <GEO_TABLES>EPSG</GEO_TABLES>
      <Horizontal_CS>
        <HORIZONTAL_CS_CODE>EPSG:32614</HORIZONTAL_CS_CODE>
        <HORIZONTAL_CS_TYPE>PROJECTED</HORIZONTAL_CS_TYPE>
        <HORIZONTAL_CS_NAME>WGS 84 / UTM zone 14N</HORIZONTAL_CS_NAME>
      </Horizontal_CS>
    </Coordinate_Reference_System>
    <Source_Frame>
      <Vertex>
        <FRAME_X unit="M">751712.2769615828</FRAME_X>
        <FRAME_Y unit="M">3548331.055235964</FRAME_Y>
      </Vertex>
      <Vertex>
        <FRAME_X unit="M">805218.2251252305</FRAME_X>
        <FRAME_Y unit="M">3301352.5596380834</FRAME_Y>
      </Vertex>
      <Vertex>
        <FRAME_X unit="M">468608.242470778</FRAME_X>
        <FRAME_Y unit="M">3239612.5590642253</FRAME_Y>
      </Vertex>
      <Vertex>
        <FRAME_X unit="M">414960.80925907975</FRAME_X>
        <FRAME_Y unit="M">3486988.9375490705</FRAME_Y>
      </Vertex>
    </Source_Frame>
    <Scene_Source>
      <MISSION>UK-DMC</MISSION>
      <INSTRUMENT>SLIM-6</INSTRUMENT>
      <IMAGING_DATE>2007-07-30</IMAGING_DATE>
      <IMAGING_TIME>16:14:39</IMAGING_TIME>
      <VIEWING_ANGLE unit="DEG">1.70751061117751</VIEWING_ANGLE>
      <SUN_AZIMUTH unit="DEG">101.74181569705586</SUN_AZIMUTH>
      <SUN_ELEVATION unit="DEG">55.227078071950686</SUN_ELEVATION>
    </Scene_Source>
  </Source_Information>
</Dataset_Sources>
</Dimap_Document>
```

 International Imaging	DMC DATA PRODUCT MANUAL	DATE: 12-Feb-2010
		DOC NO: 0115056
		ISSUE: 02
		STATUS: FINAL

APPENDIX D: RADIOMETRIC CALIBRATION REPORT

Post-Launch Calibration of the UK-DMC Satellite Sensor

Prepared for DMC International Imaging Ltd by:

Dr. Stephen Mackin
Surrey Space Centre
University of Surrey

Document Version 1.3

	DMC DATA PRODUCT MANUAL	DATE: 12-Feb-2010
		DOC NO: 0115056
		ISSUE: 02
		STATUS: FINAL

CONTENTS

1. Introduction

2. Initial Data Analysis And Characterisation

- 2.1. Deep Space Images
- 2.2. Snow Scenes

3. Procedural Overview

- 3.1. Relative Calibration
 - 3.1.1. Dark Images
 - 3.1.2. Snow Scenes
- 3.2. Absolute Calibration

4. Procedural Details

- 4.1. Relative Calibration
 - 4.1.1. Dark Images
 - 4.1.2. Snow Scenes
 - 4.1.2.1. Antarctica
 - 4.1.2.2. Greenland
 - 4.1.2.3. Geometry And BRDF Effects
 - 4.1.2.3.1. Test 1 – Nominal Acquisition / Yaw 180° Acquisition
 - 4.1.2.3.2. Test 2 – Yawed Imager For Equal Illumination Conditions
- 4.2. Absolute Calibration
 - 4.2.1. Ground Site And Observations
 - 4.2.2. Results And Processing The Coefficients
 - 4.2.3. Scaling

5. Results

6. Further work

- 6.1. Cross-Calibration
- 6.2. Stability Measurements
- 6.3. BRDF Studies

7. Summary

8. Acknowledgments

	DMC DATA PRODUCT MANUAL	DATE: 12-Feb-2010
		DOC NO: 0115056
		ISSUE: 02
		STATUS: FINAL

1 Introduction

In this document the calibration procedure of the UK-DMC satellite sensor is described. The study was carried out in several phases, the initial phase was to analyse the data and characterise the responses from dark (no signal) and bright targets. Once completed an extensive literature search was carried out to determine the best procedures to apply to calibrate such a large sensor array (20,000 detectors over two arrays).

Absolute calibration is described only in overview, as the data collection and data analysis were carried out by the Remote Sensing Group at the University of Arizona (RSG) under Kurt Thome. However, the results of the analysis are presented later in this document.

The extension of the absolute calibration of a few detectors to the whole array (the relative calibration), is described in some detail, including some of the issues related to data collection and variations in the surface response.

Finally the results of the study are illustrated (comparing the raw and calibrated data) and further work required is indicated.

2 Initial Data Analysis And Characterisation

Prior to developing the full calibration methodology, we carried out a series of tests for each detector array (Imager0 and Imager1) for each sensor (green, red and NIR bands) to characterise their response to both dark and bright targets.

2.1 Deep Space Images

Immediately after launch, UK-DMC had not deployed the gravity gradient boom and thus was more manoeuvrable. It was decided therefore to use this opportunity to collect deep space images to help characterise the sensor arrays. Only two imaging opportunities were available prior to boom deployment.

2.2 Snow Scenes

Given the size of the image arrays and the requirements for a very large swath with a uniform background radiance, a brief review of the literature pointed to targets used by the AVHRR sensor in Antarctica and Greenland (see Figure 14), which covered the required area extent and had the necessary radiometric stability. Given the autumn launch data, targets were acquired over the Antarctic, coinciding with the DOME-C site used by AVHRR and the SPOT-Vegetation instruments.

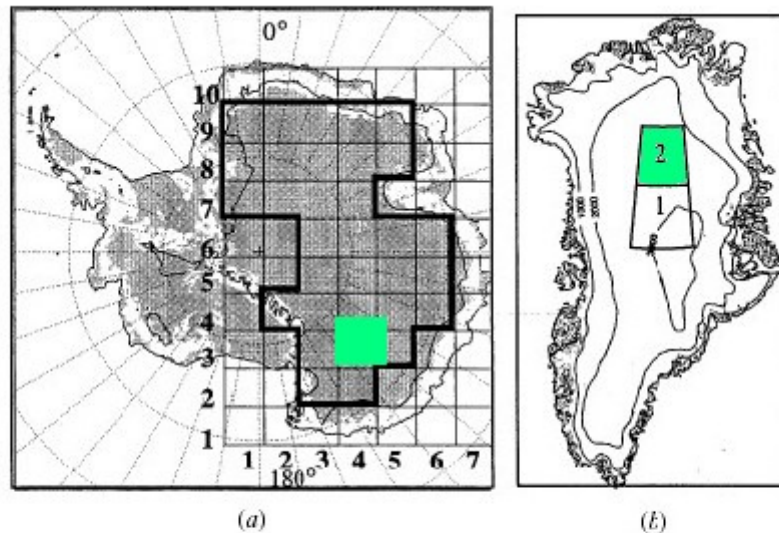


Figure 1 (a) Regions of the Antarctic continent with slope < 0.006 radians (0.34°) at 10 km resolution (shaded), with the height contour for 2000m superimposed. The 32 gridboxes (~ 444 km on a side) for which individual monthly plots of χ_{ds} are generated are outlined. (b) The two gridboxes on the Greenland high plateau used in this study. Both gridboxes are bounded by longitudes 35° and 45° W; the latitudes spanned are $72-75^\circ$ N for gridbox 1 and $75-78^\circ$ N for gridbox 2. The two maps are on different scales.

Figure 14: Site location map showing Antarctic and Greenland test sites (green boxes)⁸

3 Procedural Overview

Based on the initial data characterisation, we were able to clearly define a procedure of data collection for the relative calibration of our DMC sensor arrays. The final element required was to then tie these relative values to a set of absolute physical measurements of radiance.

3.1 Relative Calibration

3.1.1 Dark Images

The initial results of our study showed that the dark images from deep space had a fixed pattern structure for each CCD array that was not dependent on the integration time used for the image acquisition (in other words an additive component).

Figure 15 and Figure 16 show the average detector responses (in DN) across the even pixels for the red band of Imager0. Note the fixed pattern variation across the CCD array for these two deep space images. Peaks coincide in location and amplitude, suggesting a stable, additive response for our dark images. Note also the small step (pixel 4000 in Figure 15 and pixel 3000 in Figure 16), these features will be discussed later in the report.

⁸ Masonis and Warren (2001).

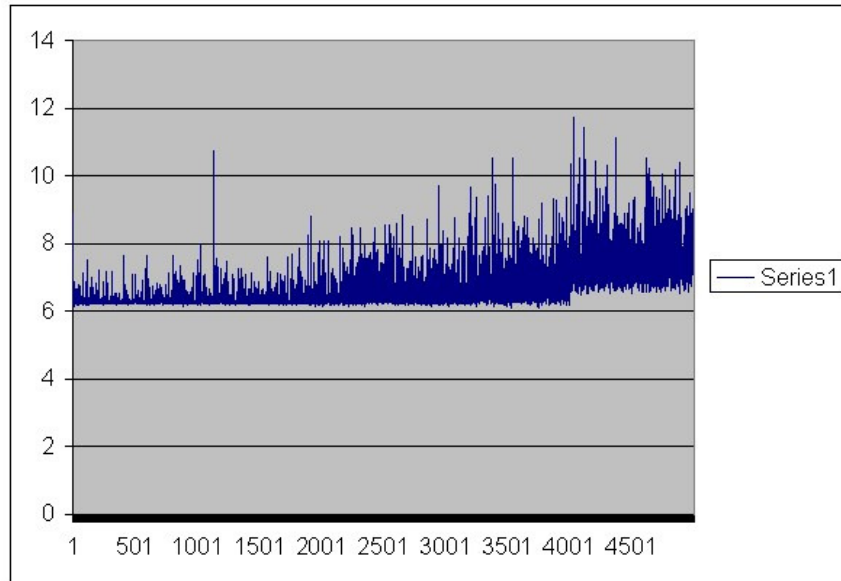


Figure 15: Red even pixels – DU000009pm (integration time 1,500 μs)

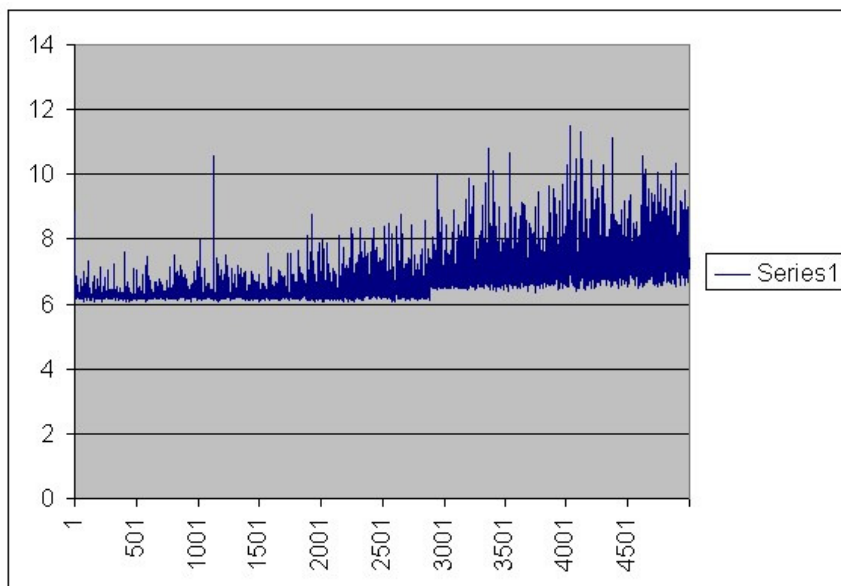


Figure 16: Red even pixels – DU000010pm (integration time 2,400 μs)

The results gave us confidence that we could extract stable measurements of the additive component for our calibration. However, as soon as the gravity gradient boom was extended, we could not carry out further observations of deep space. Hence, we had to consider alternatives to our deep space measurements. In this case we chose to observe the Pacific Ocean at night to try and derive our coefficients. The results confirmed that the Pacific Ocean at night provided the same level of information as derived from our deep space observations.

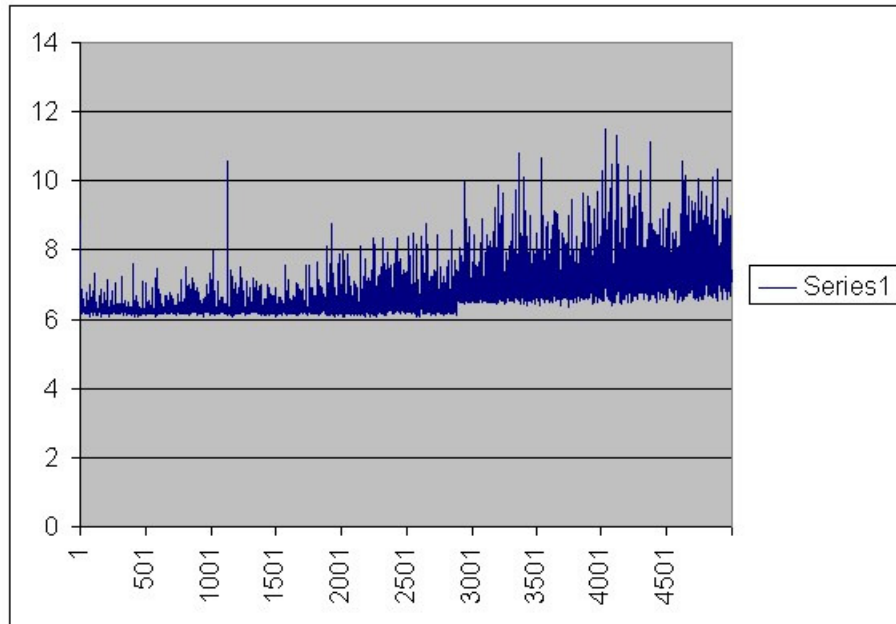


Figure 17: Deep Space image (DU000010pm red even pixels)

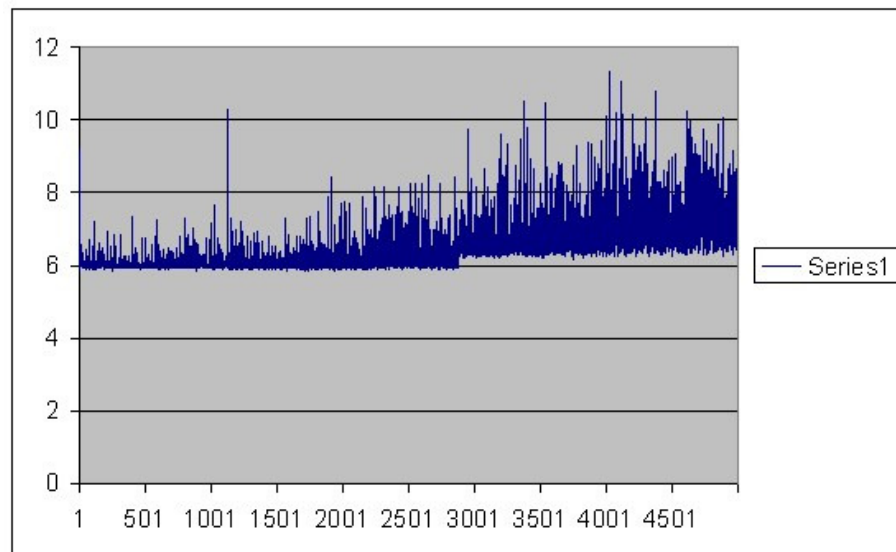


Figure 18: Pacific Ocean at night image (DU000020pm red even pixels)

In Figure 17 and Figure 18 we compare the Deep Space image for the Imager0, red band, even pixels; against the equivalent Pacific Ocean at night image. The offsets and magnitude are comparable to a high level of precision.

3.1.2 Snow Scenes

The initial results of the snow scene analysis also showed a very stable result under varying integration times, the overall scene DN scaling in proportion to the integration time in a linear manner (as determined in the lab, pre-launch).

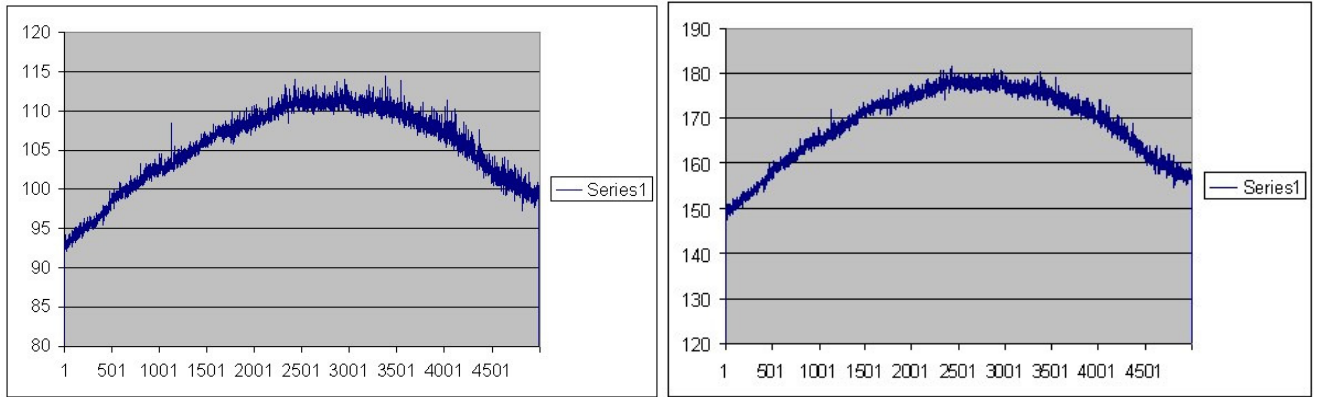


Figure 19: Comparison of Antarctic scenes DU00001cpm (left) and DU00001apm (right)

As shown in Figure 19 the overall response is similar, the DN values are different as different integration times were used. DU00001cpm had an integration time of 320 μ s, whereas DU00001apm had an integration time of 512 μ s.

The curvature of the response shown in Figure 19 is expected, as it is a function of the \cos^4 variation between a detector in the centre of the CCD array and one at the edge of the CCD array. Also, note the slight asymmetry in the snow scene response across the array.

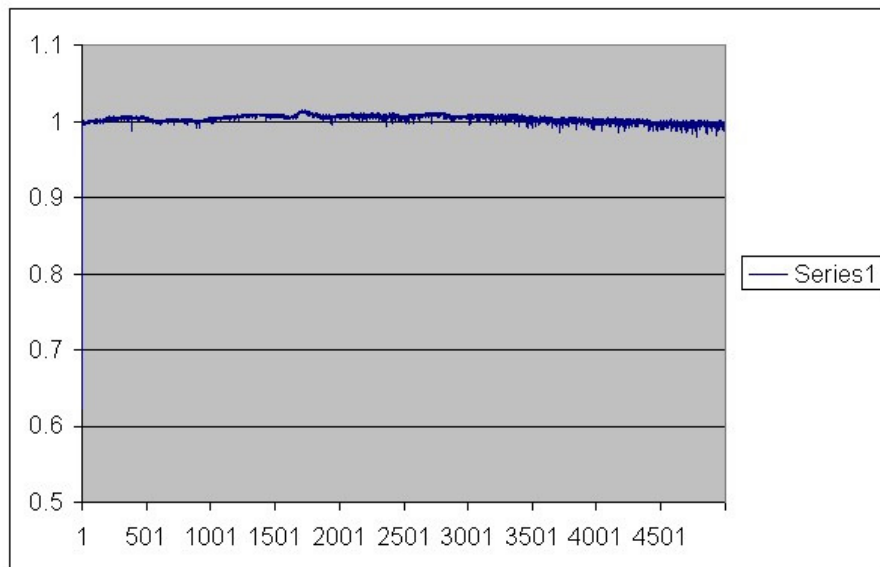


Figure 20: Ratio of the two plots in Figure 19

The results in Figure 20 suggest that the system response is stable for our snow scenes at the 1-2% level. Several other images were examined to confirm this result.

3.2 Absolute Calibration.

For an accurate absolute calibration we require a homogeneous site, with relatively stable atmospheric conditions, that is large enough to cover several pixels within our scene. We also require the necessary instrumentation at the site to characterise the surface at the time of scene acquisition and measure various atmospheric parameters such as aerosol size distribution (using a sun photometer) and variations in atmospheric parameters such as water vapour (using radiosondes).

None of this was available to us in the UK. We therefore decided to carry out a co-operative study with Kurt Thome and RSG to carry out this essential step. A two-week block of time in July 2004 was allocated for the study at the Railroad Valley site in Nevada, USA.

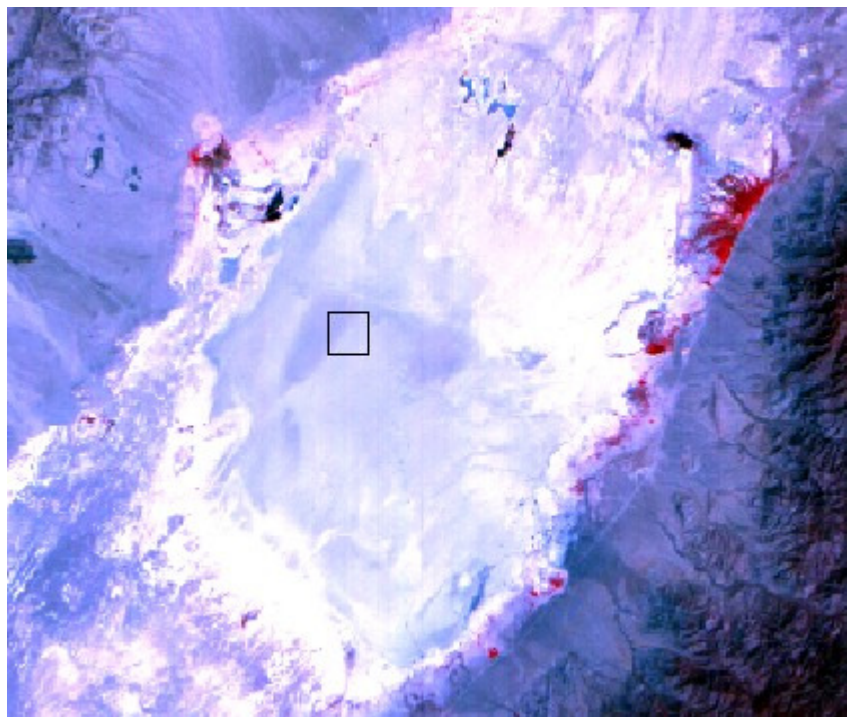


Figure 21: Railroad Valley calibration site (DMC image)

The equipment and some of the personnel were provided by RSG, along with two members of SSTL staff to help in the data collection. Ground data collection with field spectrometers, combined with atmospheric measurements were timed to occur with each overpass of all four of the satellites currently in the DMC constellation (including the UK-DMC). The ground data was retained by RSG and the results of the analysis were provided in the form of TOA radiances to SSTL.

It was decided to repeat this study on an annual basis to monitor degradation of the satellite sensor response over the satellite lifetime (nominally five years).

4 Procedural Details

In this section the detailed analysis of the dark images and snow scenes is given and the corresponding procedures to obtain the absolute calibration coefficients for the whole scene.

4.1 Relative Calibration

4.1.1 Dark Images

Initial results of comparing deep space images and those taken over the Pacific Ocean at night, showed that the pattern variation of the CCD arrays was constant and independent of the integration time. However, it was noted that there were small step features in the output data from the different data collections.

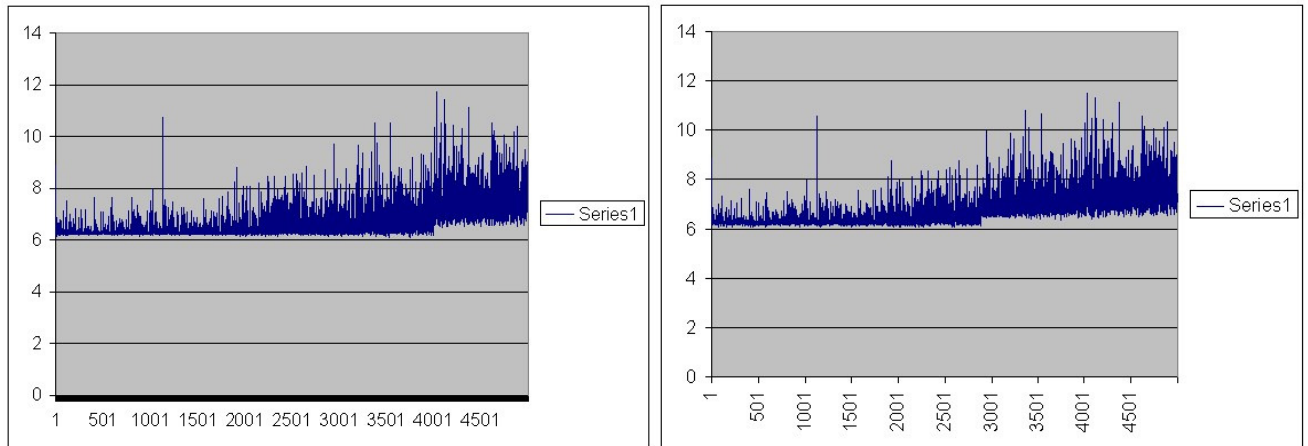


Figure 22: Comparison of dark images DU000009pm (left) and DU000010pm (right)

Figure 22 shows the comparison between two dark images of deep space; note the difference in the step position in the two plots. For any particular image these step features were in the same position for all spectral bands, but from one image to the next the position and magnitude of the step did vary. To highlight these features, we ratioed the plots, we also subtracted one plot from the other to measure the magnitude of the variations.

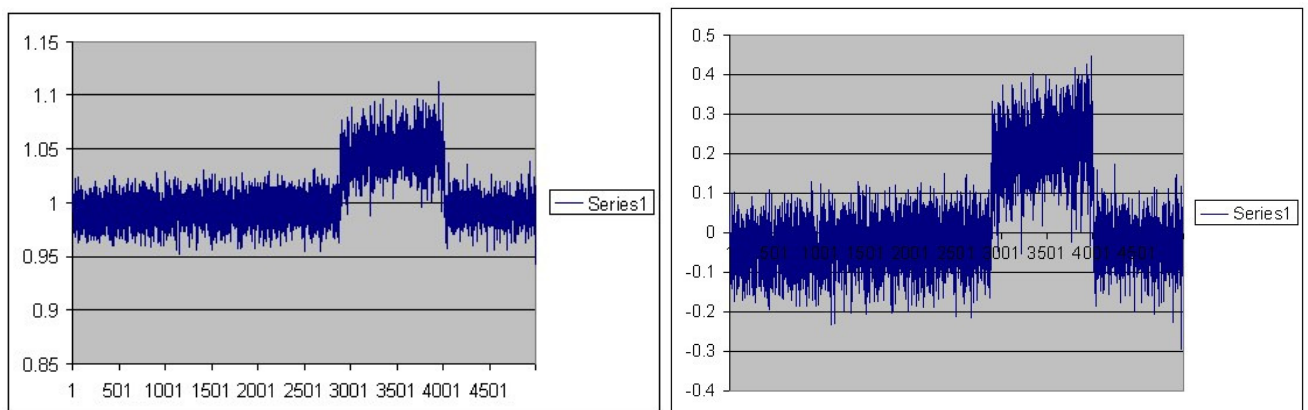


Figure 23: Analysis of the two plots in Figure 22 - ratio (left); magnitude difference (right)

The results show that the offsets produce a 5% difference in the values between two different dark images. This seems large, but only produces a 0.25 DN variation in the output values. However, it was decided to analyse all the dark images and determine the best image (most stable) to use to calculate the dark image calibration bias values to apply in the calibration process. Comparisons showed that these offsets were present in almost all the images to a larger or smaller degree.

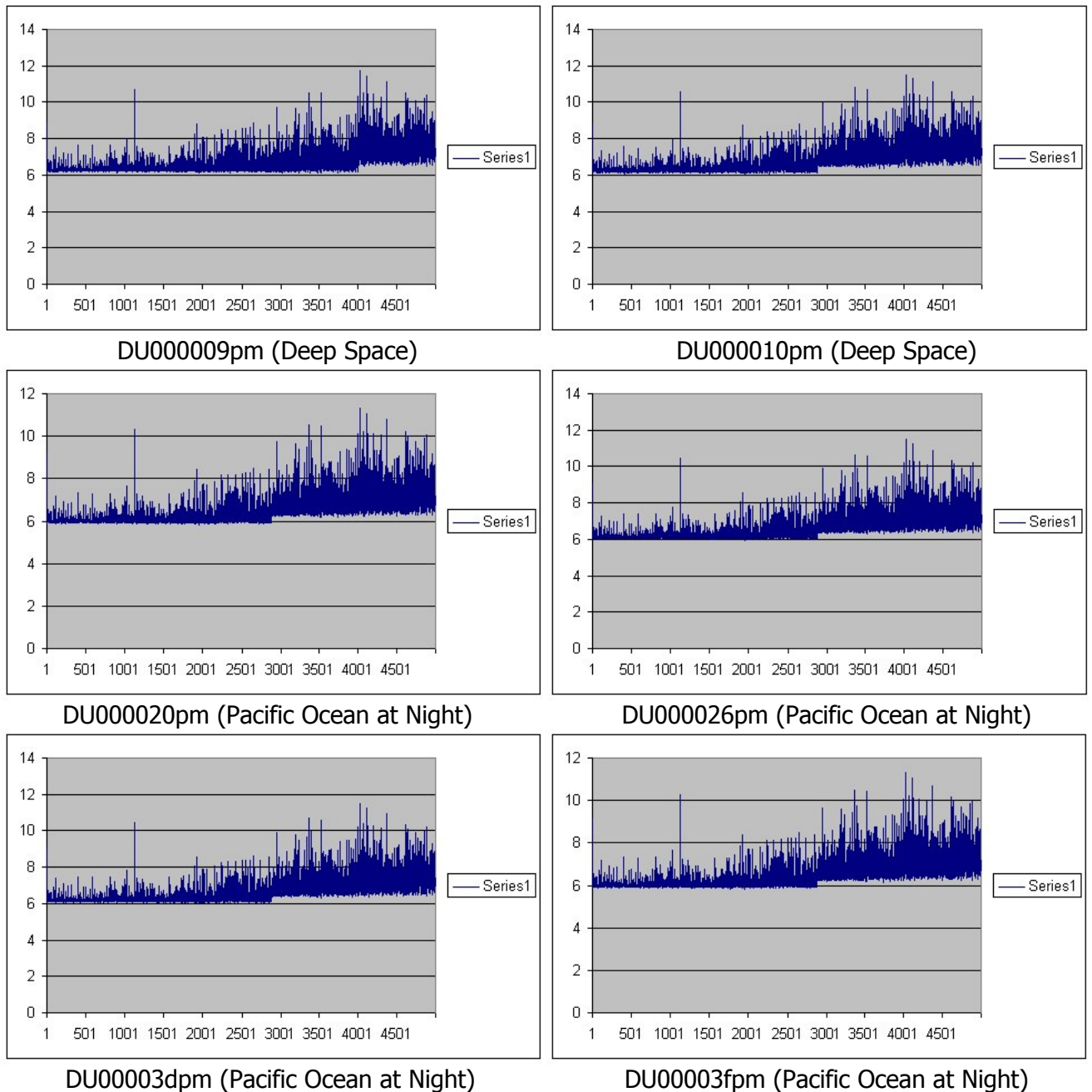


Figure 24: Comparison of the dark images for the red even pixels on Imager0

Figure 24 shows that the position of the offset, although variable, did occur in more or less the same place for any single image, the only unusual image being DU000009pm, which had a different offset

to the rest. It was decided therefore to use the deep space image DU000010pm as the baseline image for calculation of the calibration bias values.

4.1.2 Snow Scenes

4.1.2.1 Antarctica

The initial data collection of snow scenes took place over the Antarctic site (DOME-C) during the period November 2003 – February 2004. Initial data collections were saturated in the green and red bands and the integration time was therefore reduced to capture suitable images for calibration. Images were also captured in the period November 2004 – February 2005.

The data collections were remarkably cloud free, as shown by the repeatability of the results and the absence of artefacts when comparing scene acquisitions from different dates.

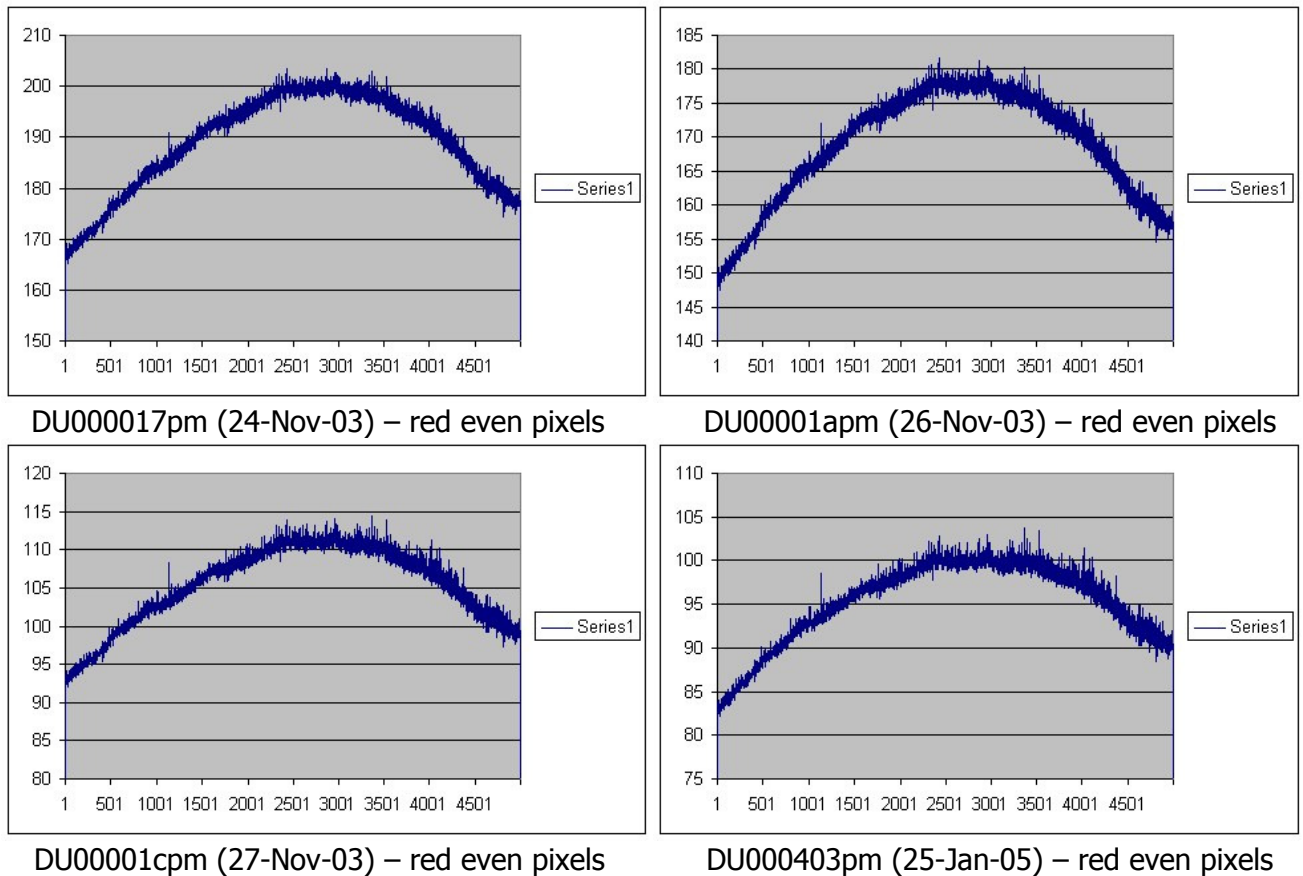
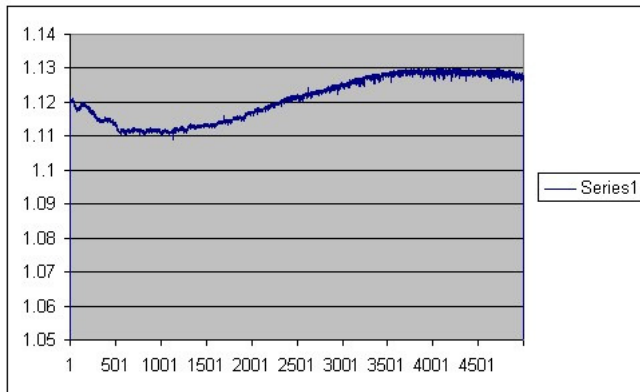


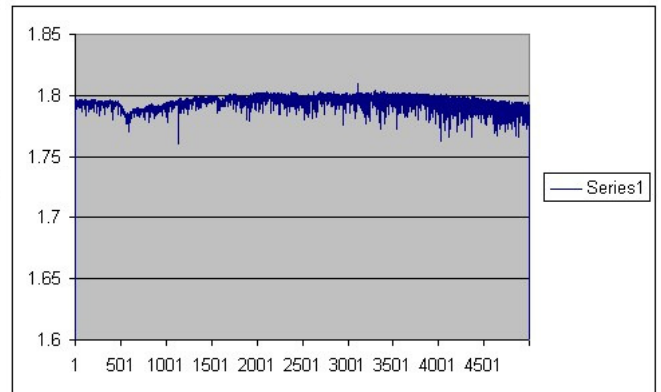
Figure 25: Comparison of the Antarctic images for the red even pixels on Imager0

Figure 25 confirms that images taken over one year after the initial data collections show the same level of stability in terms of relative response across the detector arrays (comparing DU000017pm with DU0000403pm).

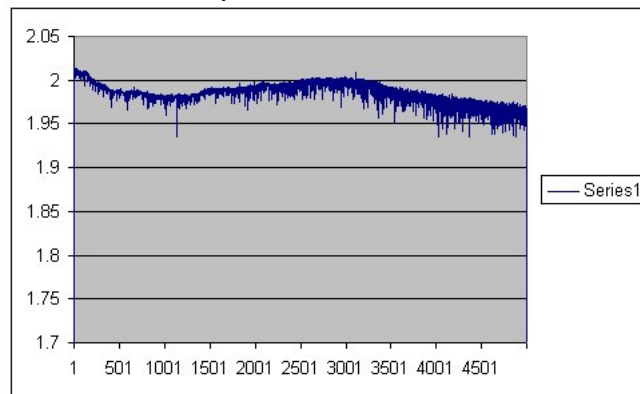
If we ratio the corresponding plots we can see any specific differences between image acquisitions. Figure 26 illustrates the ratios of DU000017pm against the other three images (DU00001apm, DU00001cpm and DU0000403pm).



Ratio of DU000017pm and DU00001apm



Ratio of DU000017pm and DU00001cpm



Ratio of DU000017pm and DU0000403pm

Figure 26: Ratio of Antarctic plots from Figure 25 for the red even pixels on Imager0

The plots in Figure 26 show that the response is reasonably consistent across the detector array. There is some structure present, which may be due to a combination of surface features, plus variations in the illumination geometry (see §4.2.3). When compared against other images, scene DU00001cpm was considered the most stable and free from artefacts. This was selected for the initial calibration of the UK-DMC to derive the calibration gain values.

4.1.2.2 Greenland

Over 30 images were taken over Greenland during the northern hemisphere summer of 2004. Almost all these images contained cloud, which could be easily discriminated from the underlying snow.

To date, no Greenland images have been used in the analysis due to the high level of cloud present in the imagery.

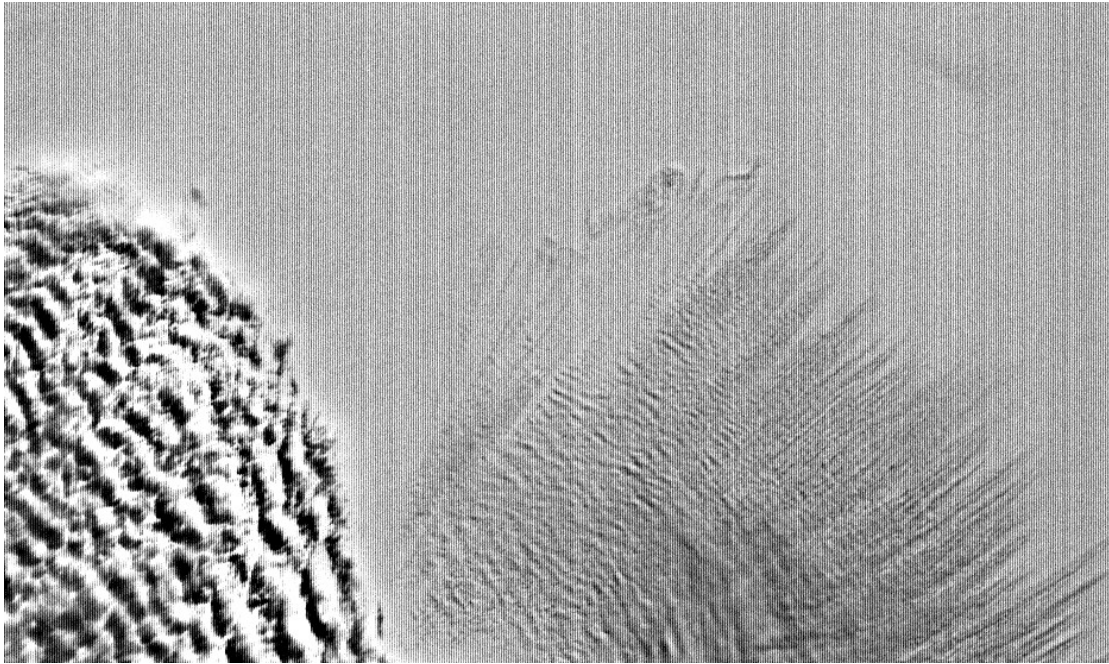


Figure 27: Subsection of a UK-DMC image over Greenland

Figure 27 shows the presence of cloud, which was typical for the Greenland images, and vertical striping due to the odd-even detector processing.

4.1.2.3 Geometry And BRDF Effects

As noted earlier in this report, the plots of the response curves for the red even pixels on Imager0 showed a marked asymmetry (Figure 25), with a much lower value on the left limb than the right, by as much as 9%.

It was considered that this variation could have three possible sources:

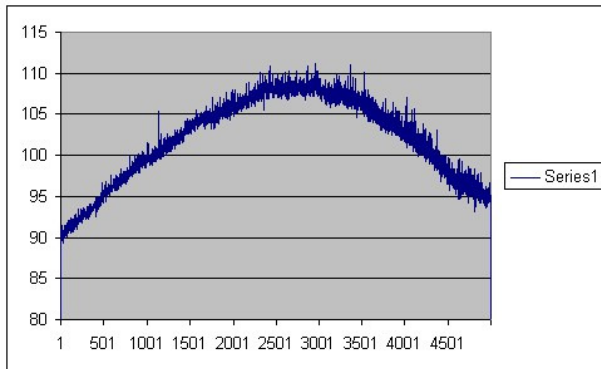
- Variation in the response of the optical system across the scene.
- Geometric considerations, a variable solar zenith angle will produce a higher response for the detector imaging an area closer to the sub-solar point.
- BRDF effects, due to the natural surface variability of snow (strongly forward scattering) over the 26° FOV of each imager.

To test this we carried out three experiments:

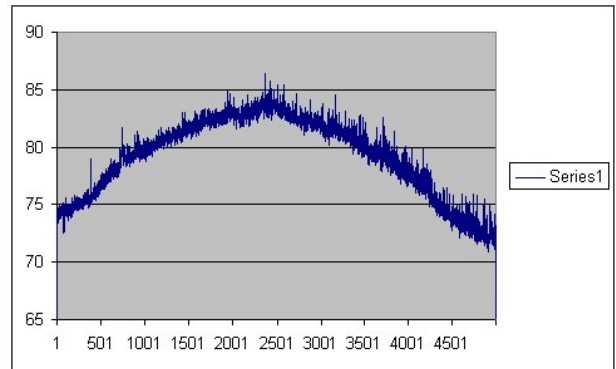
- Image acquisition during nominal spacecraft operations (spacecraft yaw=0°)
- Image acquisition when spacecraft yawed 180°
- Image acquisition when spacecraft yawed to illuminate both sides of the CCD array equally

4.1.2.3.1 Test 1 – Nominal Acquisition / Yaw 180° Acquisition

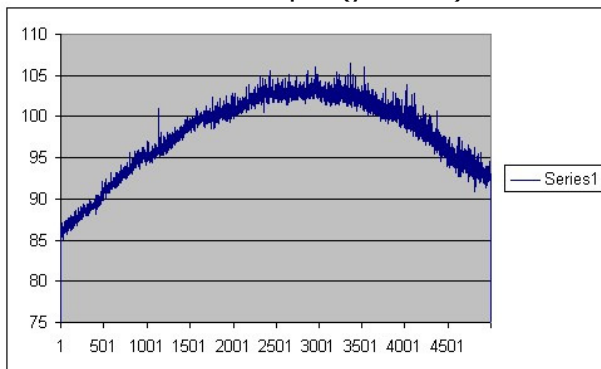
Several images were taken in January 2005 using the normal imaging orientation to provide a benchmark for the comparison against the yawed image. The plots for the red even pixels on Imager0 are shown in Figure 28. Details for each image are given in Table 23.



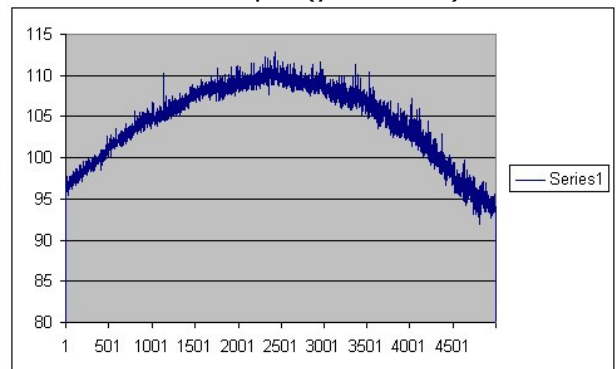
DU0003f1pm (yaw=0°)



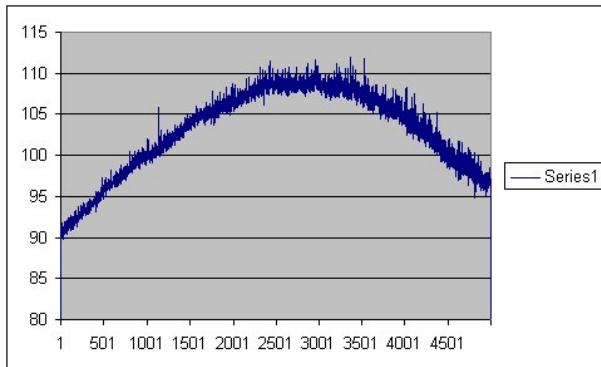
DU0003f4pm (yaw=180°)



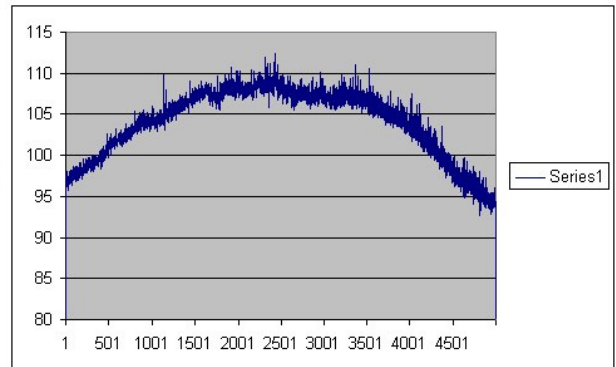
DU0003f6pm (yaw=0°)



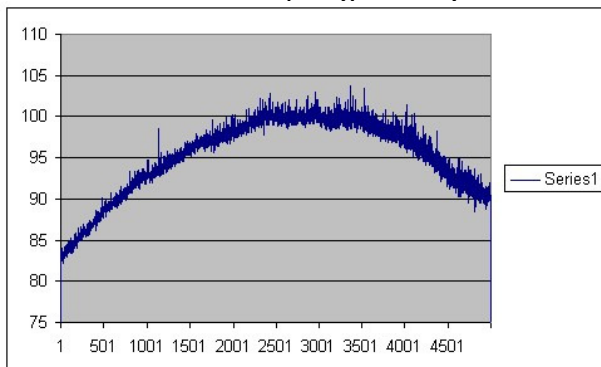
DU0003fbpm (yaw=180°)



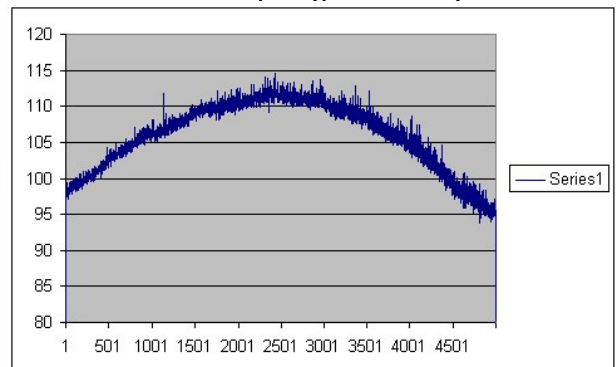
DU0003fdpm (yaw=0°)



DU000400pm (yaw=180°)



DU000403pm (yaw=0°)



DU00040epm (yaw=180°)

Figure 28: Comparison of responses for images acquired when yaw=0° and yaw=180°

In the normal imaging mode, there is a distinct asymmetry across Imager0. With a much lower value on the extreme left compared to the extreme right. However, when the spacecraft is yawed through 180°, the direction of the asymmetry is reversed, which suggests that it is largely due to surface variations in reflected radiation, rather than the optics. These variations will be due to both geometry and BRDF effects of the surface.

Scene ID	Image Date	Image Time (UTC)	Solar Elevation Angle	Spacecraft Yaw Angle
DU0003f1	19-Jan-2005	04:23:30	35.292°	0°
DU0003f4	20-Jan-2005	03:23:06	34.742°	180°
DU0003f6	20-Jan-2005	05:00:43	34.702°	0°
DU0003fb	22-Jan-2005	04:37:45	34.546°	180°
DU0003fd	23-Jan-2005	03:37:24	34.241°	0°
DU000400	24-Jan-2005	04:14:44	34.188°	180°
DU000403	25-Jan-2005	04:51:59	33.687°	0°
DU00040e	28-Jan-2005	03:28:43	32.874°	180°

Table 23: Acquisition details for the images in Figure 28

Note that the magnitude of the variation is greater in the normal flight images rather than the yawed images. This suggests that there is an asymmetry in response of the imager combined with the surface effects.

4.1.2.3.2 Test 2 – Yawed Imager For Equal Illumination Conditions

To test this we orientated the spacecraft so that each side of the imager had the same effective illumination, by yawing the spacecraft through 36.8 degrees, so that the imaging array was lined up at 90 degrees to the projected plane containing the sub-solar point.

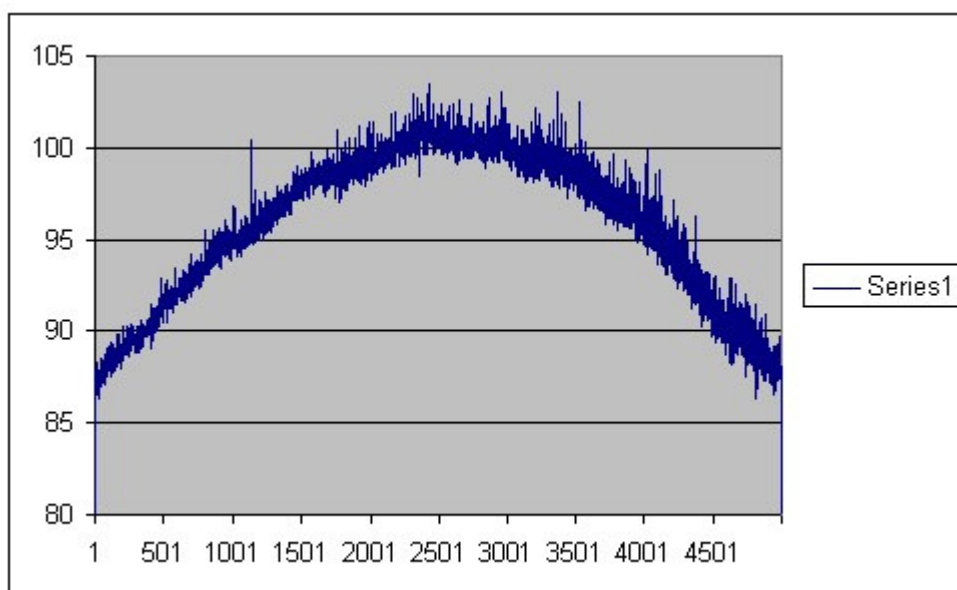


Figure 29: Response of red even pixels on Imager0 for equally illuminated scene (DU000420pm)

As can be seen in Figure 29, there is no pronounced asymmetry in the response when the scene is equally illuminated. Further work is required to identify the cause of the differences in the normal flight and yawed images in Figure 28.

However, the more uniform response from image DU000420pm (Figure 29) can be used to replace scene DU00001cpm in deriving the coefficients for calibration of the UK-DMC in future, removing a substantial part of the effects due to geometry and BRDF of the snow surface.

4.2 Absolute Calibration

In this section we will briefly describe the ground site and observations made, the results from the test site at Railroad Valley (RRV) in Nevada, USA and how the final calibration was carried out for all the detectors (20,000) over the two CCD arrays for each spectral band.

4.2.1 Ground Site And Observations

The ground measurements were performed at the small footprint test site (see Figure 30), located next to the atmospheric measurement area and CIMEL sun photometer. Table 24 shows the date, collection type and the DMC satellites that acquired an image over the test site.

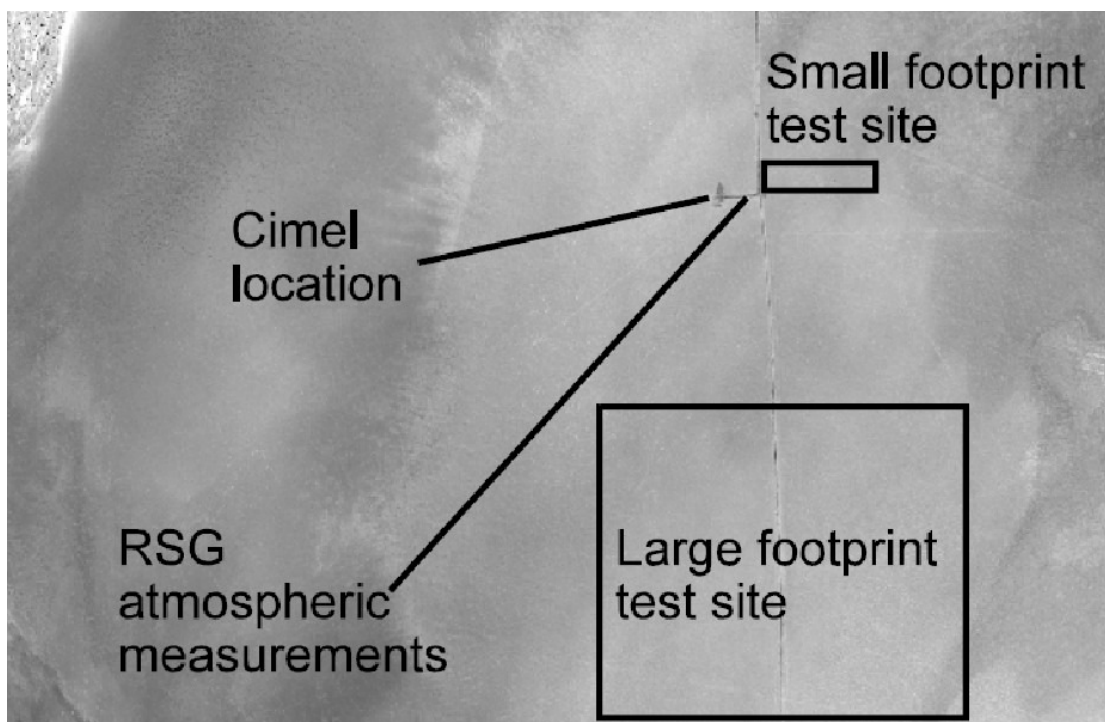


Figure 30: Railroad Valley test site (ASTER image provided by RSG)

	DMC DATA PRODUCT MANUAL	DATE: 12-Feb-2010
		DOC NO: 0115056
		ISSUE: 02
		STATUS: FINAL

Date	Collection Type	Satellite
03-July-2004	Dedicated	AlSat-1, UK-DMC
04-July-2004	Dedicated	BILSAT-1
05-July-2004	Dedicated	AlSat-1, NigeriaSat-1
06-July-2004	Poor Weather	---
07-July-2004	Dedicated	BILSAT-1, NigeriaSat-1
08-July-2004	Associated	AlSat-1
09-July-2004	Dedicated	BILSAT-1, UK-DMC
10-July-2004	Associated	NigeriaSat-1
11-July-2004	Dedicated	UK-DMC

Table 24: List of acquisitions over the RRV test site in July 2004

Most acquisitions were dedicated (the data were collected specifically for the satellite overpass), some were associated with other satellites. The important overpasses for our study were those for UK-DMC.

For each of the overpasses, ground measurements were taken, starting half an hour before the overpass, until half an hour after the overpass. Meteorological parameters were also measured at the same time.

Once the images were collected, the SSTL imaging team determined which pixels from the imagery coincided with the test site and determined the corresponding view zenith and view azimuth angles, as well as the solar zenith and solar azimuth at the time of acquisition. The values in Table 25 show the X and Y offsets in the imagery for each spectral band and the corresponding DN values captured in the raw imagery for image scene DU00017dpm, which was acquired on 03-July-2004 with a view zenith angle of 23.49°.

NIR			Red			Green		
X	Y	DN	X	Y	DN	X	Y	DN
785	1213	91	773	1216	113	786	1226	156
786	1213	98	774	1216	118	787	1226	153
786	1212	100	774	1215	117	787	1225	153
787	1212	92	775	1215	114	788	1225	157
788	1212	95	776	1215	121	789	1225	155
788	1211	100	776	1214	120	789	1224	156
789	1211	91	777	1214	115	790	1224	160
790	1211	101	778	1214	122	791	1224	154
791	1211	93	779	1214	115	792	1224	161
791	1210	91	779	1213	115	792	1223	159
792	1210	98	780	1213	123	793	1223	154
793	1210	91	781	1213	116	794	1223	156

Table 25: Pixel location and DN values from image scene DU00017dpm

Similar values were extracted for the other acquisitions, each with different view zenith angles to the calibration test site, as illustrated in Table 26.

Date	Scene ID	Imager ID	View Zenith
03-July-2004	DU00017dpm	Imager0	23.49°
09-July-2004	DU000186sm	Imager1	25.32°
11-July-2004	DU00018apm	Imager0	14.08°

Table 26: View zenith angles for the UK-DMC image acquisitions

As can be seen, the first two images were from the extremes of Imager0 and Imager1. Given that BRDF effects are more prominent at angles exceeding 18°, it was decided to use the third image (DU00018apm) as the primary acquisition to derive the calibration coefficients for the imaged area at the test site.

The RSG requested the filter specifications for each of the sensors and the corresponding information on view zenith, solar zenith and solar azimuth of each acquisition, so as to derive the equivalent radiance at the top of the atmosphere (TOA), by using a radiative transfer code to transform the measured surface reflectances to equivalent TOA radiances. Examples of the filter response data used by the RSG are shown in Figure 31.

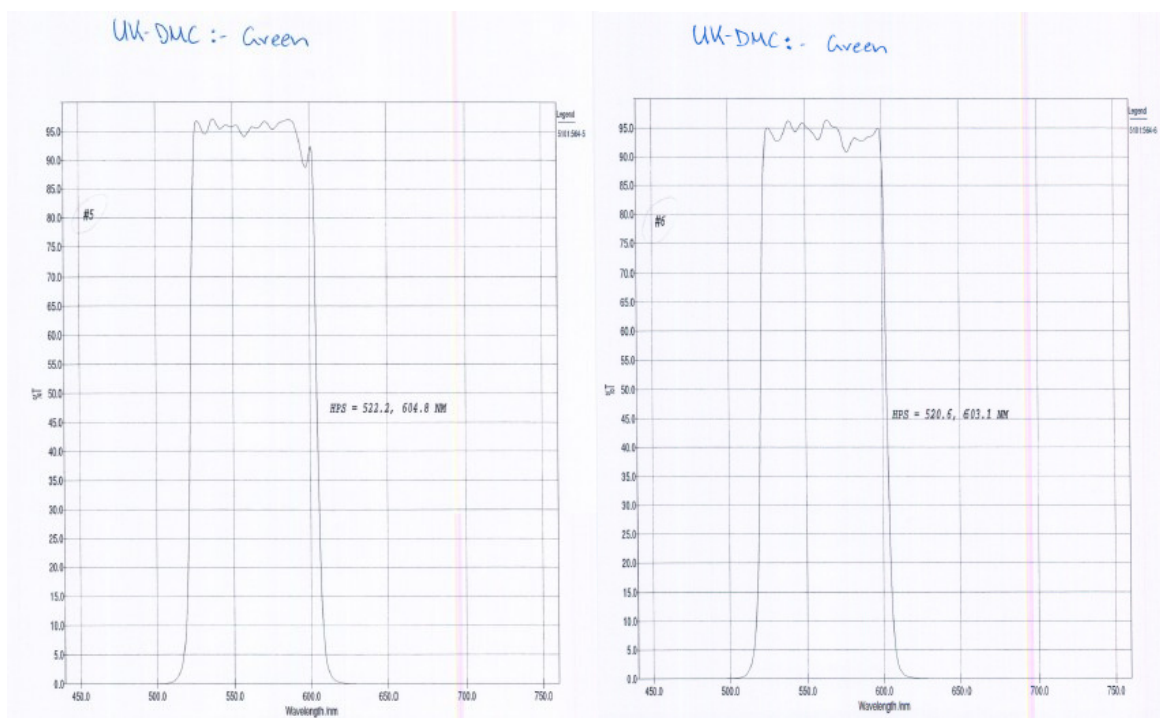


Figure 31: Filter response curves for the green spectral filter on Imager0 and Imager1

The results of the TOA calculation are split over three files for each acquisition, detailing the atmospheric conditions, the radiometry and summary radiometry values for each spectral band. These files were supplied by the RSG and example data from each file are shown in Figure 32, Figure 33, and Figure 34.



DMC DATA PRODUCT MANUAL

DATE: 12-Feb-2010

DOC NO: 0115056

ISSUE: 02

STATUS: FINAL

```

Date: 040703
Latitude:      38.4970
Longitude:    -115.691
ASR: 2K
Earth-Sun distance (AU):      1.0167045
Overpass Time:      17.4167
Overpass Angstrom      1.01795
ASR intercepts: 49970 46490 55640 47440 39900 40880 38070 37230 94760 26850
  
```

Mean molecular optical depths: 0.3742 0.3126 0.2078 0.1043 0.0546 0.0368 0.0204 0.0152 0.0108 0.0065

Note: aerosol optical depths are FITTED. To compute exactly, use airmass, intercepts, and voltage.

Jul. Day	Time	Airmass	Ozone (DU)	Angstrom	--- WATER VAPOUR ---		----- AEROSOL				
					Op. depth	Amt (g/cm ³)	0.379	0.400	0.440	0.519	0.61:
185.5537	13.2892	6.3827	0	0.000	0.318	1.439	0.000	0.000	0.000	0.000	0.000
185.5542	13.3019	6.2913	311	0.900	0.292	1.240	0.061	0.058	0.053	0.046	0.040
185.5549	13.3186	6.1757	310	0.911	0.295	1.238	0.062	0.059	0.054	0.046	0.040
185.5556	13.3356	6.0622	312	0.925	0.297	1.240	0.062	0.059	0.054	0.046	0.040
185.5563	13.3519	5.9562	312	0.938	0.299	1.239	0.061	0.058	0.053	0.046	0.039
185.5570	13.3689	5.8502	314	0.932	0.301	1.233	0.062	0.059	0.054	0.046	0.040
185.5577	13.3853	5.7510	312	0.947	0.302	1.227	0.062	0.059	0.054	0.046	0.040
185.5584	13.4019	5.6534	313	0.942	0.305	1.228	0.062	0.059	0.054	0.046	0.040
185.5591	13.4186	5.5589	318	0.958	0.306	1.225	0.062	0.059	0.054	0.046	0.039
185.5598	13.4353	5.4673	316	0.962	0.309	1.226	0.062	0.059	0.054	0.046	0.039
185.5605	13.4522	5.3771	318	0.967	0.311	1.226	0.062	0.059	0.054	0.046	0.039
185.5612	13.4686	5.2925	317	0.948	0.313	1.225	0.062	0.059	0.054	0.046	0.040
185.5619	13.4853	5.2091	318	0.951	0.315	1.225	0.062	0.059	0.054	0.046	0.040
185.5626	13.5025	5.1255	320	0.958	0.318	1.227	0.062	0.059	0.054	0.046	0.039
185.5633	13.5186	5.0496	321	0.966	0.320	1.227	0.062	0.059	0.054	0.046	0.039
185.5640	13.5353	4.9733	319	0.972	0.322	1.228	0.062	0.059	0.054	0.046	0.039
185.5647	13.5519	4.8992	320	0.973	0.325	1.231	0.062	0.059	0.054	0.046	0.039
185.5654	13.5686	4.8272	320	0.966	0.326	1.227	0.062	0.059	0.054	0.046	0.039
185.5661	13.5853	4.7572	319	0.978	0.329	1.231	0.062	0.059	0.054	0.046	0.039
185.5667	13.6019	4.6892	320	0.965	0.330	1.229	0.062	0.059	0.054	0.046	0.039
185.5674	13.6186	4.6230	322	0.953	0.332	1.229	0.062	0.059	0.054	0.046	0.040

Figure 32: Example data detailing the atmospheric conditions

Headings are: Wavelength (nanometres)
 Aerosol, molecular, and ozone optical depths,
 Gas transmittance (species listed above),
 Aerosol single-scattering albedo,
 Measured surface reflectance,
 Exoatmospheric solar irradiance,
 - computed from Thuillier plus corrected Kurucz database, scaled by square of Earth-Sun distance
 Relative radiance (reflectance of atmosphere containing no absorbing gases except ozone)
 Reflected radiance (reflectance of atmosphere containing absorbing gases)
 Absolute (top-of-atmosphere) radiance

Wavel (nm)	---- Optical Depths ----			Gas Trans.	Aerosol SSA	Surface Refl.	Solar Irrad. (W/m ² /um)	Relative Radiance	Refl. Radiance	Absolute Radiance (W/m ² /sr/um)
	Aerosol	Molec.	Ozone							
350.000	0.0732	0.5337	0.0004	0.9949	0.9501	0.1343	101.00	0.0729	0.0725	73.23
351.000	0.0731	0.5273	0.0009	0.9947	0.9501	0.1351	103.00	0.0725	0.0721	74.29
352.000	0.0729	0.5210	0.0011	0.9947	0.9501	0.1357	102.00	0.0721	0.0717	73.09
353.000	0.0727	0.5148	0.0006	0.9947	0.9502	0.1363	104.00	0.0721	0.0718	74.63
354.000	0.0725	0.5087	0.0003	0.9941	0.9502	0.1368	111.00	0.0715	0.0710	78.85
355.000	0.0723	0.5027	0.0002	0.9940	0.9502	0.1375	112.00	0.0714	0.0710	79.49
356.000	0.0722	0.4967	0.0003	0.9942	0.9502	0.1381	105.00	0.0708	0.0704	73.95
357.000	0.0720	0.4909	0.0003	0.9938	0.9503	0.1387	93.30	0.0709	0.0704	65.70
358.000	0.0718	0.4852	0.0003	0.9939	0.9503	0.1393	86.40	0.0706	0.0702	60.62
359.000	0.0716	0.4795	0.0003	0.9944	0.9503	0.1399	92.30	0.0703	0.0699	64.50
360.000	0.0714	0.4738	0.0003	0.9942	0.9503	0.1404	101.00	0.0700	0.0696	70.27
361.000	0.0712	0.4684	0.0003	0.9940	0.9504	0.1408	100.00	0.0701	0.0697	69.67
362.000	0.0710	0.4629	0.0002	0.9939	0.9504	0.1416	101.00	0.0696	0.0692	69.88
363.000	0.0709	0.4577	0.0001	0.9940	0.9504	0.1421	106.00	0.0689	0.0685	72.64
364.000	0.0707	0.4524	0.0001	0.9938	0.9504	0.1425	108.00	0.0692	0.0688	74.30
365.000	0.0705	0.4472	0.0001	0.9932	0.9504	0.1431	114.00	0.0690	0.0685	78.11
366.000	0.0703	0.4421	0.0000	0.9935	0.9505	0.1438	123.00	0.0683	0.0678	83.43
367.000	0.0701	0.4371	0.0000	0.9937	0.9505	0.1443	125.00	0.0681	0.0677	84.63
368.000	0.0699	0.4321	0.0000	0.9936	0.9505	0.1450	122.00	0.0683	0.0679	82.84

Figure 33: Example data detailing the radiometry

Prediction of at-satellite radiance - Remote Sensing Group, University of Arizona |** BAND AVERAGE RESULTS **

```

Date (mm/dd/yyyy) -- 07/03/2004
Latitude (pos. north) -- 38.4970
Longitude (pos. W of Greenwich) -- 115.691
Time (GMT, UTC) -- 17:37:19
Ground height (km) -- 1.43500
Surface pressure (mb) -- 856.100
Solar zenith angle (degrees) -- 31.7500
View zenith angle (degrees) -- 16.1472
Relative azimuth (Solar - view) -- 211.940
Aerosol Angstrom exponent -- 1.01327
Ozone (DU) -- 307.000
Water Vapour (gm/cm^3) -- 1.35000
Carbon dioxide (ppmv) -- 365.000
Earth-Sun Distance (AU) -- 1.01671

```

```

Gas transmittance is product of : Water vapour (gas and continuum)
Carbon dioxide
Oxygen
Nitrogen (N2)
HNO3
Trace gases

```

```

Headings are: Wavelength (nanometres), Aerosol, molecular, and ozone optical depths,
Gas transmittance (species listed above), Aerosol single-scattering albedo,
Measured surface reflectance, Exoatmospheric solar irradiance,
- computed from Thuillier plus corrected Kurucz database, scaled by square of Earth-Sun distance
Relative radiance (reflectance of atmosphere containing no absorbing gases except ozone)
Reflected radiance (reflectance of atmosphere containing absorbing gases)
Absolute (top-of-atmosphere) radiance

```

Channel	Band	Optical Depths			Gas	Aerosol	Surface	Solar	Relative	Refl.	Absolute
	Centre (nm)	Aerosol	Molec.	Ozone	Trans.	SSA	Refl.	Irrad. (W/m2/um)	Radiance	Radiance	Radiance (W/m2/sr/um)
1	561.6	0.0454	0.0772	0.0310	0.9915	0.9501	0.3518	1774.21	0.0902	0.0894	158.55
2	656.5	0.0388	0.0403	0.0187	0.9806	0.9483	0.3844	1520.84	0.1002	0.0983	149.49
3	833.0	0.0304	0.0156	0.0011	0.9350	0.9465	0.4201	1033.00	0.1134	0.1071	110.63

Figure 34: Example data showing the derived absolute radiance values

4.2.2 Results And Processing The Coefficients

The important values derived from the absolute calibration campaign form the final column in the table in Figure 34. These are the absolute radiance values for each spectral band on each imager. Therefore, for each imaging acquisition we now had the absolute radiance (TOA) for our target and the corresponding DN values (shown in Table 25). We can now calculate the calibration gains, using the following equation, where x is the detector number of the detectors covering the calibration target (9 detectors).

$$G_x = \frac{R_{target}}{(DN_x - BIAS_x)}$$

Equation 4

Where,

G_x is the calculated gain value for detector x

R_{target} is the measured TOA radiance for the target covered by detectors

DN_x is the measured digital number for the target covered by detector x

$BIAS_x$ is the additive term from our dark images for detector x

	DMC DATA PRODUCT MANUAL	DATE: 12-Feb-2010
		DOC NO: 0115056
		ISSUE: 02
		STATUS: FINAL

Equation 4 was applied to the nine detectors in the array that covered the target area. The results produced nine different gain values. Since these values are at most the average of two pixels per column, we have to consider that there will be a certain inaccuracy due to noise in the data (RMS noise is at the 0.8 DN level based on analysis of the dark images).

To monitor the variation induced by this, we applied the gains derived to the column mean data derived from our snow images over Antarctica, resulting in a small but measurable variation in the calculated radiances for these scenes. As we had insufficient information to determine which of the 9 pixels was the most accurate, we took an average radiance determined from the 9 pixels and set our snow scene radiance for the scene to be equal to that average.

One modification of the calibration is required to carry out this calculation of radiance for our Antarctic scene. We would normally calculate the radiance of the scene using Equation 5

$$R_{\text{scene}} = (DN_x - BIAS_x) * G_x$$

Equation 5

However, we have a variable integration time. The RRV images used a 640µs integration time, while the Antarctic scenes used a 320 µs integration time. Lab tests prior to launch showed that the DN scales up with integration time in a linear manner. Hence we need to multiply the right hand side of the equation by the ratio of the two integration times; I_s , the standard time, divided by I_t , the target time. This will produce the correct radiance.

So Equation 5 becomes Equation 6 and we can now calculate the radiance of the Antarctic scene. Or in fact 9 radiances, and use the average radiance in Equation 7.

$$R_{\text{scene}} = (DN_x - BIAS_x) * G_x * \left(\frac{I_s}{I_t} \right)$$

Equation 6

Once we have this we can now work backwards as we did in Equation 4 to derive a gain value for each detector in the array, applying the same radiance to both Imager0 and Imager1, where y is the detector number (1 to 20,000) in this case.

$$G_y = \frac{R_{scene}}{\left[(DN_y - BIAS_y) * \left(\frac{I_s}{I_t} \right) \right]}$$

Equation 7

For any new scene acquisitions we can now apply the gain and bias values derived from this calculation to directly get calibrated radiances as in Equation 8.

$$R_y = \left[(DN_y - BIAS_y) * \left(\frac{I_s}{I_t} \right) \right] * G_y$$

Equation 8

4.2.3 Scaling

The final scaling of the data product is also considered within our radiometric calibration processing. The initial data received from the satellite is in byte form. After application of the calibration coefficients, the output is a floating-point value and the dynamic range of the data is changed. An example is an image of the UK captured by Imager0 (DU00010cpm), which has a very good data range in the downloaded raw data, covering almost the whole of the 0-255 byte range (see Figure 35).

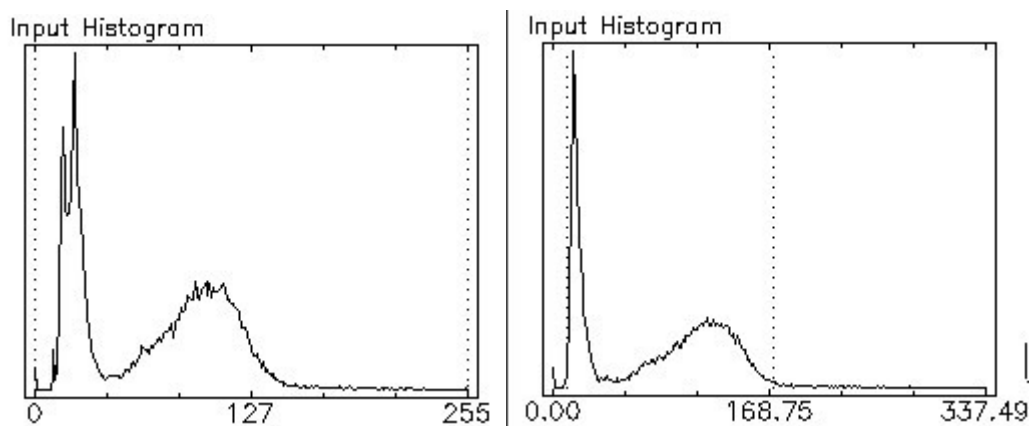


Figure 35: Histogram of original data (left); histogram of data after calibration (right)

After application of the calibration coefficients the data range is increased to cover the range 0 to 337.49, as can be seen in Figure 35.

Given the increased range and the need to keep the distributed images as small as possible, a series of compression tests were carried out on two images. The first image used a scaling where we re-

scaled the maximum value after calibration to be 255. This is the simplest form of scaling. The second image used a scaling based on the min-max method used for Landsat 5, where the minimum value in the data is scaled to zero and the maximum value in the data is scaled to 255.

The outputs were compared against the original data using a simple metric to measure data loss. The data after each scaling and quantisation was correlated against the original float data after calibration. The data loss is represented by the similarity of the scaled to this original data.

The method was tested on two very different scenes. The first scene was the UK data, which had a very large original data range. The second scene was a snow scene of Antarctica, with a very limited and narrow data range. The results are shown in Table 27.

Image	Simple Scaling	Min-Max
UK Image	99.09%	99.09%
Antarctica Image	92.07%	92.51%

Table 27: Comparison of data variation retention during scaling

As you can see, both scaling methods for the UK image show very little data loss. Over 99% of the original variation is preserved. However, with a limited data range in the original data, then large losses are apparent, with only 92% of the original variation being preserved. The losses mainly being due to quantisation losses on losing the less significant fractional numbers.

The metric used to measure the data variation retention is based on cross-correlation. This is a normalising process and so you would expect that a scene with a lot of variation would preserve most of its variation and a scene with a narrow data range to "lose" more information. Additional methods to assess data loss on scaling back within the byte range are being assessed.

For the moment it has been decided to retain a simple scaling method initially in the processing chain. The only way to preserve most of the information is to use a method similar to Landsat 7, where the data is multiplied by 100 and scaled into a short integer, preserving another two digits of the fractional data. This is being considered for the future.

5 Results

In this section we will briefly show the original image quality and that after calibration. This section is not intended to show the band-to-band radiometric integrity, but purely to show that the process does compensate for the striping artefacts of the sensor, as shown in Figure 36.

For the moment, prior to any cross-calibration exercise with other sensors, we can only assume that the radiometry is correct.

However, given that it is based on the absolute radiance values derived from the work of the Remote Sensing Group at The University of Arizona, we have high confidence that the band radiometry will be accurate to within the figure stated by the RSG (that is 5-10%).



Figure 36: Comparison of the calibrated data (left) and the raw data (right)

6 Further Work

6.1 Cross-Calibration

One area that would help in characterising the accuracy of the band-to-band radiometry is a cross-calibration exercise with another sensor with similar band characteristics. Currently we are considering more data acquisitions at our primary calibration site in Antarctica. This site at DOME-C (75°S, 123°E) has been part of an extensive study carried out using SPOT-Vegetation, which has an on-board calibrator.

The site is being run as part of a French-Italian collaboration. In past years both meteorological and tower mounted BRDF measurements have been acquired, as part of the SPOT-Vegetation calibration exercise. Our aim would be to gather images which coincided with those from the SPOT-Vegetation sensor and compare the inter-band radiometry. This would help identify any anomalies in the sensor performance and/or calibration procedure.

6.2 Stability Measurements

Additionally we need to measure the long-term stability of the instrument. We can monitor trends in behaviour using regular images over our snow-field sites and identify individual detectors that have changed in their behaviour (inducing striping in the imagery). However, if the overall optical transmission is reduced due to changes in the filter or optical performance, we cannot detect this change in absolute radiometry. Hence, we will review the absolute calibration on a yearly basis, with the next proposed absolute calibration campaign in the summer of 2005.

	DMC DATA PRODUCT MANUAL	DATE: 12-Feb-2010
		DOC NO: 0115056
		ISSUE: 02
		STATUS: FINAL

6.3 BRDF Studies

Additional work is required in characterising the snow surface at the main calibration sites. We wish to characterise the BRDF of the surface in a campaign scheduled for November 2005 – February 2006. This will consist of building up a BRDF map by yawing the spacecraft in various positions over the DOME-C site, we can build up a complete map of the BRDF variations for various solar elevation ($0^\circ - 45^\circ$), view zenith ($0^\circ - 26^\circ$) and solar and view azimuth angles.

This may require fieldwork to characterise the variation in Sastrugi (snow dunes) in terms of size and distribution across the area of study, and by modelling assess the effects they have on the determination of our calibration coefficients.

7 Summary

The UK-DMC sensor has now been calibrated using a combination of absolute measurements at the Railroad Valley site in collaboration with the Remote Sensing Group at The University of Arizona, and using “flat-field” snow images captured over Antarctica.

The overall result has removed residual striping, visible in processed post-launch imagery and provided a baseline absolute calibration.

Further work is required to compare the results of the calibration against other well-calibrated sensors and a proposed program is being developed. Additional work is addressing the possible effects of BRDF on the sensor calibration and monitoring the longer-term changes in the sensor behaviour.

These techniques are now being applied to the other satellites in the DMC constellation and will form the basis for future calibration campaigns.

8 Acknowledgements

We gratefully acknowledge the help of Kurt Thome and Chris Cattrall from the Remote Sensing Group at The University of Arizona for their help in setting up the absolute calibration activity at the Railroad Valley site in Nevada, USA and their later processing of the data.

APPENDIX E: ORTHORECTIFICATION PROCEDURE

1 Setting Up The Keystone Workstation Workspace

- 1.1 Open image to orthorectify by clicking open folder icon on the toolbar.
- 1.2 To open a zoom window of the image, right click anywhere on the image and select child (see Figure 37). Repeat on child window to open another zoom window.
- 1.3 Open reference data image as described in task 1.1 and 1.2.
- 1.4 Open a new control point list by selecting Points > Control Point List from toolbar.
- 1.5 Select Geodetic System by selecting Geodesy > Select Geodetic System from toolbar and by either entering the code or by searching the database. Once selected, click OK and the code should appear in the box.
- 1.6 Select DEM by clicking DTM > Open.

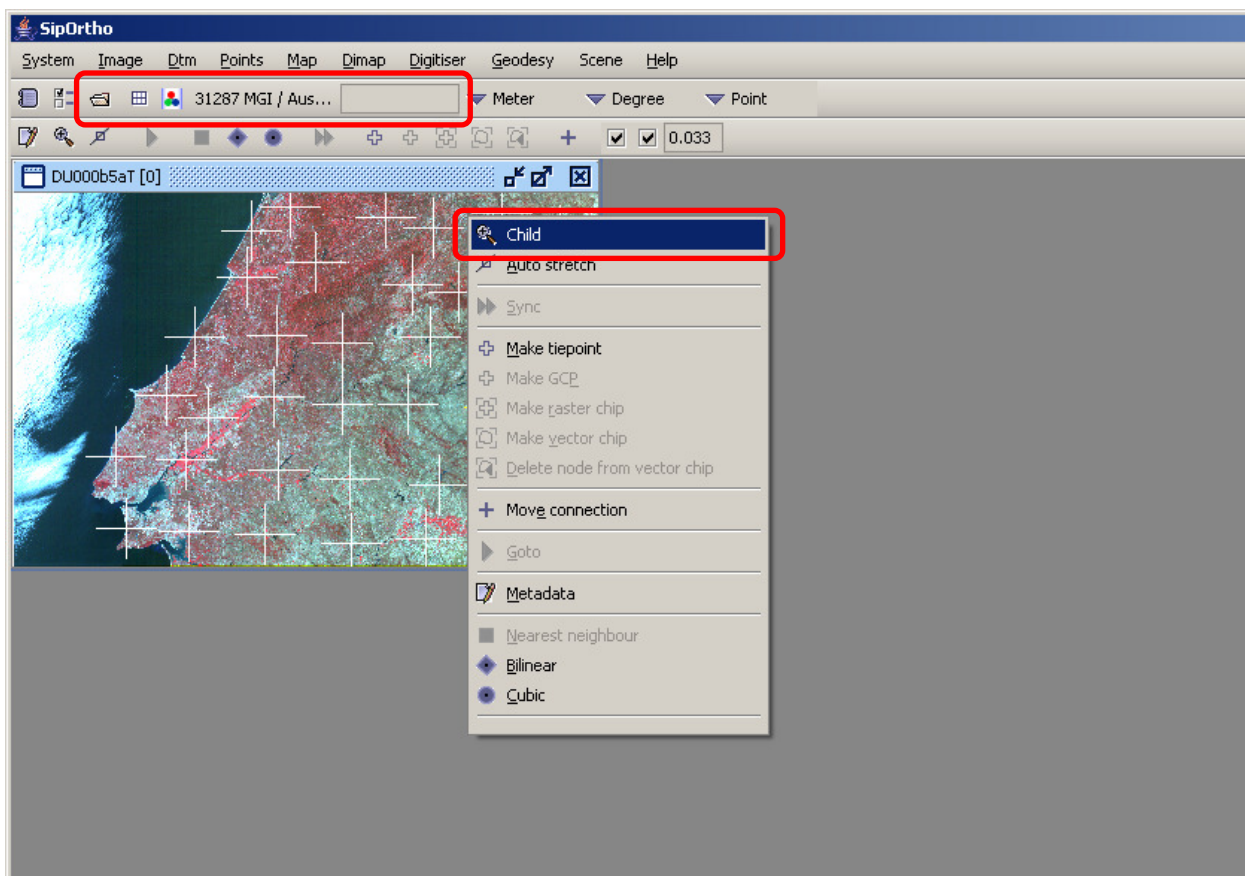


Figure 37: Keystone Workstation Workspace

2 Collecting Ground Control Points

- 2.1 Select the image to orthorectify in the left hand drop down menu on the Control Point List (see Figure 38).
- 2.2 Select the reference data image in the right hand drop down menu on the Control Point List (see Figure 38).

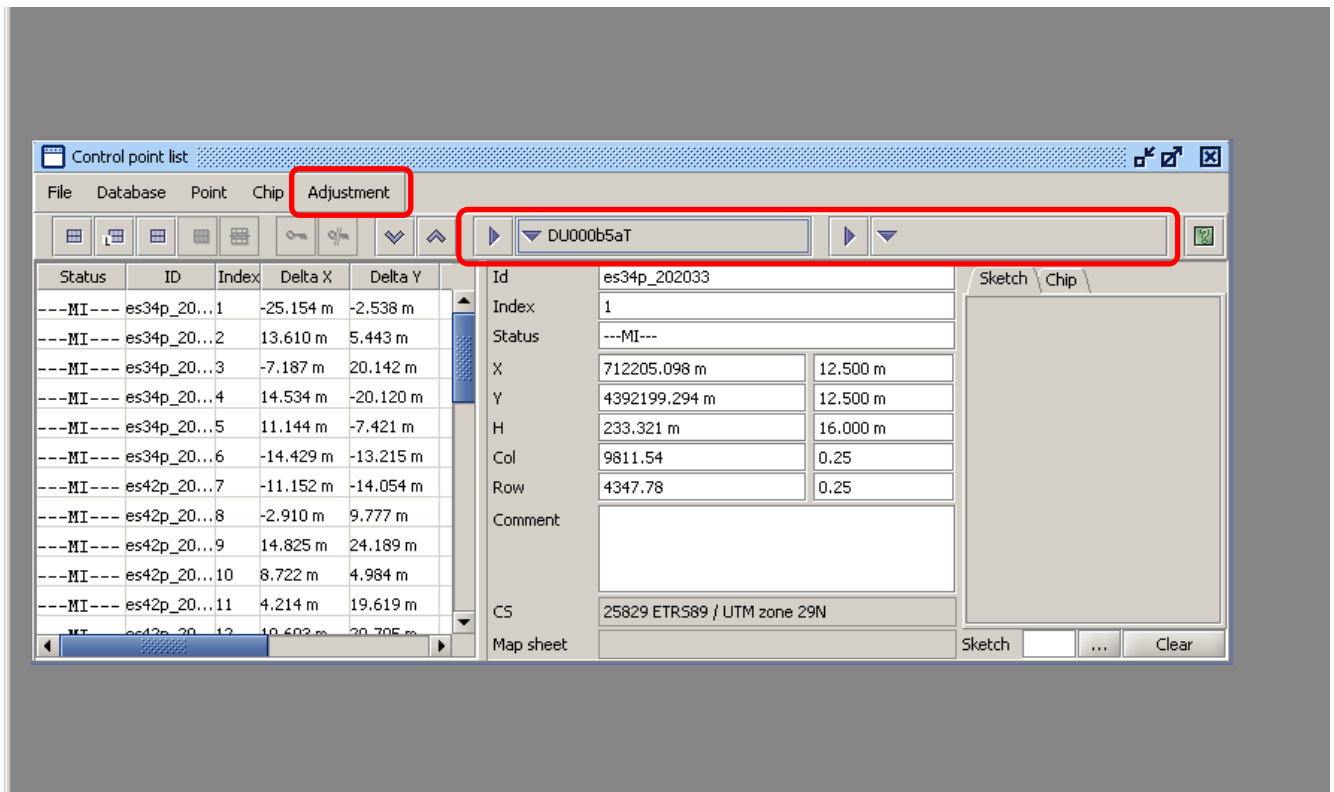


Figure 38: Control Point List

- 2.3 To place a control point, place the child view over the desired area on the image to orthorectify. Right click, and on the drop down menu that appears select sync. This will automatically move the child viewer for the reference data image to the same area.
- 2.4 In the child view on the reference data image, right click and select Make GCP. The pointer will turn into a yellow cross. Place the cross where a GCP is desired.
- 2.5 On the child viewer of the image to orthorectify, move the GCP cross to the same point on this image as it is on the reference data image. A new GCP will appear in the Control Point List.
- 2.6 To fine tune the placement of this GCP, Select Image>Image Overlay. A new window will appear which overlays the two images. Using the mouse pointer the images can be adjusted to overlay to the best fit.
- 2.7 Repeat steps 2.3 to 2.6 to produce GCPs for the remainder of the image to orthorectify, ensuring GCPs are uniformly distributed (see Figure 39).

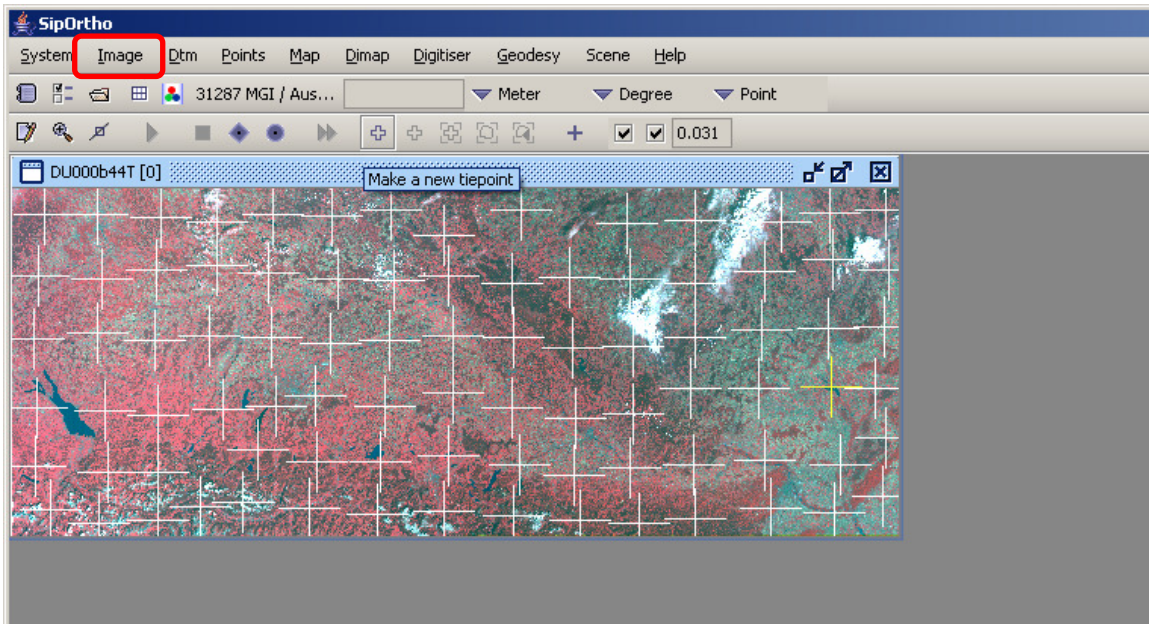


Figure 39: Distribution of GCPs

3 Editing Control Points and Running a Model

- 3.1 Select all GCPs in Control Point List. Edit the points by clicking Point>Edit Selected Points. A new window, Point List Editor, will appear. Populate the X, Y and H fields on the right hand side of the editor with the standard deviation values relevant to the reference data and DEM used. For example, when using Image2000 reference data with an SRTM DEM, the values will be 12.5m, 12.5m, and 16m respectively. Click apply.

NOTE: If more than one set of reference data is used, the GCPs may have to be edited in more than one batch with the values corresponding to the reference data.

- 3.2 With all the GCPs highlighted, click Adjustment>Adjust Rigorous Model (see Figure 38). A new window, Adjust Rigorous Model will appear. Using the navigation arrows at the bottom left hand corner of this window, skip through to the last screen available (see Figure 40).
- 3.3 Click Run.

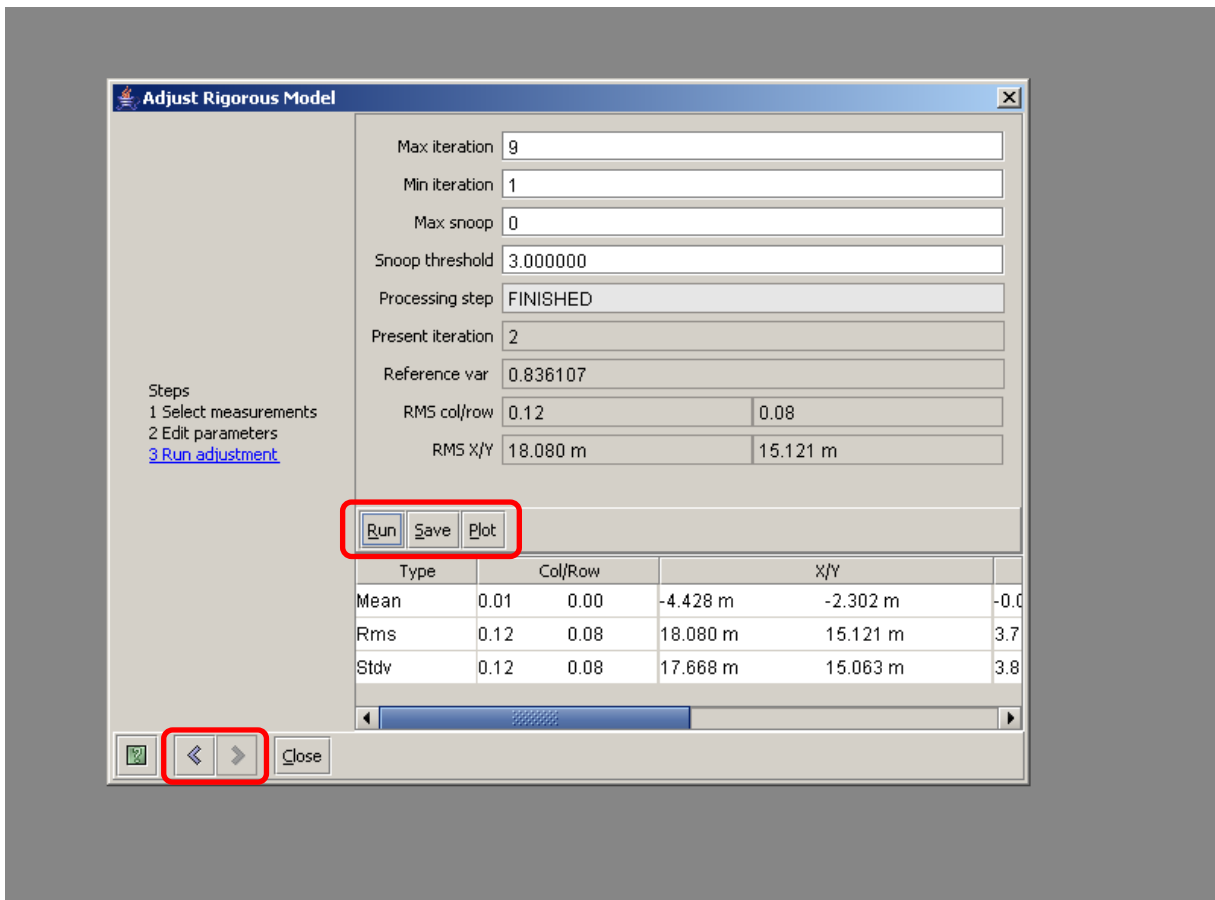
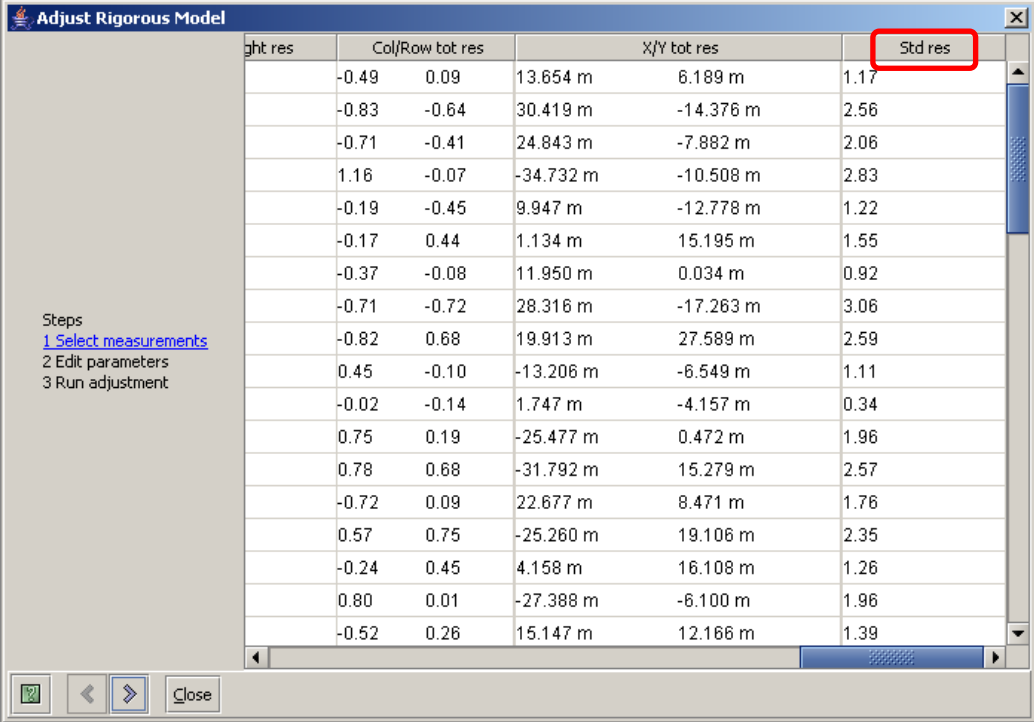


Figure 40: Adjust Rigorous Model

3.4 To achieve sub-pixel accuracy, RMS values of less than 75% of the pixel size is required. If the RMS values for X and Y are greater than this value, then clicking on Plot will show a plot of the points which can indicate if there is a particular point or area on the image to orthorectify where the errors are larger. Alternatively, by using the navigation arrows skip to the first screen to the list of all the GCPs (see Figure 41). The right hand column, labelled Std. Res., details the standardised residual error of each GCP. This value should be less than 3.0⁹. If one or more points have a standardised residual error greater than 3.0 then return to the image and re-adjust the corresponding GCPs. Repeat this adjustment process until all points have a standardised residual error less than 3.0 and the RMS values of X and Y are less than the required value for sub-pixel accuracy. Assuming there are no faults in the image itself, these standards should be achievable.

⁹ Keystone Workstation User Guide, Keystone Workstation B2239, Spacemetric



ght res	Col/Row tot res	X/Y tot res		Std res
-0.49	0.09	13.654 m	6.189 m	1.17
-0.83	-0.64	30.419 m	-14.376 m	2.56
-0.71	-0.41	24.843 m	-7.882 m	2.06
1.16	-0.07	-34.732 m	-10.508 m	2.83
-0.19	-0.45	9.947 m	-12.778 m	1.22
-0.17	0.44	1.134 m	15.195 m	1.55
-0.37	-0.08	11.950 m	0.034 m	0.92
-0.71	-0.72	28.316 m	-17.263 m	3.06
-0.82	0.68	19.913 m	27.589 m	2.59
0.45	-0.10	-13.206 m	-6.549 m	1.11
-0.02	-0.14	1.747 m	-4.157 m	0.34
0.75	0.19	-25.477 m	0.472 m	1.96
0.78	0.68	-31.792 m	15.279 m	2.57
-0.72	0.09	22.677 m	8.471 m	1.76
0.57	0.75	-25.260 m	19.106 m	2.35
-0.24	0.45	4.158 m	16.108 m	1.26
0.80	0.01	-27.388 m	-6.100 m	1.96
-0.52	0.26	15.147 m	12.166 m	1.39

Figure 41: Standardised Residual Error of GCPs

3.5 Once these requirements are fulfilled, the image is ready to be processed. On the Adjust Rigorous Model final screen click save (see Figure 40).

The meta.sip file is then processed using Keystone and the product is then subject to quality assessment.

APPENDIX F: KEYSTONE IMAGE ORTHORECTIFICATION - TECHNICAL SUMMARY

KEYSTONE IMAGE ORTHORECTIFICATION

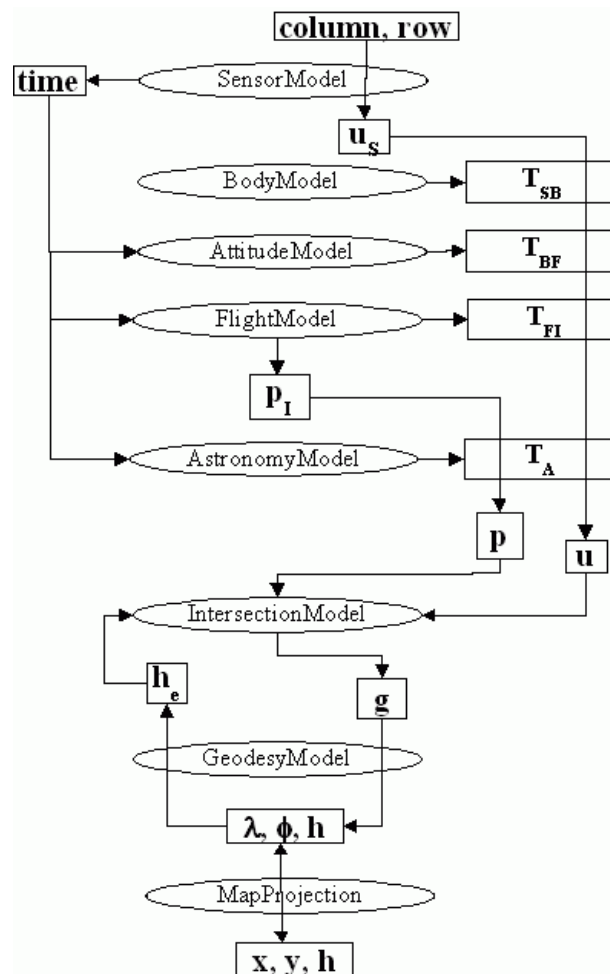
Image orthorectification is a key function of Spacemetric's Keystone system. High-accuracy image geolocation is possible through the use of rigorous photogrammetric methods using physical sensor models and advanced statistical treatment of geometric reference data.

OPTICAL LINE-OF-SIGHT MODEL

The line-of-sight model (LOS) (

Figure 42: Generic LOS model for optical sensors

) describes in an analytical way how a pixel in a satellite image is projected onto the ground using a number of distinct sub-models that can be independently modified or replaced. The diagram shows the relations between the sub-models and the flow of transformation this involves.



	DMC DATA PRODUCT MANUAL	DATE: 12-Feb-2010
		DOC NO: 0115056
		ISSUE: 02
		STATUS: FINAL

Figure 42: Generic LOS model for optical sensors

Sensor model

The sensor model takes a pixel in the satellite image and computes its look vector \mathbf{u}_s in the sensor coordinate system. It also computes the time for the instance of this look. The sensor model is initialised with instrument parameters that have been refined through an in-orbit calibration activity. The sensor model can be for a generic push-broom scanner with parameters such as focal length, detector positions in the focal plane and scan-line time interval. Alternatively, it can be a specialised model for a more complex sensor. The sensor model is typically the sub-model that is modified when implementing a new satellite system.

Body model

The body model is used to rotate the look vector from the sensor coordinate system to the satellite body coordinate system. It is used to model either intentional off-nadir sensor mounts or small misalignments in a nominal mount.

Attitude model

The attitude model is used to rotate the look vector from the body coordinate system to the flight coordinate system. The rotations between these systems result from changes in satellite attitude. This is a time-dependent variation, usually measured by devices such as Earth horizon detectors, gyroscopes or star trackers. The attitude model is initiated by a set of time-coded attitude and/or attitude rate measurements. The time of the look is used to calculate the transformation to be used.

Flight model

The flight model is used to rotate the look vector from the flight coordinate system to the Earth Centered Inertial (ECI) coordinate system. It is also used to calculate the position of the satellite. It employs orbital mechanics and is initiated by sets of parameters such as one or more ephemeris, several time-tagged position vectors or two-line elements. The time of the look is used to calculate the transformation and position to be used.

Astronomical model

The astronomical model is used to transform the position and look vectors from the ECI system to the Earth Centered Rotating (ECR) coordinate system. It is primarily a rotation of the x-axis from the Vernal Equinox to the Greenwich Meridian. The transformation is time-dependent and the time of the look is used to calculate the transformation to be used.

Intersection model

The intersection model calculates the intersection point between the look vector and an ellipsoidal Earth that is centered in the ECR system. The ellipsoidal height is also input to provide a unique position. An atmospheric model is applied to correct for the deviation caused by atmospheric refraction.

Geodesy model

The geodesy model transforms the Earth intersection point, expressed in ECR coordinates, into a geographic coordinate (longitude, latitude, orthometric height). It uses a geoid model to account for the irregularities in the Earth's zero potential surface. The result is a coordinate in the WGS84 system.

Map projection

	DMC DATA PRODUCT MANUAL	DATE: 12-Feb-2010
		DOC NO: 0115056
		ISSUE: 02
		STATUS: FINAL

The map projection transforms the geographic coordinate to a cartographic coordinate (x, y, h), by the use of a map projection that is suitable in the area of the image. There are thousands of different map projections in use for cartographic purposes in different areas all over the globe and these are referenced using standard EPSG codes. New user-defined projections can easily be defined.

Ortho-rectification

Once the line-of-sight geometric model is established for an image, it can be used for image orthorectification. The steps involved are:

- Set the output frame parameters. This includes the choice of coordinate system (map projection), bounding rectangle and pixel size for the rectified image. A minimum frame that completely contains the rectified image can be calculated automatically.
- If the image is to be orthorectified then a DEM is associated with the image. Otherwise a reference elevation is selected as the projection surface.
- Compute locations of output pixels in the input image. This inverse line-of-sight transform is not performed for every pixel as computationally this would be too costly. Instead, it is performed through the use of a regular grid over the image. The density of the grid is adjusted to be tight enough that a bilinear interpolation of positions within a grid cell is sufficiently accurate.
- Resample the input image by interpolating the non-integer positions of the output pixels. The interpolation method is selectable from among standard methods, such as cubic convolution, bilinear and nearest neighbour, while any other interpolation/filtering kernel can be added in the form of coefficients tables.
- The rectified image is saved in the required image format.

Model parameter adjustment

Prior to the image orthorectification the parameters of the line-of-sight model can be adjusted to fit a set of ground control points (GCPs). This has the goal of achieving an improved geometrical accuracy in the output product. A GCP consists of a 3-dimensional ground coordinate (x, y, h) and its estimated accuracy (s_x, s_y, s_h). An image point (IP) consists of a position in the satellite image (column, row) and its estimated accuracy ($s_{\text{column}}, s_{\text{row}}$). Marking the position of a GCP in the satellite image consequently gives a constraint on the model parameters. A number of such measurements give rise to a system of constraint equations that can be solved by least-squares adjustment.

An optimal least-squares solution should employ the “generalised least squares” approach. This makes full use of all a priori information, including start values for the parameters and their estimated accuracies. Details on how the generalised least-squares method is applied to the satellite line-of-sight problem are found in references [1] and [2].

Tie-points (TPs) are image measurements that connect locations in different images. In the “generalised least squares” approach, they are treated as IPs with small (zero) variance measured for GCPs with high (infinite) variance. In this way TPs can conveniently be accommodated in the same generalised least-squares solution.



DMC DATA PRODUCT MANUAL

DATE: 12-Feb-2010

DOC NO: 0115056

ISSUE: 02

STATUS: FINAL

	DMC DATA PRODUCT MANUAL	DATE: 12-Feb-2010
		DOC NO: 0115056
		ISSUE: 02
		STATUS: FINAL

The positioning of GCPs in an image (IP measurement) can be achieved using different tools:

- Manual positioning in an image viewer. A simple colour balancing of the image allows the GCP feature to easily be identified. It is also important that the image can be correctly zoomed so that the sub-pixel position of the feature can be measured.
- Automated pointing using image chips. The chip is a small section from another image, extracted around the GCP. The position of the chip in the raw image is found by normalised cross-correlation of image pixel grey levels. It is necessary to correctly re-sample in order to achieve a common geometric space for the chip and raw image. In this way it is possible to estimate the sub-pixel location of the best fit. In the case of ground control, the chip is extracted from a previously orthorectified image, while in the case of tie-points, the chip is extracted from the raw image to which it is to be tied. It is possible to handle both these types of chips.

Automatic model adjustment to reference data sets

The measurements of GCPs can be automated if suitable reference data sets are available. The reference data must be in the form of reference images covering the scene area. The reference images are ortho-rectified images with an accuracy as good as or better than the desired accuracy of the resulting image. The spectral response of the reference images must match the target image in at least one band, so that they are sufficiently correlated for successful matching.

The automatic model adjustment is based on strategies involving:

- Automatic selection of reference images and DEM covering the image to be corrected.
- Selection of large numbers of potential GCP locations.
- Hierarchical matching in different resolutions.
- Robust methods for gross error detection.
- Least-squares adjustment of LOS model parameters.

After the successful model adjustment, the target scene is ready for orthorectification. If an automated model adjustment fails to produce the required accuracy a manual GCP identification process can be undertaken in the reference data sets, and the model re-adjusted to enhance the accuracy.

This automatic model adjustment is used in the Keystone server provided to DMCIi at their UK receiving station. This carries out automatic adjustment of all DMC image acquisitions as a pre-process to that improves upon the initial image geolocation provided by the platform pointing data alone. A global coverage of ortho-rectified Landsat TM imagery is successfully used as reference imagery in this systematic process.

	DMC DATA PRODUCT MANUAL	DATE: 12-Feb-2010
		DOC NO: 0115056
		ISSUE: 02
		STATUS: FINAL

Geometric accuracy performance

Spacemetric's software has a long-standing reputation in achieving unsurpassed geometric accuracy in operational environments. The key factors are:

- Precision: The analytical LOS models are rigorous and well calibrated and allow precise modelling of the sensor geometry.
- Robustness: The use of analytical models with carefully weighted parameters makes it possible to achieve high accuracy even when there is limited ground control.

The models allow half-pixel accuracy or better to be achieved if the ground control is of sufficient quality. This has been verified during many years of operational use by users including Metria, Sweden, and through tests carried out by the EC Joint Research Centre in the context of quality tests within the Control with Remote Sensing activity.

The principles and performance of the methodology are documented in numerous technical papers, a selection of which is referenced below and are available for download through Spacemetric's homepage (www.spacemetric.com).

Referenced documents

- [1] Westin, T.: Precision rectification of SPOT imagery. *Photogrammetric Engineering & Remote Sensing*, Vol. 56, No. 2, February 1990, pp. 247-253.
- [2] Westin, T.: Pass processing and extrapolation of SPOT image geometry. *Photogrammetric Record*, 13(78), 1991, pp. 919-925.
- [3] Westin, T.: Empirical models for attitude variability of the SPOT 1 satellite, *Photogrammetric Record*, 13(78), 1991, pp. 913-918.
- [4] Westin, T.: Inflight calibration of SPOT CCD detector geometry. *Photogrammetric Engineering & Remote Sensing*, Vol. 58, No. 9, September 1992, pp. 1313-1319.
- [5] Westin, T.: Photogrammetric Potential of JERS-1 OPS. *International Archives of Photogrammetry and Remote Sensing*. Vol. XXXI, Part B4, Vienna 1996, pp. 937-942.
- [6] Westin, T.: Geometric Rectification of European Historical Archives of Landsat 1-3 MSS Imagery. *Proceedings of the ISPRS workshop "Sensors and Mapping From Space 1999"*, Hannover, Germany, September 27-30, 1999.
- [7] Westin, T.: Geometric Modelling of Imagery from the MSU-SK Conical Scanner. *Bulletin SFPT*, no 159, pp. 55-58, 2000.
- [8] Westin, T., and Forsgren, J., 2001: Orthorectification of EROS A1 images. *IEEE/ISPRS Joint Workshop on "Remote Sensing and Data Fusion Over Urban Areas"*, Rome, Nov. 8-9, 2001
- [9] Vassilev, V., Popova, S., Mangolini, M., Garnier, A., Westin, T., Åstrand, P., Milenov, P.,: Orthorectification Tests Continued...Formosat-2, conference presentation, MARS PAC Annual conference 2007, Geomatics in support of the CAP, Madrid, Spain. 12th-14th November 2007
- [10] Vassilev, V., Popova, S., Mangolini, M., Garnier, A., Westin, T., Åstrand, P., Milenov, P.,: Orthorectification of Formosat-2 Data for Use in the Common Agricultural Policy Control with Remote

	DMC DATA PRODUCT MANUAL	DATE: 12-Feb-2010
		DOC NO: 0115056
		ISSUE: 02
		STATUS: FINAL

Sensing Programme, conference presentation, MARS PAC Annual conference 2006, Geographical information in support of the CAP, Toulouse, France. 27th-29th November 2006

[11] Westin, T., Edgardh, L.: Automatic geo-registration of satellite imagery, MARS PAC Annual conference 2006, Geographical information in support of the CAP, Toulouse, France. 27th-29th November 2006

APPENDIX G: WEBLINKS

DIMAP

<http://www.spotimage.fr/dimap/spec/dimap.htm>

DMCII

<http://www.dmcii.com>

Eastman Kodak KLI-10203 Linear CCD Data Sheet

http://www.micronkk.com/1_imaging/kodak/DataSheet/KLI-10203%20Rev.6.pdf

Eastman Kodak KLI-14403 Linear CCD Data Sheet

<http://www.kodak.com/global/plugins/acrobat/en/business/ISS/datasheet/linear/KLI-14403LongSpec.pdf>

GLCF

<http://glcf.umiacs.umd.edu/index.shtml>

GLOBE

<http://www.ngdc.noaa.gov/mgg/topo/globe.html>

OGP Surveying & Positioning Committee

<http://www.epsg.org/>

Spacemetric

<http://www.spacemetric.se/>

SRTM

<http://srtm.csi.cgiar.org/>

SSTL

<http://www.sstl.co.uk>

TIFF Revision 6.0

<http://partners.adobe.com/public/developer/en/tiff/TIFF6.pdf>